THE OLIGOMERIZATION OF PROPENE OVER NICKEL SYNTHETIC MICA-MONTMORILLONITE

BY

LESTER LANCE JACOBS

B.Sc. (ENG) (CAPE TOWN)

Submitted to the University of Cape Town in fulfilment of the requirements for the degree of Master of Science in Engineering.

ACKNOWLEDGEMENTS

I would like to express my sincere appreciation to Prof. C.T. O'Connor and Dr. M. Kojima for their assistance and guidance throughout the duration of my study.

Many thanks to Messrs S. Harms, S. Swartz, P.M. Dickens, K. Moller and D. McClean for their friendship and helpful advice over the years.

The following people and Institutions are also gratefully acknowledged :

SASOL and the Council for Scientific and Industrial Research for financial and technical assistance. In particular, Mr K. Kriel of SASOL and Dr. M. Scurrell of CSIR.

All on the Chemical Engineering Department staff.

The Council for Mineral Technology for the fluorine analyses.

Harshaw/Filtrol for the catalyst samples.

Dr. K. Hertzog for his assistance with the TG-DTA studies.

Miss B. Williams for the mass spectroscopic analysis.

A very special thanks to Maria for her companionship over the years and to Michèle for the excellent typing of the thesis.

I would also like to thank my parents, Henry and Francina, for their constant support.

SYNOPSIS

The catalytic oligomerization of propene to liquid fuels using synthetic mica montmorillonite (SMM) as well as the effect of incorporating nickel into the lattice and nickel, cobalt and zinc into the interlayer spaces was investigated.

NiSMM is more active for propene oligomerization than SMM, although the product selectivity (60% of the oligomers boiled at above 453 K) is similar. The increase in activity of NiSMM is attributed to an increase in the surface acidity of the catalyst. The maximum activity over the nickel exchanged catalyst occurs at a nickel loading of 0.057 wt %. It is proposed that the bond strength of the acidic hydroxyl groups are perturbed by the polarizing effect of the divalent cation (Co, Zn or Ni) present in the interlayer spaces of SMM. The reduction of nickel, ion exchanged into SMM, removes the induction period associated with SMM and increases the catalyst lifetime. However, reduction of the lattice nickel results in a decrease in catalyst lifetime although the Bronsted acidity has increased. It is proposed that the metallic nickel present in reduced NiSMM may promote dehydrogenation of high molecular weight hydrocarbons thus causing rapid deactivation of the catalyst by increasing the formation of "graphitic" coke.

The lifetime of NiSMM is greatly reduced by using a wet propene feed and reacting at higher temperatures (443 K) due to the generation of Bronsted sites and increased coke formation rates, respectively. Deactivation of the catalyst is associated with a "graphitic" coke build up. The RON of the petrol fraction is 94.5 and the hydrogenated diesel fraction has a cetane number less than 35.

TABLE OF CONTENTS

CATPOLY

LIST OF FIGURES

Chapter 1

Chapter 2

Chapter 3

Chapter 4

Chapter 7

LIST OF TABLES

Chapter 1

Chapter 3

Chapter 4

Chapter 7

NOMENCLATURE

ASTM	-	American Society for Testing of Materials
BET	-	Brunauer Emmet Teller
D	-	Dimer
DTA	-	Differential Thermal Analysis
GC	-	Gas Chromatography
H	-	Hexamer
HEP+	-	Heptamer +
IP	-	British Institute of Petroleum
LPR	-	Liquid Production Rate (gram liquid product per gram catalyst per hour)
MOGD	-	Mobil Olefins to Gasoline and Distillate
NMR	-	Nuclear Magnetic Resonance
NiIXSMM	-	Nickel Ion Exchanged SMM
NiSMM	-	Nickel Substituted Mica Montmorillonite
P	-	Pentamer
RON	-	Research Octane Number
SMM	-	Synthetic Mica Montmorillonite
TE	-	Tetramer
TG	-	Thermogravimetry
T.I.C.	-	Total Ion Current
TR	-	Trimer
WHSV	-	Weight Hourly Space Velocity

1. INTRODUCTION

The production of synthetic fuel from coal has been practised in South Africa for three decades. The process, which involves the conversion of carbon monoxide and hydrogen to hydrocarbons, was invented by Frans Fischer and Hans Tropsch in 1922 (Jager, 1978). Because of the abundance of coal in South Africa, the Anglo Transvaal Consolidated Investment Co. (Anglo Vaal) acquired in 1935 the South African rights to the German Fischer-Tropsch (F-T) process (Hoogendoorn, 1974). In 1943, rights to the American variation of the F-T process were procured. In 1950 an agreement was reached between the South African government and Anglo Vaal in which the Anglo Vaal rights were taken over by the government, with the subsequent formation of the South African Coal, Oil and Gas Corporation (SASOL). Commercial operation started in 1955 with the SASOL 1 plant at which the planned output of 223 000 tons per annum of primary products was reached two years later (Hoogendoorn, 1974). With the rise in crude oil prices in the 1970's a second much larger plant (SASOL 2) was built. The production capacity was increased dramatically in 1980 when SASOL 2 came on stream with 1 400 000 tons of motor fuels per annum, and was boosted even further in 1982 when SASOL 3 came on line with the same production capacity (Snel, 1986).

The SASOL process uses two types of reactors, the Arge fixed bed and the Synthol fluidized bed reactors. Table 1.1 shows a typical product spectrum for the two reactors (Jager, 1978). It can be seen from Table 1.1 that less than 50 % of the product from the Synthol reactor is in the gasoline and diesel range. The remaining products CH_4, C_3 and C_4 alkenes and wax are processed by catalytic reforming, oligomerization, and cracking, respectively. Approximately 30 % of the total gasoline

Selectivities, %	Fixed Bed		Synthol	
CH_4	5.0		10.0	
C_2H_4	0.2		4.0	
C_2H_6	2.4		6.0	
C_3H_6	2.0		12.0	
C_3H_8	2.8		2.0	
C_4H_8	3.0		8.0	
C_4H_{10}	2.2		1.0	
Petrol C_5-C_{12}	22.5		39.0	
Diesel C_{13}-C_{18}	15.0		5.0	
Heavy Oils C_{19}-C_{21}	6.0		1.0	
C_{22}-C_{30}	17.0		3.0	
wax C_{31}^+	18.0		2.0	
NAC	3.5		6.0	
Acids	0.4		1.0	
	C_5-C_{12}	C_{13}-C_{18}	C_5-C_{10}	C_{11}-C_{14}
% Paraffins	53	65	13	15
% Olefins	40	28	70	60
% Aromatics	0	0	5	15
% Alcohols	6	6	6	5
% Carbonyls	1	1	6	5
% n-Paraffins	95	93	55	60

Table 1.1 : Typical hydrocarbon product spectrum from a fixed bed and Synthol reactor.

and diesel product is obtained by alkene oligomerization over phosphoric acid via a catalytic polymerization process. However, the diesel fuel produced is of a relatively poor quality (cetane number of hydrogenated liquid product lies between 33 and 35). It is desired, therefore, to improve characteristics such as the density and viscosity of the diesel fuel. Several processes have been suggested to improve diesel selectivity such as Low Temperature (493 K) F-T processing (Jager et al, 1982; Dry, 1982) and improved alkene oligomerization.

At this stage, the second option is attracting considerable interest. An efficient and economic modification to the CATPOLY process would be to use a catalyst which is capable of producing a heavier diesel fuel by selectively oligomerizing propene and butene to linear products in the C_{12+} range.

The present study investigated the oligomerization of light alkenes to liquid fuels using synthetic clay type catalysts, namely synthetic mica montmorillonite (SMM), nickel substituted synthetic mica montmorillonite (NiSMM) and nickel-exchanged SMM. The main objective of the work was to improve the quality of the liquid fuel produced. The experimental work was carried out in a high pressure integral reactor. The liquid product was characterized using gas chromatography (GC), mass spectroscopy, nuclear magnetic resonance and ASTM fuel techniques.

1.1 ALKENE OLIGOMERIZING CATALYSTS

The polymerization of olefins to produce liquid fuels on a commercial scale began in 1931 (Oblad et al, 1958). Initially, thermal polymerization was employed until the introduction of the first catalytic process in 1935 (Ipatieff et al, 1935).

CAT BOL Y

Phosphoric acid is the most widely used acid catalyst for olefin polymerization. It has been employed commercially as 103-110 % phosphoric acid on a Kieselguhr support. Phosphoric acid has been used principally for the polymerization of C_3 and C_4 olefins. These catalysts are used in fixed bed flow type reactors at temperatures ranging from 373 to 523 K and pressures from 30 - 50 atm (Langlois, 1953). However, product yield and quality was relatively insensitive to operating conditions (Mc Mahon et al, 1963). Propene and butene polymerization over phosphoric acid yields polymers mainly in the gasoline range (C_5 - C_{12}). Oblad et al (1958) reports that butene polymerization yields 90 % dimer and 10 % trimer. By operating at conversions between 80 and 90 % the polymers produced from propene have a RON of 94, whilst from a mixed C_3 - C_4 feed the product has a value of 97. The cetane number of the diesel fraction after hydrogenation lies between 33 and 35. The activity and the lifetime of the phosphoric acid catalyst is sensitive to the water partial pressure in the reaction zone (Mc Mahon et al, 1963). Water rates sufficient to obtain an acid strength of 103 % are recommended since this results in good catalyst lifetime. No regeneration facilities are required since the combination of high pressure and low reaction temperature prevents excessive coke deposition. Although the phosphoric acid catalyst is used extensively,

the process is plagued by corrosion problems.

A variety of other solid acid catalysts have been proposed in recent years. Silica-alumina has been employed industrially for the polymerization of butene at reaction temperatures from 373 to 523 K (Thomas, 1945). The liquid product resulting from reaction at 440 K and 45 atm (LHSV = 7) contained about 52 % dimers with an octane number of the hydrogenated product equal to 95. Propene oligomerization was carried out at a higher reaction temperature of 520 K. However, the catalyst deactivated rapidly. The polymer made under these conditions contained about 10 % dimers and 60 % trimers (Thomas, 1945). Johnson (1955) showed that the polymerization activity of silica-alumina increased with acid strength and that a linear relationship exists between acidity, as measured by ammine titration, and the rate of propene polymerization. Shephard et al (1962) reported that Bronsted acid sites of silica-alumina were required to polymerize propene while the Lewis acid sites promote aromatics and coke formation.

Shape selective zeolite-Y catalysts have also been investigated as catalysts to improve liquid products selectivities for propene and butene oligomerization (Fasol, 1983, Occelli et al, 1985). Fasol (1983) found that optimum reaction conditions for butene oligomerization to be 573 K and 50 atm resulting in a product consisting of 60% dimers, 35% trimers and 5% tetramers. Occelli et al (1985) investigated propene oligomerization over HY. Reaction conditions were similar to that used by the above worker (50 atm, reaction temperature = 573 K, WHSV = 1 h^{-1}). Propene conversion was about 40 weight % and the product was mainly in the gasoline range (90%) and highly branched. Datka (1980) studied the effect of the degree of cation exchange on butene oligomerization using

NaHY/21, NaHY/40 and NaHY/77. He found that the rate of oligomerization increased with the degree of cation exchange of the catalyst. He also found that the more active the zeolite Y, the more branched the product formed.

ZSM-5, which has been shown to be highly reactive for olefin reactions after intensive study by the Mobil Research and Development Corporation, is used in the MOGD (Mobil Oil to Gasoline and Distillate) process. In the MOGD process light olefins are converted to higher molecular weight gasoline and diesel fuel (Tabak, 1981). Anderson et al (1980) suggested that the catalytic activity of ZSM-5 is due to the Bronsted acid sites, since Na-ZSM-5 had a very low activity and the activity of H-ZSM-5 was quenched by ammonia. Occelli et al (1985) investigated the oligomerization of propene over H-ZSM-5 at WHSV = 1 h^{-1} and 48 atm. The optimum reaction temperature (conversion = 98 wt %) was 640 K and the liquid product contained mainly gasoline (80 %). At temperatures below 470 K the catalyst had low activity. However, conditions could be varied to maximize the diesel fuel range products (C_{12} - C_{20}) (Tabak et al, 1986). The MOGD process employs a liquid product recycle and thus by varying reaction conditions and the recycle composition a maximum gasoline or diesel yield can be obtained. Marsh et al (1984) reports the following product spectrum for two operating modes at 540 K and 42 atm :

diesel mode - 13 wt % gasoline; 79 % diesel

gasoline mode - 52 wt % gasoline; 32 % diesel

Occelli et al (1985) found that the synthetic fuel produced over ZSM-5 had a low degree of branching ($CH_3/CH_2 < 0.5$). He proposed that the average molecular size of oligomers produced was controlled by the pore size. Tabak et al (1986) stated that at conditions which maximize

diesel production, the product was shown to be 100 % olefinic. The overall branching was not extensive, with one branched methyl per five carbon atoms. The gasoline product from oligomerization over ZSM-5 has a RON of 92, and after hydrogenation of the heavier fraction (C_{11} - C_{20}) a cetane number of 56 is obtained.

Synthetic clays, SMM and NiSMM, have been shown to oligomerize products in the range C_{12} to C_{18} (Bercik et al, 1978; Fletcher, 1984). These catalysts offer considerable potential for processing low chain olefins to a variety of useful products such as high performance jet fuels and low pour hydraulic and transformer oils. Product yield and lifetime data will be discussed in Section 1.2.3.

The use of cation exchange resins in the oligomerization of butene to liquid fuel has been investigated (Haag, 1967; Schumann, 1983). The oligomerization reaction was performed at low reaction temperatures (373 - 400 K) and 15 atm. The liquid product consisted mainly of dimers (65%) and trimers (30%), and was highly branched. The RON of the gasoline fraction (C_6 -C_{12}) was 97 and the diesel fuel range (C_{12}-C_{18}) yielded a cetane number of 35.

The dimerization of low molecular weight olefins has also been investigated extensively. The use of nickel oxide silica-alumina for C_2 - C_4 olefin dimerization at low reaction temperatures (353 K) has been shown by a number of workers (Glockner and Barnett, 1970, Pine et al, 1970; Hogan et al, 1955; Holm et al, 1957). Hogan et al (1955) reported that the reaction rate of propene oligomerization over nickel oxide silica-alumina at 40 atm was highest in the temperature range of 340 - 360 K (system in the liquid phase), whilst conversion declined

rapidly above 370 K (psuedocritical temperature). At 68% conversion, the product contained 72% dimers, 19% trimer and 6% tetramer. The RON of the product formed was about 90. However work by Glockner and Barnett (1970) revealed that the product selectivity could be varied by sulphiding the NiO_2 SiO/Al_2O_3 catalyst. At a reaction temperature of 420 K, 85 % dimers and 10 % trimers were formed with ethylene oligermerization over the unsulphided catalyst as opposed to 42 % dimers, 28 % trimers and 13 % tetramers when the catalyst was presulphided. The dimers and trimers showed an average of 85 % linearity. Cobalt oxide on activated carbon is known to dimerize C_2 - C_6 olefins (Schultz et al, 1966; Addy and Hill, 1966; Weise, 1977). Oligomerization reactions were carried out using propene as feed, the pressure at 20 atm and the reaction temperature 298 K. The polymer produced contained about 96 % dimers (hexenes) with 56 % straight chain hexenes (Hill, 1967).

Other catalyst types for alkene polymerization include Friedel Crafts catalysts, e.g., BF_3 (Oblad et al, 1958), organometallic catalysts (e.g. $TiCl_4$-$Al(C_2H_5)_3$) (Doi et al, 1982) and Ziegler type catalysts. Natural clays such as kaolinite and montmorillonite have been shown to polymerize styrene (Solomon, 1968).

1.2 NATURAL AND SYNTHETIC CLAY CATALYSTS

1.2.1 NATURAL CLAYS

In industry, clay minerals have been widely employed as catalysts for a number of hydrocarbon reactions including polymerization, isomerization and cracking (Davidtz, 1976; Voge, 1958; Swartz-Allen and Matijevic, 1974). They are also used as catalyst supports and starting materials in catalyst manufacture. Today, acidic clays are commercially used for the purification of hydrocarbons by removing olefinic components and colouring matter (polar compounds) (Jasra and Bhat, 1985). Because of their layered structure and ability to swell, clay minerals can absorb bulky and long chain molecules (Jasra and Bhat, 1985). In nature, these minerals form an integral part of the conditions in soil profiles where organic matter is continuously undergoing change. The acidity of clays is believed to have had a role in petroleum formation in nature. (Johns and Shimoyama, 1972).

1.2.1.1 CRYSTAL STRUCTURE AND CHARGE DISTRIBUTION

Clay minerals are composed of small plate-like particles ranging in diameter from a few hundredths of a micron to several microns. Each of these platelets consists of one or more unit layers. Clays exist predominantly as two-layer and three-layer silicates.

In a two-layer clay, such as halloysite, the unit layer is composed of one sheet of silica and a sheet of alumina and is thus a 1:1 phyllosilicate (Grim, 1968). Kaolinite, an example of a 1:1 phyllosilicate, is neutral (i.e. layer charge is zero) as shown in Figure 1.1 (Brown, 1972). Three layer clays, such as montmorillonite,

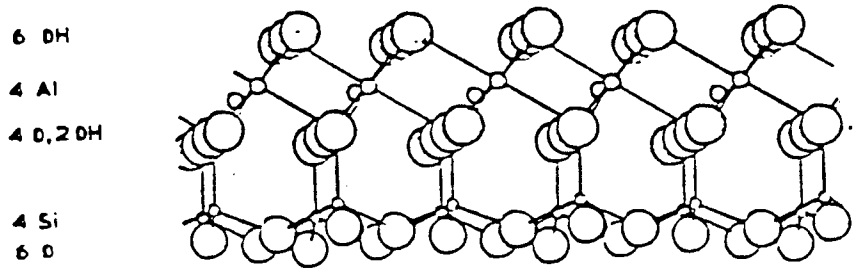

Figure 1.1 Structure of Kaolinite (Brown,1972)

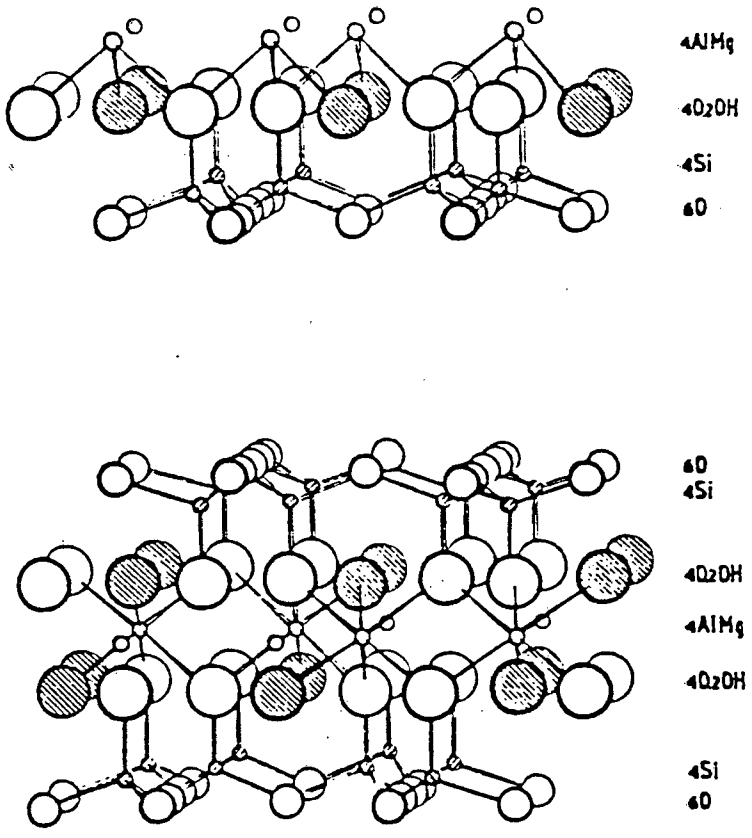

Figure 1.2 Structure of Pyrophyllite (Brown,1972)

have a unit layer consisting of a sheet octahedral alumina or magnesia sandwiched between two sheets of tetrahedral silica. Montmorillonite belongs to the smectite group and is a 2:1 phyllosilicate (Grim, 1968). A schematic representation of the crystal structure of the parent material of this mineral, pyrophyllite, is shown in Figure 1.2. (Brown, 1972). From Figure 1.2, three distinct sheets can be seen. The inner sheet consisting of octahedrally co-ordinated aluminium ions, shares two thirds of its oxygen with the outer tetrahedrally co-ordinated silicon sheets. The remaining oxygens are included in hydroxyl groups. The term 2:1 layer lattice is derived from this layered structure (Farmer and Russel, 1964). In the neutral clay, the layers are held together by weak van der Waals forces. The silicates show hexagonal symmetry (Farmer and Russel, 1964) with the oxygen atom of the structural hydroxyl groups projecting into this hexagonal hole.

It can also be seen from Figure 1.2 that only two out of the three possible octahedral positions per unit cell are occupied. The mineral is termed dioctahedral. In the case of talc (Mg^{2+} in the octahedral position instead of aluminium), where all the octahedral positions are filled, the clay is termed trioctahedral.

Electrokinetic studies of certain clays indicate that clay particles carry a net negative charge which is compensated by positive counter ions (Swartz-Allen and Matijevic, 1974). This negative charge on the clay lattice is believed to be due to isomorphic substitution, lattice imperfections, broken bonds at the edges of particles and exposed structural hydroxyl groups (Grim, 1968).

Literature suggest that the main source of the negative charge is isomorphic substitution within the lattice (van Olphen, 1963; Grim, 1968; Farmer and Russel, 1964; Davidtz, 1976). In the 2:1 layer silicates (mica and montmorillonite), there are two positions that the replacing cation can occupy, viz., Al^{3+},Fe^{3+} for Si^{4+} in the tetrahedral layer and Mg^{2+}, Fe^{2+} for Al^{3+} in the octahedral layer. This results in a net negative charge of approximately 0.5 to 2 per unit cell. Table 1.2 gives typical examples of phyllosilicates and their respective layer charges.

TYPE LAYER LATTICE	GROUP χ = LAYER CHARGE	EXAMPLES
2 : 1	PYROPHYLLITE $\chi \sim 0$	PYROPHYLLITE, TALC
	SMECTITE $\chi \sim 0.5\text{-}1$	MONTMORILLONITE, MONTRONITE, HECTORITE
	MICA $\chi \sim 2$	MUSOVITE, BIOTITE
2 : 1 : 1	CHLORITE VARIABLE	PENNINE
1 : 1	KAOLINITE-SERPENTINE	KAOLINITE, HALLOYSITE

TABLE 1.2 TYPICAL PHYLLOSILICATES (Brindley, 1964)

The cations which balance the lattice negative charge are usually associated with water molecules (water-cation complex) and can be ion exchanged (Lewis, 1955; Kerns and Mankin, 1968; Cariatti, 1983). Kerns and Mankin (1968), amongst others, found that the degree of hydration (swelling) of the clay is related to the interlayer cation and the site of the layer charge deficiencies (i.e. the strength of the bond between the cation and the clay layer). The degree of hydration increases with decreasing lattice layer to interlayer cation bonds per unit cell and increasing octahedral/tetrahedral charge deficiency. Where a high degree of substitution occurs, with a layer charge of approximately 2, little or no water is present and the clay is non-exchangeable (e.g. mica). Montmorillonite with a lower layer charge (0.5 - 1) has exchangeable interlayer cations which are associated with a water layer of variable thickness (Farmer and Russel, 1964).

Cation exchange capacities of different montmorillonites varies from 85 to 160 meq / 100 g, whereas the exchange capacity of kaolinite samples range from 1.5 to 20.2 meq / 100 g (Lewis, 1955). Surface area determinations of montmorillonite have been made (Thomas and Bohor, 1968). Using nitrogen as adsorbent, the calculated surface area ranged from 61 m^2/g for Li-montmorillonite to 138 m^2/g for Cs-montmorillonite.

1.2.1.2 SURFACE ACIDITY OF MONTMORILLONITES

Clay minerals have the ability to protonate bases and catalyze many organic reactions even though the interlayer cations are not protons (Frenkel and Mortland 1974; and Raman, 1968). Stul (1983) showed that the introduction of organic cations ($(CH_3)_4N^+$) into the clay lattice

improved its activity for isomerization. Walter (1967) reported that the presence of small exchangeable cations in clays enhances the decomposition of glycerol.

The surface acidity of montmorillonite has been suggested to result from the water molecules strongly polarized by the cation on the clay surface. NMR studies (Frenkel, 1974) indicated that water adsorbed on the montmorillonite is 10^6-10^7 times more dissociated than in liquid water. Farmer and Mortland (1966) found that the acidity of Mg-montmorillonite increased as the clay was dehydrated. The polarization forces of the cation, which are dispersed via hydrogen bonding, increases as the number of co-ordinated water molecules around it decreases with the result that the degree of polarization, and in turn the clay's proton donating ability, increases.

Mortland and Raman (1968) and Frenkel (1974) have shown that the acidity of the clay is strongly influenced by the polarizing ability of the exchangeable cation. The acidity was found to decrease in the order Al^{3+}, Mg^{2+}, Na^{+}. The presence of organic exchange cations on montmorillonite gave an improved performance for olefin isomerization than inorganic cation exchange montmorillonite (Stul et al, 1983).

It appears that the hydrated water of the exchanged cation is acidic, and can be represented as :

(1) $$[M(H_2O)_x]^{n+} \underset{\longleftarrow}{\xrightarrow{K_1}} [M(H_2O)_{x-1}(OH)]^{(n-1)+} + H^+$$

(2) $$[M(H_2O)_x(H_2O)_y]^{n+} \underset{\longleftarrow}{\xrightarrow{K_2}} [M(H_2O)_{x-1}(OH)(H_2O)_y]^{(n-1)+} + H^+$$

where M is the exchangeable ion, x the amount of inner sphere co-ordinated water, y the amount of outer sphere co-ordinated water, and K_1, K_2 the ionization constants for the two systems. Equation (1) represents the drier system with directly co-ordinated water, while equation (2) represents a moist system. It has been shown that K_1 is greater than K_2, indicating that the drier system is the more efficient proton donor (Mortland and Raman, 1968).

Schainberg and Kemper (1966) have shown that the protonation ability of clays are affected by the site of the lattice charge. Frenkel (1974) suggested that the greater acidity of montmorillonite with octahedral substitution to be due to a weaker cation attachment to the lattice than when substitution occurs in the tetrahedral layer. Mortland and Raman (1968) postulated that the polarization of water by the cation was dependent on the electrostatic field around the cation and the total dipole moment of co-ordinated water. The electrostatic field was in turn related to the force exerted by the clay structure itself on the cation. This force may be expressed as Coulomb's Law Relationship (Kerns and Mankin, 1968) :

$$F \propto \frac{C^+C^-}{r^2}$$

where C^+ and C^- represent charges entering bond formation and r is the distance of separation. This equation implies that a charge deficiency in the tetrahedral layer would form a stronger layer-cation bond than would one in the octahedral sheet.

Acid catalysis by clays have been employed in early catalytic cracking processes. Acid clays are prepared by washing with mineral acids

(Coleman and McAuliffe, 1954), electrodialysis (Davidtz, 1976) and ammonium exchange followed by thermal decomposition (Russel and White, 1966). Coleman and McAuliffe (1954) found that Al-saturated clays had little catalytic effect as opposed to H-saturated clays. Activity was proportional to the H ion concentration of the clay. Frenkel (1964) reported that the surface acidity of Al-montmorillonite is nearly equal to heat-treated H-montmorillonite is transformed to Al-montmorillonite upon heating (Mathers et al, 1954). However, the surface acidity of unheated H-montmorillonite. This is expected since H-montmorillonite is the highest indicating that the hydrogen ion is a source of strong surface acidity. The acid site strength of H-montmorillonite ranged from $H_0 = -3.7$ to $H_0 = 4.6$. Benesi (1957) reported acid strengths with $-H_0$ values up to 8.2.

Davidtz (1976), who studied the dehydration of t-butyl alcohol over H-clays, showed that the activity of H^+-exchanged layer silicates is directly proportional to the tetrahedral exchange capacity. The catalytic inactivity of the octahedral sites was thought to be due to the protonic centres in the octahedral sheet forming an unstable arrangement which is lost during deammoniation.

Solomon (1968) has reported that clays (including montmorillonite) catalyze the polymerization of unsaturated compounds. He found that kaolonite was more active than montmorillonite followed by pyrophyllite. Talc (Mg^{2+} only in octahedral layer) was not active. The results indicated that the presence of aluminium in the octahedral sheet is important and that the crystal edges are involved in the hydrocarbon reactions. Solomon and Rosser (1965) suggested that the catalytic activity was related to aluminium in the octahedral co-ordination at the

crystal edges (mineral acting as a Lewis acid site).

1.2.1.3 NATURAL CLAYS AS CATALYSTS

Clay minerals are known to catalyze numerous organic reactions. Clays were used as petroleum cracking catalysts (Voge, 1958), where reaction temperatures are in the range 673 K - 773 K, and for the isomerization of hydrocarbons.

Acid clays can be used to catalyze reactions such as sucrose inversion, ester hydrolysis (Coleman and McAuliffe, 1954) and ethanol oxidation (Grim, 1968). The dehydration of organic molecules can be catalyzed by a clay surface (Davidtz, 1976). Acid treated clays catalyze alkylation of aromatic rings by alcohols, alkyl chlorides and alkyl ethers (Swartzen-Allen and Matijevic, 1974). Alkylation of aromatics by reaction with olefins is enhanced by acidified clays.

Acid treated clays have the ability to polymerize olefins (Solomon, 1968). The sodium substituted clays were not active with respect to styrene polymerization. However, other work has shown that Cu, Zn, Cd, Al and Co montmorillonite are active for the reaction (Swartzen-Allen, 1974).

1.2.2 SYNTHETIC CLAYS

As discussed in Section 1.2.1, initial catalysts used for the cracking of petroleum feedstocks were made from acid-treated montmorillonites. However, this type of clay contained lattice iron (Fe^{3+}) which was activated by the feed sulphur resulting in the formation of coke

deposits. It was also found that this catalyst was not stable at the higher regeneration temperatures in catalytic cracking (Swift, 1977). Synthetic silica-alumina cracking catalysts were discovered (Ashley and Innes, 1952) that were iron free and more stable at higher regeneration temperatures. They also gave a better product quality than the acid-treated montmorillonite. In the early 1960's zeolite-containing catalysts were developed resulting in an improved activity and selectivity to the desired products. In recent years there has been renewed interest in synthetic clay-like materials for catalytic applications. These synthetic materials are mainly aluminosilicates that are ordered in two dimensions. These clays are thermally very stable and can be synthesized directly in the ammonium form so that one is able to generate the acid form by heating the clay.

This literature review will cover the structure, characterization, acidity and activity for a number of hydrocarbon reactions for the following synthetic clays :

i) Synthetic mica montmorillonite (SMM)
ii) Nickel substituted synthetic mica montmorillonite (NiSMM)
iii) Other metal substituted SMM.

1.2.2.1 SYNTHETIC MICA MONTMORILLONITE

1.2.2.1.1 SYNTHESIS

The synthesis of three-layer clays was first reported in the work by Noll (1930) and Roy (Iiyama and Roy, 1963).

The hydrothermal synthesis of a randomly interstratified layer lattice silicate (SMM) was reported in a publication by Granquist and Pollack (1967). SMM was synthesized from a slurry of diatomite (silica) and bayerite (alumina) in an aqueous solution of NaOH at 573 K. From this mixture the sodium form of SMM was obtained. The synthesis method was improved by Granquist et al (1972) so that the ammonium form was crystallized directly, during which partial F/OH substitution occurred.

1.2.2.1.2 STRUCTURE

SMM is a 2:1 layered aluminium silicate consisting of randomly interstratified expandable and non-expandable dioctahedral layers. Wright et al (1972) showed that the infrared spectra of SMM and the natural clay muscovite are very similar. The small differences were attributed to the lower lattice aluminium content of SMM, the greater (Si, Al) ordering in muscovite, and the higher fluoride/hydroxyl substitution in SMM. The unit cell of SMM may be presented as follows :

$$[(Al_4)^{OCTA}(Si_{8-x}\ Al_x)^{TETRA}\ O_{20}\ (OH,F)_4]^{x-}\ x/n\ M^{n+}$$

where x is the number of tetrahedrally co-ordinated aluminium ions and thus represents the net negative charge on the unit cell. M is the charge-balancing cation(s).

Wright et al (1972) determined the value of the x to be approximately 1.5. Due to the uncertainty regarding the average charge on the charge-balancing hydroxy-aluminium species the cation M^{n+} is represented as :

$$M^{n+} = w\ NH_4^+ + y\ [Al(OH)_{3-z}]^{z+}$$

where the primary charge balancing ion is given as NH_4^+.

The structure of the SMM lamellae is shown in Figure 1.3 and the bonds in the matrix are shown in Figure 1.4. It can be seen that two out of the three octahedral positions are filled and thus SMM is a dioctahedral clay.

Electron microscopy studies (Wright et al, 1972) showed the bulk material to have a platelike structure, having platelets of an average diameter of 1000 A. Based on a BET surface area of 160 m^2g^{-1} and a density of 2.55 $g.cm^{-3}$ (from X-ray unit all measurements), the average number of layers per platelet is calculated to be about 5 giving an approximate platelet thickness of 50 A (as shown in Figure 1.3).

The surface area of SMM was observed to drop from 160 m^2g^{-1} to 135 m^2g^{-1} after activation at 923 K. The loss in surface area was ascribed to increased platelet-to-platelet association (Wright et al, 1972).

Uncalcined SMM had a flouride/silicon ratio of 0.1 and contained 175 meq NH_4^+ / 100 g.

1.2.2.1.3 CATALYST CHARACTERIZATION

The methods used to characterize SMM included thermal analysis, application of non-aqueous indicators (Fletcher, 1984); X-ray diffraction (Wright et al, 1972; and nitrogen adsorption (surface area). Fletcher (1984), who performed a thermal analysis on SMM showed that the structure of the clay was stable up to 1200 K. Physisorbed water which accounted for 7.5 % of the mass of the catalyst was completely desorbed by 423 K. Deammoniation and dehydroxylation which resulted in a further 8 % mass loss was complete by 1000 K. Wright et al, (1972) suggested

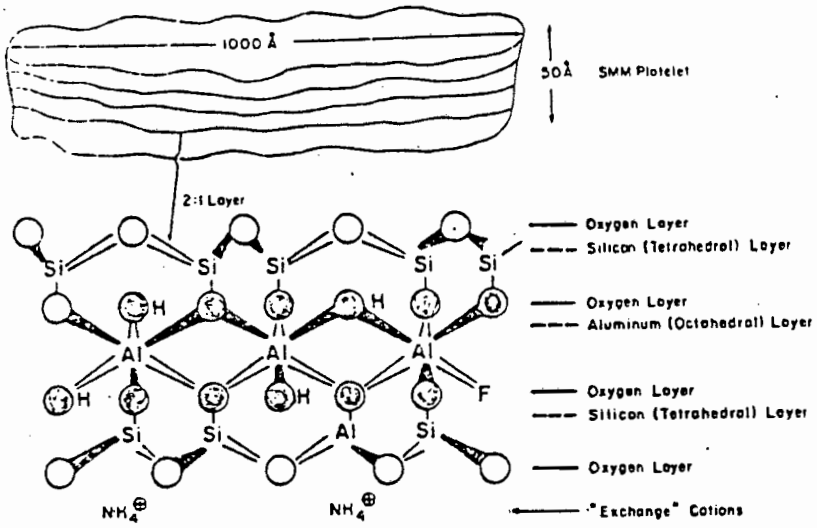

Figure 1.3 Structure of SMM lamella (Swift,1977)

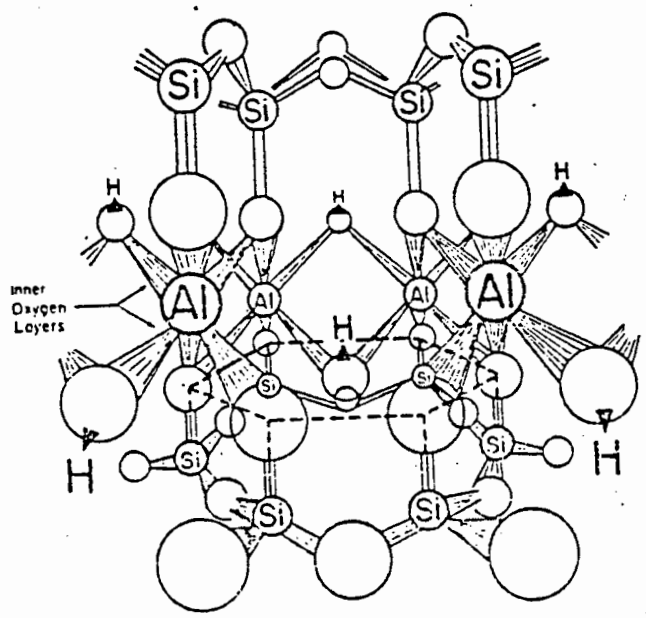

Figure 1.4 Connection of dioctahedral layer to tetrahedral layer in SMM (Swift,1977)

that the presence of ammonium, as opposed to other cations, promoted the dehyroxylation of the catalyst.

The acid strength of SMM after dry calcination between 773 and 923 K was reported to lie between an H_0 value of -5.6 and -8.2. Rehydration at room temperature decreased the acid strength to between -5.6 and -2.4, and rehydration at 923 K to between -2.4 and +1.5. (Fletcher, 1984).

X-ray diffraction studies of SMM (Wright et al, 1972) gave a non-integral ØØl sequence and irregularly shaped peaks which were indicative of mixed layering. Wright et al (1972) found basal spacings of 1Ø.4 A and 12.5 A to occur in the proportion 2:1. Upon hydration the 1Ø.4 A spacing persisted at 1ØØ % humidity (mica-like nature), whilst the 12.5 A spacings swelled to 17.3 A upon the addition of ethylene glycol and collapsed to 1Ø.8 A in dry air exhibiting montmorillonite behaviour. Calcining SMM at 923 K caused an irreversible collapse of basal spacing to 9.4 A indicating that the platelet edges and faces were of catalytic importance. These results were confirmed by Fletcher (1984) who reported an average $d_{ØØl}$ interlayer spacing of 11.Ø8 A which collapsed to 9.7 A upon calcination at 773 K.

Fletcher (1984) reported that the catalyst contained slit-shaped pores and that after activation at 773 K the interlayer spaces were not accessible to nitrogen. The 'external' surface area of the activated SMM was calculated to be 114 m^2g^{-1}. This value was lower than the 135 m^2g^{-1} reported by Wright et al (1972) after activation at 923 K.

1.2.2.1.4 ACTIVATED SMM STRUCTURE

Wright et al (1972) showed that deammoniation and dehydroxylation occurred simultaneously although final deammoniation preceded dehydroxylation. A similar result was obtained by Fletcher (1984) who found that these reactions were complete by 1000 K.

Granquist and Kennedy (1967) demonstrated that SMM sorbed about 1% water at 763 K and 24 torr water vapour pressure, and that lattice fluoride appeared to be responsible for much of this uptake. The sorption was found to regenerate partially the structural hydroxyls.

The structure of dehydroxylated clay minerals is a subject of controversy (Grim, 1968). SMM, as stated earlier, is very similar to muscovite. The structure of muscovite has been investigated by Vedder and Wilkins (1963) and Eberhart (1963). Wright et al (1972) suggested a configuration which caused minimum disruption of the unit cell since the infrared spectra of SMM and muscovite change slightly upon activation. The overall equilibrium process was represented as :

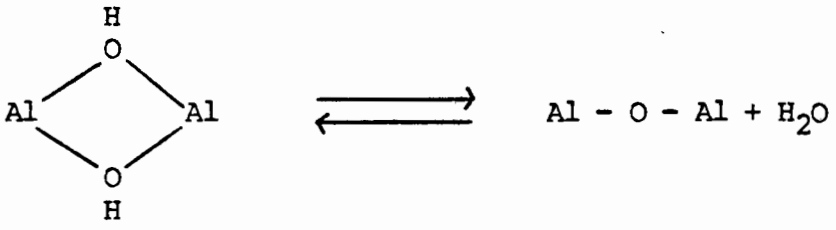

OCTAHEDRALLY CO-ORDINATED Al 5 - CO-ORDINATED Al

Wright et al (1972) suggested that the protons resulting from deammoniation enter sites within the lattice. Some of the protons may be lost according to

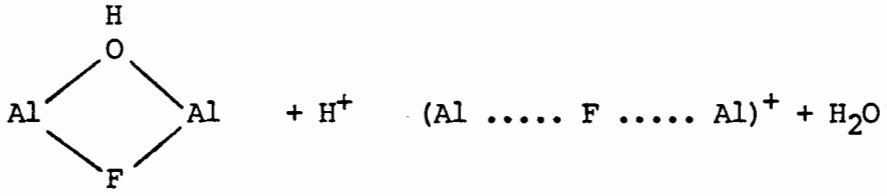

where $(Al \ldots\ldots F \ldots\ldots Al)^+$ assumes the charge balancing role. The remaining protons were eventually lost since the OH bands in the infrared (3670 cm^{-1}) were absent after 24 h evacuation at 923 K. The protons could react with the tetrahedral aluminosilicate lattice by a mechanism similar to that proposed by Uytterhoeven et al (1965) :

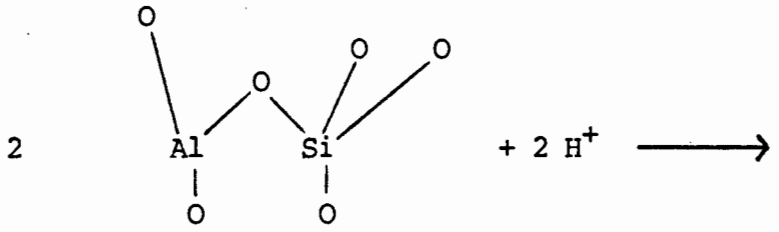

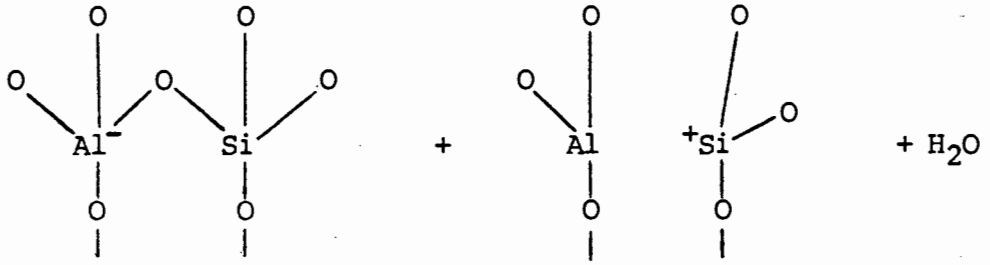

Russel and White (1966) reported that upon deammoniation and dehydroxylation a band at 3470 cm^{-1} of the infrared developed. This observation was in agreement with that of Wright et al (1972) who found that the 3470 cm^{-1} band to be stronger in fluoride-free SMM at high temperatures. Fletcher (1984) reported that a band at 3460 cm^{-1} grew in intensity and then started to drop at about 500 K. The above workers believe the 3470 cm^{-1} band to be a result of an interaction between the

protons from deammoniation and the oxygen of the structural hydroxyl. Russel and White (1966) referred to this species as a proton perturbed lattice hydroxyl group. The electron withdrawing proton near the oxygen of the hydroxyl group weakened the O-H band and therefore lowered its frequency. The addition of ammonia caused the disappearance of the 3470 cm^{-1} band thereby confirming the above proposal. The postulate made by the above workers is that the protons drop into the empty tetrahedra adjacent to the (OH, OH) or (OH,F) pairs in the octahedral layer. Wright et al (1972) suggested that the dehydroxylation of the dioctahedral is proton-catalyzed.

1.2.2.1.5 ACIDITY OF SMM

The nature of acid sites present on SMM were investigated by solid state infrared studies (Fletcher, 1984; Wright et al, 1972) and temperature programmed desorption studies (Fletcher, 1984) using pyridine as the probe molecule.

Wright et al (1972) reported values of 2.5 meq Bronsted and 1.5 meq Lewis-bound pyridine per 100 g of calcined NH_4^+-SMM giving a total acidity of 4 meq per 100 g. Fletcher (1984) found that the amount of Bronsted acidity decreased as the calcination temperature increased. At a calcination temperature of 770 K there was no longer evidence of Bronsted acidity.

Upon addition of water to dehydroxylated SMM, Lewis sites were observed to convert to Bronsted sites. Quantitative measurements suggested a reversible one to one interconversion of these acid sites. Using the integrated absorbance coefficients of Hughes and White (1967), Fletcher

(1984) computed the number of Lewis sites per gram of SMM after calcination at 773 K to be 2.4 x10^{19} sites g^{-1}. This was the exact value obtained by Wright et al (1972). The findings of the pyridine desorption infrared runs indicated that Lewis sites hold pyridine to higher temperatures than Bronsted sites. Fletcher (1984) found that calcination at 923 K resulted in the generation of only Lewis acid sites which existed at particle edges and faces. Wright et al (1972) attributed the Lewis acidity to trigonal aluminium at the edge of the tetrahedral layers. The actual amount of Lewis acidity versus the theoretical amount (approximately 20 meq / 100 g) indicated that only a fraction of the aluminium ions have trigonal configuration. The conversion of Lewis to Bronsted acidity by the addition of water is represented as :

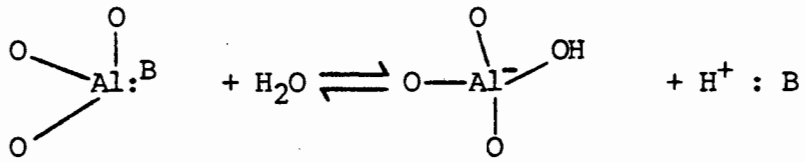

where B is a base.

The density of acidic sites as measured by pyridine adsorption, 2.4 x 10^{19} g^{-1}, is low compared to the site density of 32 x 10^{19} g^{-1} reported for the faujasites (Hughes and White, 1967).

Temperature programmed desorption (TPD) experiments were carried out to investigate the acid strength and distribution on SMM (Fletcher, 1984). At a low calcination temperature of 521 K the acidity was mainly due to polarized water and ammonium ions. As the calcination temperature was increased there was a shift to a higher peak desorption temperature. The effect of the calcination medium (air, hydrogen, nitrogen) was shown

to be negligible in the TPD spectrum. An interesting feature of the TPD results was that the amount of adsorbed pyridine increased by an order of magnitude upon exposing SMM to water. This did not occur when the water was evacuated at 426 K. This increase is attributed to the polarized physisorbed water holding the pyridine. The above worker also found that the lattice charge played a crucial role in retaining pyridine.

The TPD peak resulting from calcination at 923 K yielded a Lewis acid site concentration of 1.7 x $1Ø^{19}$ sites g^{-1}. This compared well with the equivalent value of 1.8 x $1Ø^{19}$ sites g^{-1} determined in the IR studies (Fletcher, 1984).

1.2.2.1.6 CATALYTIC ACTIVITY OF SMM

Although SMM has a much lower acid site density than zeolitic catalysts, it has comparable catalytic activity. A possible explanation is that because of the platelike nature of SMM, the measured acidity is representative of accessible acidity, whereas due to diffusional limitations, only a fraction of the measured acidity of the zeolites is actually catalytically active under dynamic conditions (Thomas and Brarmby, 1968).

The catalytic activity of SMM for cracking was first reported by Capell and Granquist (1966). The catalyst had an exchange capacity of 1.97 meq / g and was converted to its active form by exchanging with ammonium ions followed by deammoniation at 773 K. The catalytic activity of the catalyst, which had a surface area of 115 m^2g^{-1}, was compared to that of

an alumina synthetic cracking catalyst, a sulphur-resistant natural halloysite cracking catalyst and a steam -H_2S treated fresh commercial halloysite catalyst. SMM was observed to be twice as active as the sulphur resistant natural clay and 1.5 times more active than the synthetic alumina catalyst. It was also shown that SMM had a better product selectivity. Workers at the Baroid Division of N.L. Industries compared the cracking activity of SMM with three commercially available zeolitic catalysts (Swift, 1972). Their results showed that SMM had similar activity to the zeolitic cracking catalysts.

Hoffman and Granquist (1974) found that by coating kaolinite particles with a layer of SMM a catalyst with high cracking activity and improved mechanical strength resulted. Hattori et al (1973) investigated the isomerization of hydrocarbons over SMM. They reported that with silica alumina, the H^+ ions do not undergo easy exchange with hydrocarbon molecules during isomerization, whereas with SMM there was a high degree of exchange. The high cracking activity was due to this 'exchangeability'.

SMM as a support for hydrogenation metals has been patented by many workers (Csiesery and Kittrell, 1972; Jaffe and Kittrell, 1972; Kittrell et al, 1972; Malasky, 1972).

Csiesery and Kittrell (1972) showed that the introduction of low concentrations of other metal ions (Mn, Cr, Fe, Co) into the SMM lattice affected its catalytic performance for hydrocracking. The addition of Ø.5 wt % Fe on PdSMM resulted in a dramatic decrease in the deactivation rate of the catalyst.

1.2.2.2 NICKEL AND OTHER METAL SUBSTITUTED SMM

The charge requirement of SMM may also be met by six divalent ions such as Ni^{2+}, Zn^{2+}, Co^{2+} and Mg^{2+}. Because of their size and charge, these ions are able to substitute for Al^{3+} causing, in certain cases, all the octahedral positions to be filled resulting in a trioctahedral clay. A mixed dioctahedral-trioctahedral clay may be formed which is directly related to the concentration of the divalent ions in the synthesis clay material.

The synthesis of metal substituted SMM is similar to that of SMM with the exception that the reaction mixture of the hydrothermal synthesis includes a source of the divalent cation(s). In the case of NiSMM, nickel acetate, nickel fluoride and nickel nitrate are suitable salts to use. The preparation and characterization of these metal-substituted 2:1 layer lattice aluminosilicates has been described by Granquist (1976) and Black et al (1976). A simplified formula for these synthetic materials is :

$$[(GY)^{OCTA}\ (QR)^{TETRA}\ O\ (OH,F)]^{-}[M^{+}] \cdot H_2O$$

where G is a trivalent ion with a maximum ionic radius of Ø.75 A (Al); Y is a divalent ion with a maximum radius of Ø.75 A (Ni, Co, Zn, Cu); Q is a tetravalent ion such as Si and R is a trivalent ion with a radius less than Ø.64 A (Al). M^{+} is the exchangeable ion. In most cases, a hydrogenation component such as platinum or palladium was deposited on the clay after synthesis.

1.2.2.2.1 STRUCTURE AND CHARACTERIZATION

The structure of NiSMM is similar to that of SMM except that Ni now substitutes for the aluminium in the octahedral layer. NiSMM clays readily crystallize, for varying amounts of nickel added, to form a trioctahedral silicate that may or may not contain aluminium. Therefore, a mixed dioctahedral-trioctahedral phase will be formed from mixtures of NiO, Al_2O_3 and SiO_2 that contain less than the required amount of nickel for 6 nickel atoms per unit cell (Granquist, 1976). Black et al (1976) found this maximum weight percentage nickel that could be incorporated in SMM to be 36 %. Swift (1977) observed that formation of the mixed phases by X-ray diffraction, where the trioctahedral (Ø6) reflection (>1.5 A) increased while the dioctahedral (Ø6) reflection (<1.5 A) decreased with increasing nickel atoms / unit cell. Black et al (1976) developed a linear correlation relating the intensity of the trioctahedral reflection and the average nickel per unit cell.

X-ray diffraction was used by the above workers to characterize NiSMM with varying nickel atoms / unit cell. Basal spacings were observed to vary between 1Ø and 13.5 A. Generally, as the Ni atoms / unit cell increased the interlayer spacing increased. A basal spacing of 11.32 A was reported for NiSMM containing 1 Ni atom / unit cell (Black et al, 1976).

The TG-DTA curve was similar to SMM (Fletcher, 1984) except that the DTA of the NiSMM sample exhibited a sharp endothermic peak at 121Ø K which may be due to crystallization of the mineral (Wright et al, 1972).

Swift and Black (1974) reported that the incorporation of nickel into the SMM lattice via synthesis resulted in a significant increase in the stable surface area. The results of this study is shown in Table 1.3.

CATALYST*	NICKEL CONTENT (WT%)	APPROX. Ni ATOMS / UNIT CELL	SURFACE AREA ($m^2.g^{-1}$)
A	Ø	Ø	145
B	6.75	1	199
C	14.3	2	23Ø
E	21.6	3	3Ø2
F	26.4	4	254
G	3Ø.5	5	258
H	35.7	6	332
I	15.Ø	-	94

TABLE 1.3 : EFFECT OF NICKEL INCORPORATION

* CALCINATION TEMPERATURE = 81Ø K

A loss in surface area is observed in catalyst I (made by impregnating catalyst A (SMM) with nickel nitrate). Swift (1977) stated that the surface area decreased as Zn is included in the matrix, although a more crystalline structure is formed.

1.2.2.2.2 NICKEL REDUCIBILITY AND ITS EFFECT ON ACIDITY

Nickel substituted mica montmorillonite (NiSMM) has been shown to be highly active for a number of hydrocarbon reactions including

hydroisomerization and hydrocracking (Swift and Black, 1974; Black et al, 1976). The origin of the high activities found for NiSMM catalysts, especially the reduced form, is not fully understood.

Robschlager et al (1984) compared the Bronsted acid site distribution of unreduced NiSMM and beidillite (SMM) and found that there was no significant difference in the acid site strength. The activity of beidillite and unreduced NiSMM was shown to be similar for n-pentane hydroisomerization.

It has been reported that upon the reduction of NiSMM in flowing hydrogen at elevated temperatures, a highly active catalyst for hydroisomerization and hydrocracking is formed (Heinerman et al, 1983; Robschlager et al, 1984). During the reduction process, the Ni^{2+} ion in the octahedral layer is converted to its metallic form. Swift (1977) postulates that the metallic nickel atoms formed are expelled from the lattice due to ionic radius expansion, i.e. Ni^{2+} (radius = Ø.69 A) is reduced to metallic nickel of radius 1.25 A. The metallic nickel atoms combine on the surface of the catalyst to form nickel crystallites of varying diameters. Swift (1977) stated that the rate of nickel reduction does not become appreciable until 698 K. Heinerman et al (1983) investigated the reduction of NiSMM using temperature programmed reduction (TPR) and found that the initial nickel crystallites were formed at a reduction temperature of 723 K.
Introducing Pt or Pd lowered this temperature to about 653 K. Robschlager et al (1984) observed the reduction of Pd NiSMM to start between 473 K and 573 K. The lower reduction temperature for Pt or Pd impregnated NiSMM is expected since Pt and Pd are known to catalyze the

reduction of nickel (Swift and Black, 1974). Heinerman et al (1983) found that the degree of reduction increased with increasing reduction temperature. At 723 K after reduction for 16 h, 7.9 % of the nickel present in NiSMM (21 wt% Ni) was reduced. This percentage increased to over 20 % at 753 K. TEM results showed that after reduction at 713 K for 16 h, Ni crystallites of sizes from 5 to 15 nm were formed (Robschlager et al, 1984). Swift (1977) observed that after 1/3 of the nickel of a 15 % NiSMM sample was reduced nickel crystallite growth (agglomeration) occurred.

The basic NiSMM structure remained unaffected when samples contained an appreciable amount of octahedral aluminium. However, Heinerman et al (1983) found that upon the reduction of 22 % Pd-NiSMM (3 Ni/unit cell), the structure was partly destroyed. Swift (1977) and Robschlager et al (1984) suggested that the reoxidation of the reduced clay would not lead to the complete reincorporation of the nickel.

Heinerman et al (1983) investigated the acidic sites of NiSMM by infra-red analysis, using NH_3 as a probe. These workers found that upon the reduction of NiSMM (20 wt% Ni) the number of Bronsted sites increased four times while the Lewis sites decreased by a quarter. This was confirmed by Robschlager et al (1984) who studied the thermal desorption of pyridine from Pd-NiSMM. Their results showed a five-fold increase in the Bronsted acidity. The Lewis sites did not vary much. The results obtained by the above workers suggest that the newly formed acidic sites were responsible for the increased acidity of NiSMM compared with SMM. The reduction process may be presented as :

$$Ni^{2+} + H_2 \longrightarrow \underset{\text{Metallic Nickel}}{Ni^{o}} + \underset{\text{Bronsted Site}}{2H^{+}}$$

The desorption experiments showed that the new Bronsted sites are strongly acidic, since most pyridine desorbed at higher temperatures than acid sites formed after calcination. It is known that the relative amounts of Bronsted and Lewis sites depend strongly on the amount of water in the system (Wright et al, 1972; Fletcher, 1984). However, the reduction of NiSMM in different hydration states still caused a marked increase in the total number of acid sites. Heinerman et al (1983) estimated that the total number of sites were doubled by the reduction treatment.

The Lewis and Bronsted acidity of Pd-SMM did not change during reduction indicating that the water formed during Pd reduction did not affect the balance between Lewis and Bronsted sites and no new Bronsted sites were formed. Robschlager et al (1984) suggested that Pd is already metallic after calcination and was no longer located in exchange positions.

1.2.2.2.3 CATALYTIC ACTIVITY OF NiSMM

NiSMM and CoSMM have been reported to catalyze hydrocarbon reactions including hydroisomerization and hydrocracking (Swift and Black, 1974), oligomerization of olefins (Bercik et al, 1978) and hydrotreating (Swift and Vogel, 1979).

Swift and Black (1974) evaluated hexane hydroisomerization activity of Pd-SMM, Pd-NiSMM (with varying nickel loadings) and Pd-H-mordenite. The

catalysts were reduced at 623 K. Pd-NiSMM catalyst was observed to be 20 times more active than Pd-SMM and approximately 1.7 times more active than Pd-H-mordenite demonstrating the importance of nickel incorporation in the SMM structure. The maximum activity was obtained using a catalyst containing 5 Ni atoms / unit cell. Robschlager et al (1984) and Heinerman et al (1983) provided evidence that hydroisomerization may be described by a dual function mechanism in which the metal sites (nickel and/or palladium) are responsible for (de)hydrogenation and acid sites for the isomerization of the hydrocarbon.

Black et al (1976) reported that, for hydrocracking of hexane and raffinate, presulphiding the catalyst improved its activity and selectivity. Pd-NiSMM with 2 Ni atoms per unit cell gave the most promising results yielding LPG with a minimum amount of undesired products. Black and Swift (1974) studied the effect of cobalt and zinc in the SMM lattice. They found that there was an increase in hexane hydroisomerization activity with increasing cobalt content. However, the increase in activity was not as marked as the catalyst with a corresponding amount of nickel. ZnSMM exhibited low activities for hydrocracking.

1.2.2.2.4 PILLARED NiSMM

Swelling clays can be crosslinked with inorganic metal hydroxide oligomers to yield a stable pillared clay with similar properties to zeolites (Endo et al, 1981). Gaaf et al (1983) have reported the application of this technique to NiSMM. Crosslinking of a swellable NiSMM clay with a solution of hydroxy-alumina oligomer in water results in an expanded lattice accompanied by catalytically more active

catalyst. The BET surface area of the clay investigated increased from 170 to 230 m^2g^{-1}.

1.2.3 SMM AND NiSMM AS OLIGOMERIZING CATALYSTS

Fletcher (1984) investigated the activity of SMM for the oligomerization reaction. He studied the effect of varying calcination and reaction conditions on the oligomerization of propene over SMM in a fixed bed reactor at 61 atm and WHSV = 1.5. He reported that the presence of Lewis acid sites gave high activity and long catalyst lifetime. The catalyst deactivated rapidly in the presence of water and this observation was attributed to the conversion of Lewis to more active Bronsted sites. Calcining at low temperatures (520 K), which caused the formation of mainly Bronsted sites, resulted in poor catalyst lifetime. The sites formed by polarized water were shown to be inactive for propene oligomerization. The optimal condition for propene oligomerization was a calcination temperature of ca 770 K and a reaction temperature of 420 - 460 K. Approximately 55 vol % of the liquid product boiled above 453 K (diesel fraction).

Bercik et al (1978) showed that NiSMM is an active catalyst for oligomerizing C_3 - C_4 olefins. The reaction conditions were similar to that of the above worker. It was found that with proper sulphiding of the catalyst, product quality could be improved and a sulphur-containing feed could be used without affecting the catalyst lifetime. The sulphided NiSMM was very active for propene oligomerization yielding dimer and trimer product with a research octane number (RON) of 98. The yield of gasoline, kerosine and heavier products could be controlled by the degree of sulphiding of the catalyst. A feed containing 39 wt %

propene oligomerized over NiSMM (13.8 % Ni, 3.6 % F) at 433 K, 6.1 MPa and LHSV of 0.98 resulted in 80 % propene conversion for 10 days. Of the oligomer product, 50 % vol % boiled above 453 K. The hydrogenated liquid product could be suitable for inclusion in diesel fuel.

1.3 OBJECTIVES OF THE RESEARCH

The present research investigated the effect of nickel in synthetic mica montmorillonite (SMM) on the oligomerization of propene. The activity, selectivity and lifetime of the catalyst were monitored. Nickel can be incorporated into SMM by direct substitution for Al^{3+} in the octahedral layer during synthesis or by ion-exchanging for NH_4^+ ions in the interlayer spaces of SMM (NiIXSMM). Reduced NiSMM has been shown to be a highly active catalyst (Black et al, 1974) and the effect of nickel reduction on the catalysts was therefore studied. An attempt was made to establish the significance of the metallic sites formed after reduction. The elements Co and Zn were also exchanged into SMM and studied using the above reaction.

In order to gain some understanding of the coke deposits on SMM and NiSMM, thermogravimetric studies were performed.

The liquid product was analyzed using gas chromatography, mass spectroscopy, nuclear magnetic resonance and ASTM fuel tests.

2. MECHANISM AND THERMODYNAMICS OF POLYMERIZATION

2.1 MECHANISM OF POLYMERIZATION

Catalytic polymerization reactions are classified as following either free-radical or ionic mechanisms. Ionic mechanisms are further subdivided into cationic or anionic polymerization (Oblad et al, 1958).

Examples of catalysts, co-catalysts and the idealized Bronsted acid formed for cationic polymerization are :

Catalyst	:	$AlCl_3$	SiO_2-Al_2O_3
Co-catalyst	:	HCl	H_2O
Idealized Bronsted acid	:	$H^+(AlCl_4^-)$	$H^+(Al(-O-Si)_4)$

All of the above catalysts can generate carbonium ions in alkenes by adding the proton from the acid to the extra electron pair in the double bond (pi electrons). Alkenes may undergo different types of polymerization :

1. true polymerization;
2. conjunct polymerization; and
3. co-polymerization.

In true polymerization, the products consist of alkenes having molecular weights which are integral multiples of the monomer alkene, i.e.

$$xC_nH_{2n} \longrightarrow C_{xn}H_{2xn}$$

The second type, conjunct polymerization, yields a complex mixture of alkanes, alkenes, alkadienes, cyclo-alkenes and alkanes, and aromatics with the number of carbons not corresponding to integral multiples of

the monomer. Interpolymerization of two different alkenes is termed co-polymerization.

The term oligomerization will be used in this report to include the overall processes discussed above, occurring during the reaction of olefins over acid catalysts. This is largely true polymerization with some conjunct polymerization (also depends on reaction conditions).

2.1.1 TRUE POLYMERIZATION

The carbonium ion mechanism, which follows the rules stated below, is the most widely accepted mechanism of polymerization (Oblad et al, 1958). This mechanism incorporates the following steps :

i) The formation of an electron deficient carbon according to Markovnikoff's rule, i.e. the proton is added to the carbon atom holding the greatest number of hydrogen atoms.

ii) The isomerization of carbonium ions to a stable form.

iii) The allowance for absence of products where such products of reaction are prevented by steric hindrance.

2.1.2 CONJUNCT POLYMERIZATION

The extent to which conjunct polymerization takes place depends largely on the catalyst in use and the reaction conditions. It may result in the formation of saturates :

$$R\text{-}CH_2\text{-}CH{=}CH\text{-}R^1 + H^+ \rightleftharpoons RCH_2\text{-}C^+H\text{-}CH_2R^1$$

$$RCH_2\text{-}C^+H\text{-}CH_2R^1 + RCH_2\text{-}CH{=}CHR^1 \rightleftharpoons \underset{\text{(SATURATE)}}{RCH_2\text{-}CH_2\text{-}CH_2R^1} + RC^+H\text{-}CH{=}CH\ R^1$$

For conjunct polymerization the significant reactions are (Oblad et al, 1958).

1. Initiation by proton addition
2. Propogation by olefin addition
3. Chain termination by proton expulsion
4. Chain termination by proton transfer
5. Chain termination by addition of hydride ion
6. Depolymerization to same or other chain length than that of original olefin.
7. Isomerization
8. Hydrogen exchange
9. Cyclization, equivalent to self-alkylation or self-polymerization
10. Loss of hydride ion

2.1.3 PROPENE OLIGOMERIZATION

Solid phosphoric acid is the most widely used catalyst for propene oligomerization. In this process, known as the CATPOLY process, trimerization occurs more readily than dimerization. A liquid product consisting of about 50% nonenes, 25% dodecenes and less than 5% hexenes was formed in the presence of solid phosphoric acid at 433 K and 1 MPa (Schmerling and Ipatieff, 1950). The reason for the low yield of dimer can be explained in terms of the relative stability of the propene dimer and monomer carbonium ions. The dimer can generate a tertiary carbonium ion which is more stable, and will thus exist for a longer time before expelling a proton, than the secondary carbonium ion of the monomer. Therefore it is more probable that the dimer will add to another monomer than that the monomer will dimerize.

The mechanism for propene oligomerization is shown below :

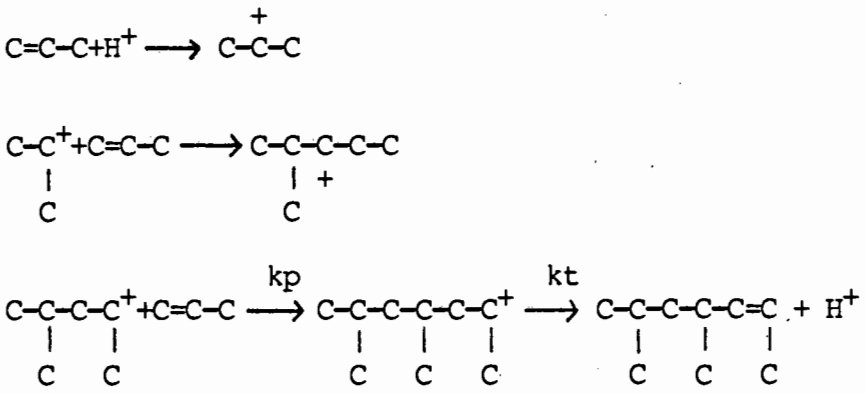

where kp = rate of further alkene addition (polymerization)

kt = rate of proton expulsion to form an alkene (termination)

According to Germain (1969) the dimer should have the following structure :

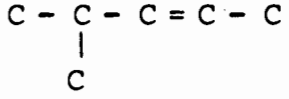

However, skeletal isomers will be present under most reaction conditions (Schmerling and Ipatieff, 1950) and thus the following possibilities exist for the hydrogenated dimer of propene :

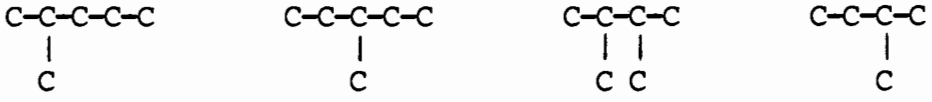

The individual reaction steps for polymerization is presented by Flory (1964) :

Let M represent the monomer, A the catalyst, SH the co-catalyst and A.SH the catalyst / co-catalyst complex.

$$A.SH + M \longrightarrow HM^+ + AS^-$$

$$M_x^+ + AS^- + M \xrightarrow{kp} M^+_{x+1} + AS^-$$

$$M_x^+ + AS^- \xrightarrow{kt} M_x + A.SH$$

$$M_x^+ + AS^- + M \xrightarrow{ktr} M_x + HM^+ + AS^-$$

where ktr is the rate of carbonium ion transfer.

It is further shown (Flory, 1969) that the average degree of polymerization is given by :

i) $X_n = (kp/kt)\ [M]$ if chain termination dominates over chain transfer

ii) $X_n = kp/ktr$ if chain transfer dominates over termination

The carbonium ion mechanism does not hold for all acid catalysts. Hassan et al (1977) found that the primary product, 3-methylpentene, of propene dimerization over zeolite catalysts could not be explained by a carbonium ion mechanism. Examination of the results suggested that a mechanism of dimerization similar to that proposed by Imai et al (1968) occurred. This mechanism assumes the formation of an intermediate of a cyclobutane derivative. The compounds are formed when a propene molecule reacts with an adsorbed one of the zeolite surface as follows :

$$2CH_3 - CH = CH_2 \rightleftharpoons$$

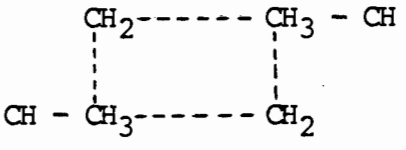

(I)

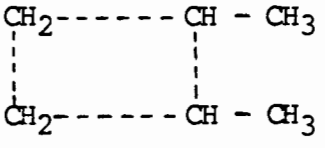

(II)

The dimethyl cyclobutanes, I and II, formed are unstable complexes and are either converted to the initial molecules or undergo a bond rupture. The bond rupture of the two complexes leads to the formation of extremely unstable complexes which undergo rearrangement and hydrogen redistribution. The rearranged structure desorbs as a propene dimer. If the rate of desorption is relatively slow, the formed dimer can adsorb another propene molecule forming a similar unstable complex which again is converted either to the initial state or undergoes bond rupture and hydrogen redistribution to form propene trimers. Similarly if trimers are not rapidly desorbed they can adsorb another propene molecule forming, in the same manner, tetramers.

2.2 THERMODYNAMICS OF POLYMERIZATION

Oblad, Mills and Heinemann (1958) have considered the thermodynamics of the oligomerization of olefinic hydrocarbons. Their study, however, has been made on the basis of theoretical reactions of gaseous mono-olefins oligomerizing to give gaseous olefins of higher molecular weight, and therefore, the study does not account for such factors as deviation of gases from ideality and phase changes occurring at certain reaction conditions.

A plot of the free energy change for the dimerization reaction versus temperature given by Figure 2.1 shows that generally low temperatures favour polymerization (Oblad et al, 1958).

It can also be seen that at any given temperature the dimerization of ethylene to 1-butene is more favoured than that of other light olefins which have similar free energy changes for dimerization.

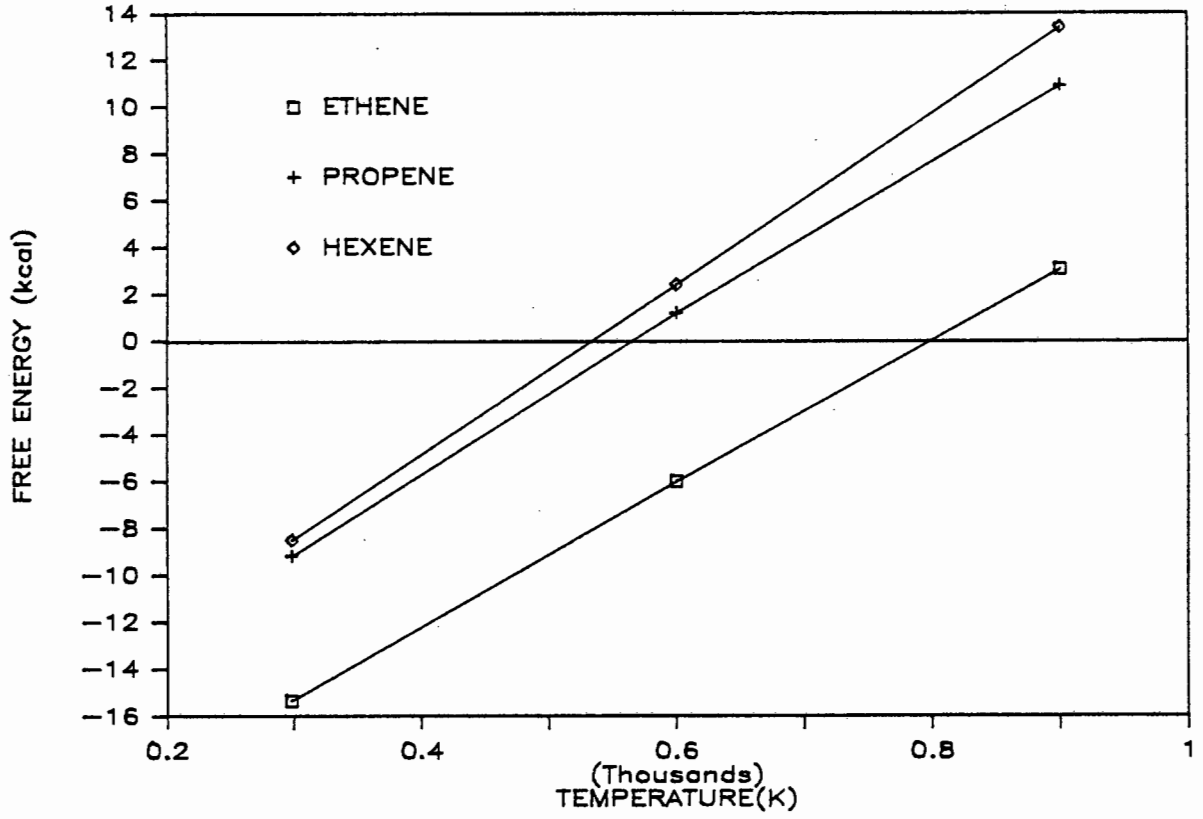

Figure 2.1 Dimerization of light olefins

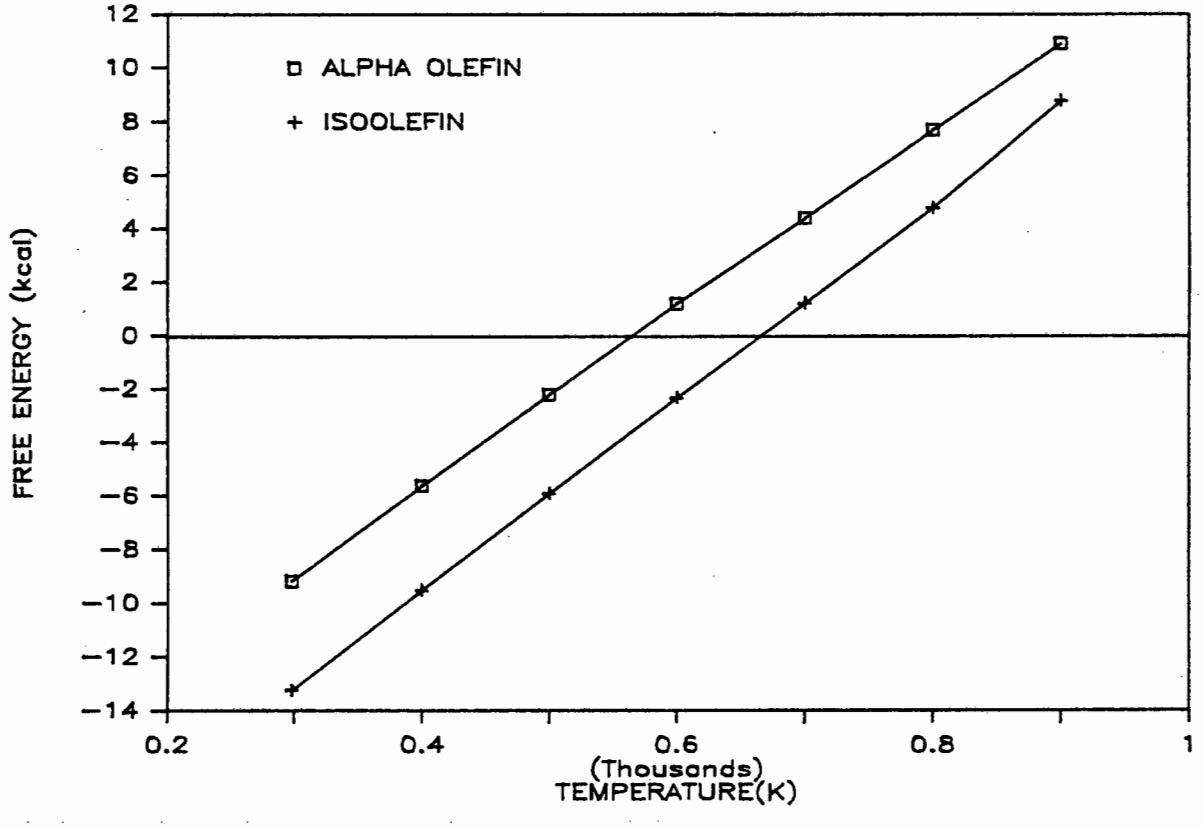

Figure 2.2 Polymerization of propene into isomers

From Figure 2.2, it can be seen that the dimerization of terminal bond olefins to isomers of the corresponding higher olefins at a given temperature is more favourable than the dimerization to the higher terminal olefins. Hence the equilibrium conversion of an alpha olefin to a higher alpha olefin will always be less than the corresponding conversion of an alpha olefin to an isoolefin. The dimerization of beta olefins or isoolefins to the corresponding higher olefins will be similar to the alpha olefin - alpha dimer relationships. However, the dimerization of beta olefins or isoolefins to higher alpha olefins will always be the least favourable reaction (Oblad et al, 1958).

The effect of pressure and temperature on the equilibrium position of the dimerization reaction :

$$2C_3^{=} \longrightarrow \text{1-hexene}$$

is shown in Figure 2.3 (Oblad et al, 1958). It is clear that the oligomerization reaction is favoured by low temperatures and high pressures.

Figure 2.4 shows that the free energy change for the formation of higher polymers as a function of temperature for propene. It can be seen that at temperatures above 550 K the reverse reaction, i.e. cracking, occurs. Also illustrated in this graph is the fact that at higher temperatures lower oligomers will predominate, whereas at low temperatures the higher polymers will predominate at equilibrium.

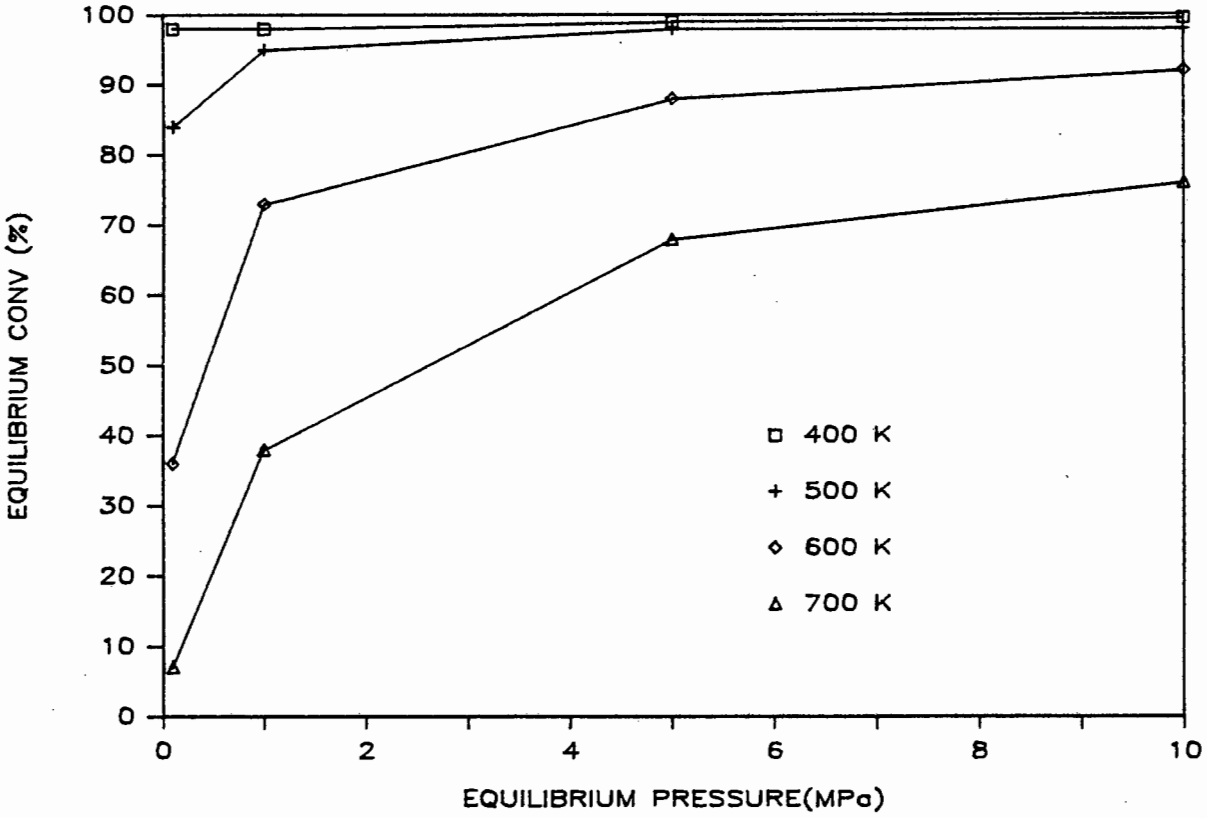

Figure 2.3 Effect of pressure and temperature

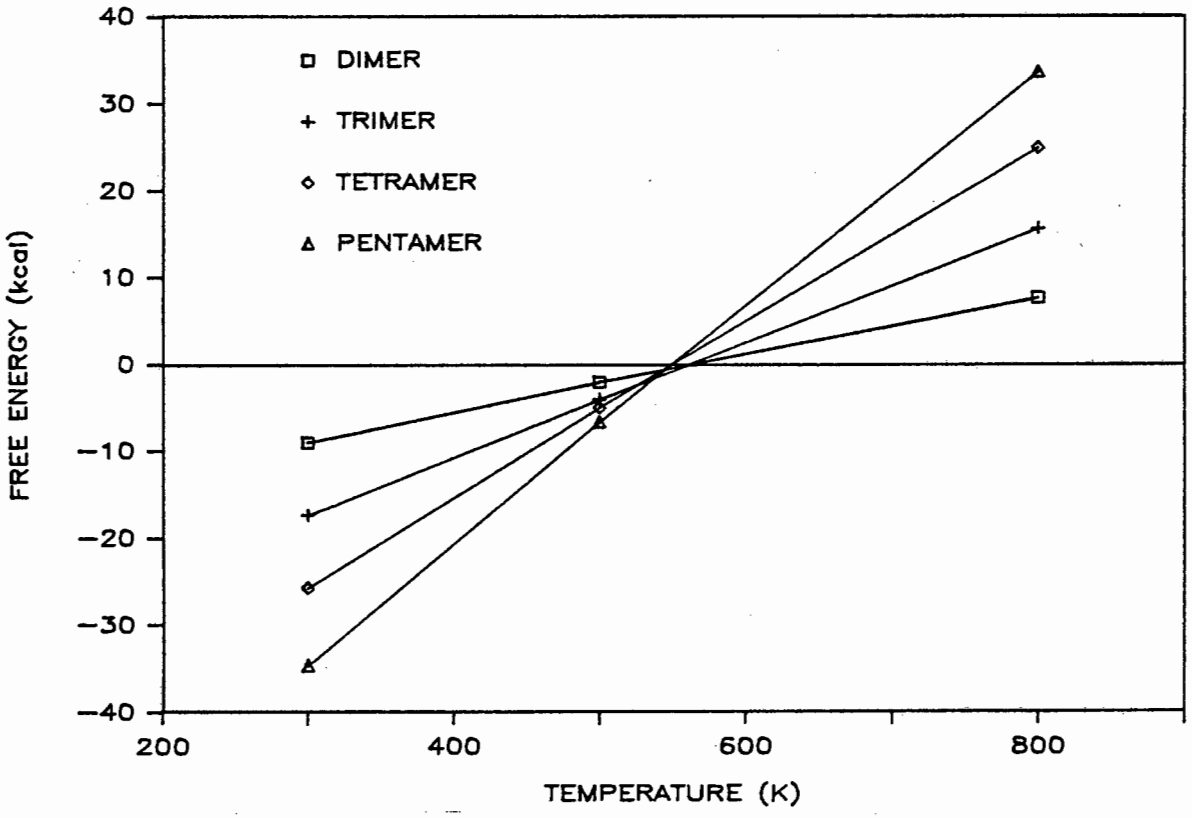

Figure 2.4 Polymerization into higher olefins of propene

3. EXPERIMENTAL METHODS

3.1 CATALYST PREPARATION

3.1.1 CATALYSTS

The catalysts (7% NiSMM and SMM) used in this work were supplied by the Filtrol Corporation (USA). Both catalysts were in their ammonium form and were obtained as powder (< 500 micron). All catalyst samples were washed in deionized water, filtered and oven-dried at 80°C overnight.

3.1.2 PREPARATION OF NICKEL ION-EXCHANGED SMM

3.1.2.1 Ion-exchange procedure

NH_4^+-SMM (<0.25mm) was ion-exchanged in aqueous nickel nitrate solutions in a well mixed glass reactor flask (Gallezot and Imelik, 1973; Elliot and Lunsford, 1979). The effects of time length of mixing, initial concentration of the solution, exchange in a heated, open and closed system, and repeated exchange using fresh solution were studied.

Large volumes of diluted solution (<0.05N) were used to avoid any pH increase due to partial hydrolysis and precipitation of nickel salts. Thus the pH of the system was monitored during the ion exchange treatment. Other exchange ions, viz., cobalt and zinc were introduced into SMM in a similar manner.

3.1.2.2 Atomic absorption spectroscopy

The nickel content of the washed and dried samples was determined by AA spectroscopy. The catalyst samples were dissolved in hydrofluoric acid as follows :

i) 5 ml of HF (38%) was added to Ø.25 g of catalyst.

ii) 5 ml of concentrated sulphuric acid was added tothe HF-catalyst mixture.

iii) The solution was heated for 45 minutes at 363 K.

iv) If the catalyst was not completely dissolved, another 5 ml of HF plus 2Ø ml of deionized water was added and the solution was further heated at 363 K for 1 h.

v) The solution was then cooled and diluted to 25Ø ml in a plastic volumetric flask.

The instrument was set up as recommended by the manufacturer : the gas pressures, slit widths and other controls were adjusted to values prescribed in the manual (Varian, 1979). Operating conditions and typical interferences are shown in Appendix 1.

Because differences in viscosity, surface tension and/or specific gravity between the sample and the standard solutions could not be eliminated, the method of standard additions (Welz, 1976) was used to determine the nickel concentration in the sample. The method used is described in Appendix 1.

The maximum exchange capacity of NH_4^+-SMM was determined using the procedure described by Kunin and Myers (197Ø).

3.2 CATALYST CHARACTERIZATION

The catalysts were characterized by X-ray diffraction, surface area calculations, fluorine content determination and thermal analysis.

3.2.1 X-RAY DIFFRACTION

The basal spacing (i.e. the distance between the base of one 2:1 layer and the next) of clays can be measured by X-ray diffraction. Since the 2:1 layer does not alter much in size after physical treatments, any changes observed in the basal spacing (which includes the interlayer space) can be attributed to changes in the height of the interlayer spacing. XRD studies were carried out to determine whether there were any differences in the basal spacing (interlayer spaces) between NH_4^+-SMM, 7% NiSMM and nickel ion-exchanged SMM.

A Phillips diffractometer was used with the settings as follows :

Radiation	:	CuK_{alpha}
Voltage	:	40 kV
Current	:	3 mA
Slits	:	1/2", 1/2", 1"
Scan Range	:	4^{o} - 30^{o} (2 Theta Degrees)

3.2.2 FLUORINE CONTENT

The fluorine content of 7% NiSMM and SMM were determined at the Council of Mineral Technology. To determine the fluorine content, the sample was decomposed by heating to 1273 K in zinc oxide and sodium carbonate. After the complete disintegration of the material, the sample was filtered and the filtrate was acidified with nitric acid. Fluoride was determined by the addition of a portion of the sample to a solution containing zirconyl chloride and erichromecyanin. The extent to which the zirconium-erichromecyanin solution was bleached was measured using a

spectrophotometer and the fluoride content was determined from a calibration graph (Look and Steele, 1984).

3.2.3 SURFACE AREA DETERMINATION

The BET surface areas of the catalyst samples were determined at the CSIR, using a Carlo-Erba Sorptometer 1800 with nitrogen as the adsorbate. The adsorption measurements were performed at the temperature of boiling liquid nitrogen. The samples were outgassed at about 473 K before carrying out the adsorption measurements to pressure of 10^{-3} Pa.

3.2.4 THERMAL ANALYSES

Thermal analyses, which is described in Section 3.5.7., were used to study the thermal stability of the fresh catalysts and mass losses during calcination. The technique was also extensively used to determine weight % coke on spent catalysts.

3.3 ETHANE HYDROGENOLYSIS REACTIONS

In order to estimate the extent of nickel reduction and the dispersion of metallic nickel on 7% NiSMM, ethane hydrogenolysis ($C_2H_6 + H_2 \longrightarrow 2CH_4$) was used as a probe reaction. The reduction procedure and catalyst pretreatment may be of vital importance for the oligomerization of propene over reduced NiSMM. An optimum dispersion level of the metal on the acid support is desirable since this increases the specific activity of the metal (Yates and Sinfelt, 1967; Darling and Moss, 1966; Boudart, 1972; Taylor 1964; Carter et al, 1966). Ethane hydrogenolysis is a structure - sensitive reaction (Boudart, 1972) and will be sensitive to changes in the metal dispersion.

The following parameters and their effects on the activity of NiSMM were considered :

1. reduction temperature
2. reduction time length
3. reaction temperature
4. calcination temperature
5. effect of NH_4^+ ions on reduction

3.3.1. DESCRIPTION OF FLOW REACTOR SYSTEM

Ethane hydrogenolysis was carried out at atmospheric pressure. Hydrogen gas was passed over a deoxy-unit and 5A molecular sieves and C_2H_6 (99.999%) was passed over 5A sieves. The reactor was a 1/2" diameter stainless steel tube surrounded by a furnace. Glass beads were packed in the top section of the reactor to preheat the feed and to produce plug flow. 0.6 g of catalyst (<250 micron) was placed in the reactor, supported by a wire mesh disc. A thermowell containing an iron-constantan thermocouple extended upward into the catalyst bed and positioned at the centre of the catalyst bed. The reactor temperature was controlled by means of a Eurotherm temperature controller. The catalysts were pretreated with high purity hydrogen and nitrogen. The product gases were analyzed using a Varian 3700 with a column of n-Octane/porasil C at 323 K.

The following operating conditions were used :

- H_2/C_2H_6 molar ratio of 2, total feed flow rate of 15 ml min^{-1} (STP) and a reaction temperature range between 473 K and 573 K. Thermal cracking was shown to become significant above 623 K.

3.3.2 PROCEDURE FOR RATE MEASUREMENTS

In a typical run, the fresh catalyst was reduced above 450°C and then cooled to reaction temperature in flowing hydrogen. At the reaction temperature, the ethane/hydrogen flow was then started and continued for a period of five minutes. At the end of the reaction period the products were analyzed chromatographically. The ethane flow was then discontinued while maintaining the hydrogen flow until the catalyst activity was restored (approximately 15 minutes). By this method a reproducible catalyst activity was attained. The reactor conditions were changed and the reaction procedure repeated.

Ethane conversion was kept below 5% to minimize mass and heat transfer effects and to maintain differential conditions. To obtain rate data, ethane hydrogenolysis was carried out at four different temperatures. The reaction rate was computed as follows :

$$r = F/W\ (C) \quad \text{where } F = \text{g moles } hr^{-1}\ C_2H_6$$

$$W = \text{weight nickel (g)}$$

$$C = \text{conversion to methane (\%/100)}$$

3.4 THE OLIGOMERIZATION REACTOR SYSTEM

3.4.1 LAYOUT

The reactor system used for propene oligomerization is shown schematically in Figure 3.1. The feed (propene/propane) was stored as a liquid under its vapour pressure in an inverted Cadac No. 7 domestic gas cylinder. The feed flowed from the cylinder over two sets of 3A molecular sieves and a 30 micron filter to a high pressure diaphragm

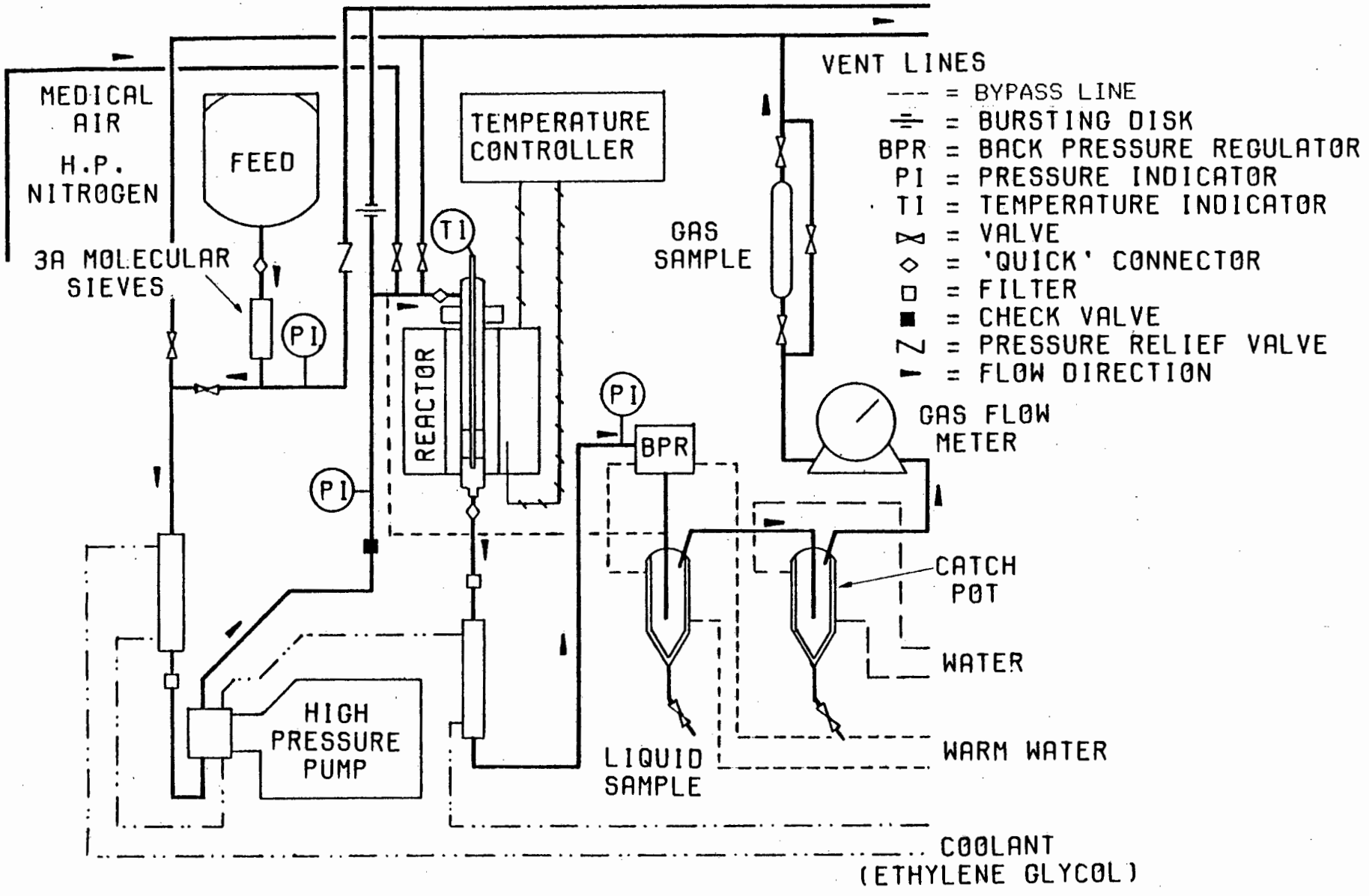

Figure 3.1 Schematic of Reactor System (Rautenbach,1986)

pump (Lewa Model HK-1). An ethylene glycol/water mixture at 280 K cooled the liquid feed to increase the pump head and thereby avoid cavitation. The pump raised the system pressure to that set by the backpressure regulator. Variation in the pump temperature often made it difficult to maintain the flow rate constant for all experiments and therefore it is indicated for each experiment. From the pump the feed passed via a 3-way valve to the reactor and a dome loaded diaphragm-type backpressure regulator (Grove, Mity Mite model 591XW), where the system pressure was reduced to atmospheric. A filter protected the backpressure regulator against damage from eluted fine catalyst particles, while a cooler was introduced before the backpressure regulator to protect the diaphragm during high temperature runs (above 423 K).

A line bypassing the reactor was used during start-up together with a needle valve positioned after the first set of molecular sieves. Phase separation of the reactor effluent took place in a jacketed catch-pot maintained at 285 K.

A second catch-pot removed any condensables which might have been carried over from the first. The backpressure regulator was heated to about 323 K since it was found that the cooling which resulted from the flash vapourization of the unreacted gas could be severe enough to 'freeze' the diaphragm in an open position. After separation in the catch-pot the effluent gas flow was measured with a gas meter, sampled and finally vented. Liquid products which collected in the catch-pot was drained at desired intervals. All tubing upstream of the pump was 1/4" o.d. whilst downstream of the pump 1/8" tubing was used. All metallic sections and all the fittings were made of 316 stainless steel.

3.4.2 THE REACTOR

A small integral reactor based on a design by Snel (1982) was used in this study. 2 mm diameter glass beads were packed in the preheat section to achieve effective liquid distribution and heat transfer. The overall length of the preheat section was 130 mm. The stainless steel reactor was clad with a copper block which served as a heat sink. Two 500 W cartridge heaters connected in parallel were inserted in the copper block and used to control the reactor temperature. The complete reactor (including the heat sink) was insulated with fibre glass. A voltage regulator was connected in series to a Eurotherm temperature controller so that the heat input could be controlled during start-up. The cartridge heaters extended the full length of the copper block and provided a stable and uniform reactor temperature up to 773 K. Temperatures in the preheat and catalyst bed sections of the reactor were measured with a Chessel 306 temperature recorder by inserting a thermocouple down the central thermowell to the desired position.

The reactor was identically packed for most experiments performed in this study, thus ensuring identical feed distribution and catalyst bed geometry. The packed reactor volume is shown in Figure 3.2.

Herskowitz and Smith (1978) found that uniform liquid distribution is ensured in a packed bed when the ratios of the bed diameter to the particle diameter, d_b/d_p, and the bed length to the bed diameter, l_b/d_b exceeded 18 and 5, respectively. From Figure 3.2 these ratios are $d_b/d_p = 9$ and $l_b/d_b = 8$ for the preheat section of the reactor.

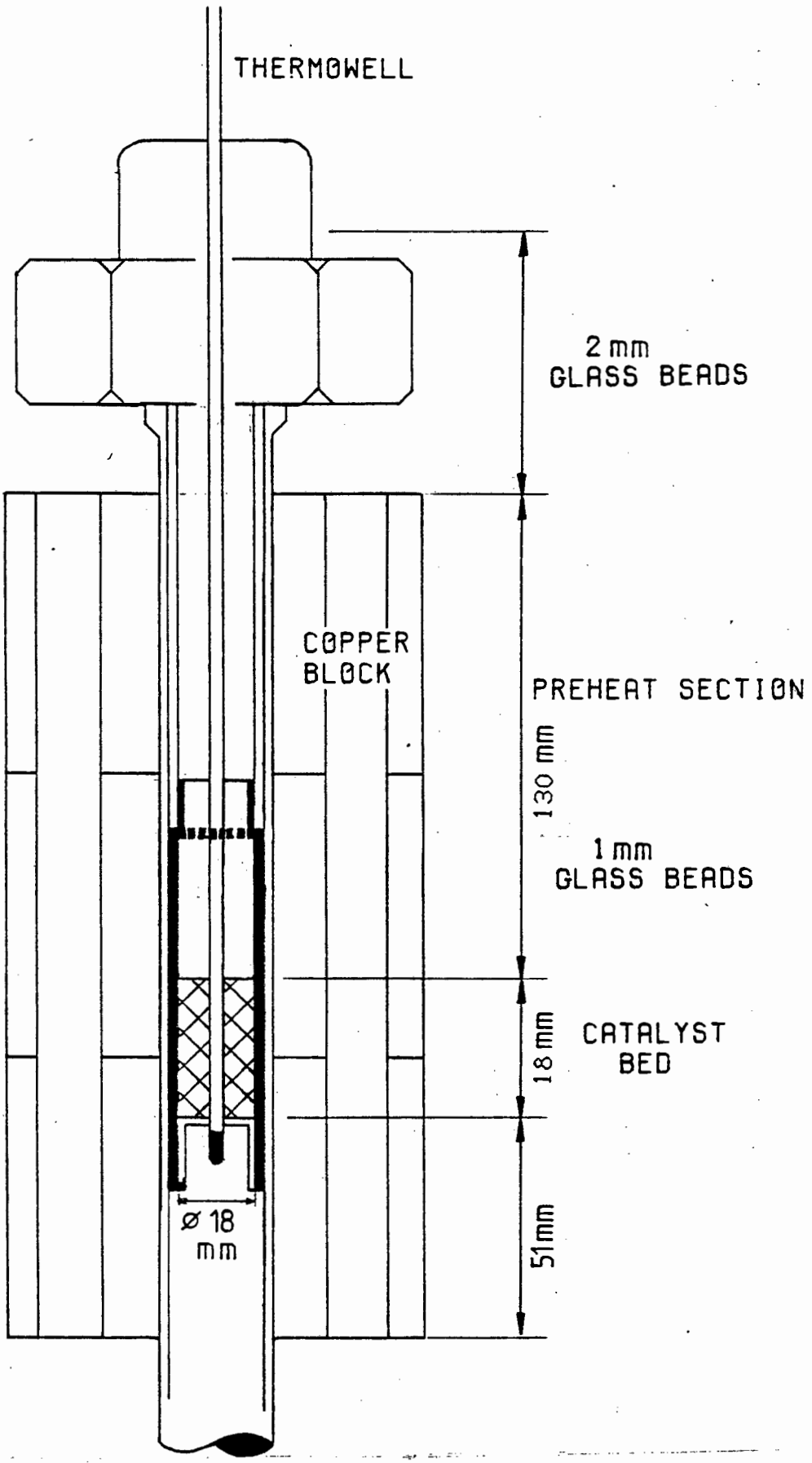

Figure 3.2 Packed reactor volume (Rautenbach,1986)

Although the ratio d_b/d_p is somewhat lower than desired it is hoped that the excessive length of the preheat section will ensure good liquid distribution.

3.4.3 CATALYST PRETREATMENT

The catalyst size and mass, calcination gas, calcination temperature and period were the same in all the experiments. The catalyst used were sieved and 3g of the 106-212 micron fraction was packed into the reactor. The average volume of the catalyst packing was 3.5 cm^3 with a bulk density of 0.86 gcm^{-3}. Calcination was achieved in flowing high purity nitrogen (N_2 = 99.995% by vol, O_2 = 10ppm, moisture = 10VPM) dried over 3A molecular sieves. The nitrogen flow of 1500-2000 h^{-1} SGHSV was maintained at a calcination temperature of 773 K. The catalyst temperature was raised slowly over 1 h interval and held at the set temperature for 4 h after which it was cooled overnight in the same carrier stream used during calcination.

High purity H_2 (3500 h^{-1} SGHSV) was used to reduce the selected catalyst samples. H_2 was passed over 3A molecular sieves and a deoxy-unit before entering the reactor. Prior to reduction, the catalyst was calcined as described above. After calcination the reactor was cooled to the desired reduction temperature and H_2 was passed over the catalyst bed for an average period of 16 h. The bed was then cooled in the same dry H_2 flow used during reduction.

In certain experiments metallic nickel was removed from the reduced NiSMM lattice by carbon monoxide (99.999%) treatment (Heinemann et al, 1983; van Santen et al, 1984). The carbon monoxide flow was kept

constant at 1500 - 2000 h^{-1} SGHSV and the catalyst bed temperature was maintained at 140°C for different treatment periods. The $Ni(CO)_4$ formed was decomposed by passing the exiting gas through nitric acid. The amount of nickel leached out of the catalyst could then be determined by AA analysis on the nitric acid solution.

3.4.4 OPERATION

The feed used in all the experiments was a 4:1 mixture of propene/propane (99% purity) obtained from Sasol.

Considerable work was done in developing an appropriate start-up procedure. During preliminary runs, it was found that if the feed gas was passed rapidly over the 3A molecular sieves (section 4.5) a temperature runaway (typically from 393 K to 473 K) in the catalyst bed was observed, followed by immediate deactivation of the catalyst. It was important to ensure that the feed was adequately dried. This was achieved by the introduction of a bypass line. This diverted the feed from the reactor to remove the initial wet batch of feed, before slowly introducing the feed (usually a feed rate of 24 g/h) into the reactor system. Control of the heat input was also critical during start-up to prevent temperature runaway.

A detailed description of the operating procedure, including start-up, steady state operation and shut-down is outlined in Appendix 2.

At low weight hourly space velocities (WHSV) (1 - 2 h^{-1}), conversion is close to 100% for many pretreatment and reaction conditions and differences in activity are not easily observed. Hence a WHSV of 8 to 9 h^{-1} was chosen so that differences in catalyst activity could be

observed. This also increased the rate of liquid product formation, thereby deactivating the catalyst more rapidly. Oligomerization experiments were typically completed in less than 50 h. Experimental conditions for most oligomerization runs were :

Catalyst charge	:	3 g
Calcination temperature	:	773 K
WHSV	:	8 (+ 10%) h^{-1}
Operating pressure	:	5 MPa
Reduction temperature	:	723 - 763 K
Reaction temperature	:	363 - 453 K

1/16" extrudates were used for an oligomerization run at low space velocity. In this case, 11 g of catalyst was charged to the reactor. The volume of the catalyst bed was 38 cm^3 with a bulk density of 0.3 $g.cm^{-3}$.

3.4.5 CALCULATION PROCEDURE

The mass balances over the integral reactor were calculated using the differences between the mass of hydrocarbons fed to the pump and the combined masses of the liquid product collected and the effluent gases. The percentage loss was determined as follows :

$$\% \text{ loss} = [1 - \{(\Sigma \text{ weight of liquid product i}) + \Sigma \text{ weight of effluent gas i})\}/(\text{total wt of propane and propene fed})] \times 100$$

where the (Σ weight of liquid product i) is directly measured by adding the weights of all liquid samples collected and the (Σ weight of effluent gas i) is calculated by the formula :

Σ wt of effluent gas i = $P\Delta V/RT \times M$

where ΔV = (final gas meter reading - initial gas meter reading),

T = ambient temperature,

P = atmospheric pressure,

and M = average molecular weight of exit gas.

Total wt of propane and propene fed is determined from the weight change in the feed cylinder.

Because the feed rate was low (24 g/h), and weighing the feed cylinder over a short time interval might cause inaccurate flow rate measurements, the flow rate through the integral reactor was calculated from the exit liquid and gas mass rate. The WHSV was based on the total feed stream (propene and propane) since the propane acted as a diluent and affected the reactor residence time. The reaction data yielded the following information :

- Liquid product formation rate expressed in terms of grams of liquid product (excluding dissolved monomer) obtained per gram of catalyst per hour.
- Conversion to liquid product, mass % conversion =

$$\frac{\text{mass of liquid product (excl. monomer) formed}}{\text{mass of propene fed}} \times 100$$

- Liquid product composition which is expressed in terms of mass % dimer, trimer, etc. collected over a time period.
- Effluent gas composition. This data is expressed in terms of mass % since the response factors for components were determined.

3.5 ANALYTICAL METHODS

3.5.1 FEED GAS

Table 3.1 gives a typical analysis of the feed gas used:

COMPONENT	MASS %
ETHANE	0.8
PROPANE	19.1
PROPENE	78.8
ISO-BUTANE	Ø.2
n-BUTANE	Ø.3
n-BUTENE	Ø.7
ISO-BUTENE	Ø.1

Table 3.1. Feed Gas Composition

3.5.2 GAS ANALYSIS

The analysis of the effluent gas and feed streams was performed using a 6 mm by 3 m stainless steel column packed with n-Octane/Poracil C.

The G.C. settings used were as follows :

Detector : Flame ionization

N_2 flow rate : 41 ml/min

H_2 flow rate : 31 ml/min

Air flow rate : 3ØØ ml/min

Injector temperature : 423 K

Detector temperature : 523 K

Column temperature program	:	10 min @ 323 K, 10 K/min to 398 K, 5 min @ 398 K.
Column pressure	:	30 psig @ 323 K
Sample Volume	:	10 μl

A typical chromatogram and the retention times and response factors for the different components are given in Appendix 3.

3.5.3 LIQUID PRODUCT ANALYSIS

The liquid products were analyzed on a 6 mm ID, 3.8 m long glass column packed with 3% OV-101 on Chromosorb W-HP. The following G.C. settings were used :

Detector	:	Flame ionization
N_2 flowrate	:	30 ml / min
H_2 flowrate	:	30 ml / min
Air flowrate	:	300 ml / min
Injector temperature	:	523 K
Detector temperature	:	573 K
Column temperature programme	:	313 K (5min); 10 K/min to 453 K; 30 K/min to 573 K; 5 min at 573 K.
Column pressure	:	18 psig at 313 K.
Sample volume	:	2 μl

The liquid composition was determined using a Varian 3400 gas chromatograph with a Varian 8000 liquid autosampler linked to a Vista 401 data system for integration.

The liquid product formed consists of a large number of isomers of the various oligomers, and it was therefore difficult to identify all the peaks. The liquid fuel analysis was thus based on carbon number groupings. Mass spectroscopy was used to determine approximate transition points between successive carbon number groupings. The cut-off points were not distinct and a certain amount of overlap occurred. This is mainly due to the fact that branched hydrocarbons have much lower boiling points and hence retention times than their straight chain counterparts. Since true polymerization of the feed was predominant, the carbon number groupings were renamed in terms of oligomer fractions as shown in Table 3.2.

CARBON No. GROUPING	OLIGOMER	RETENTION TIME RANGE (MIN)
Dissolved gases C3	Monomer	Ø - 1.Ø2
C6 - C7	Dimer	1.Ø2 - 4.7Ø
C8 - C1Ø	Trimer	4.7Ø - 11.2Ø
C11 - C13	Tetramer	11.2Ø - 15.7Ø
C14 - C16	Pentamer	15.7Ø - 18.5Ø
C17 - C19	Hexamer	18.5Ø - 2Ø.5Ø
C2Ø+	Heptamer+	2Ø.5Ø - 28.ØØ

TABLE 3.2 : G.C. RETENTION TIMES

It has been shown that for hydrocarbons the relative response factors are approximately one (Dietz, 1967), and thus the results (area %) should be a reasonable representation of mass percentage composition. A comparative G.C. - mass spectrum is shown in Section 4.4.7.1.

3.5.4 DETERMINATION OF THE WATER CONTENT IN THE OLEFINIC FEED

The water content of the feed dried over molecular sieves and the wet feed was determined using a Panametrics Model 600/700 Hygrometer. This is a direct reading instrument which responds to water vapour pressure over the range 0.0001 ppm to 200 000 ppm in gases and 0.001 ppm to 3000 ppm in liquids. The dew point, which corresponds to a specific vapour pressure, is read directly. The moisture sensing probe is essentially an aluminium oxide capacitor. The hygrometer response is rapid, insensitive to temperature and flowrate fluctuations, and measures the vapour pressure of water only.

Water content was calculated as follows :

1. $ppm_v = P_w/P_t \times 10^6$

where ppm_v = parts per million by volume

P_w = vapour pressure of water at measured dew point

P_t = total pressure of the system

2. $ppm_w = ppm_v \times \frac{M_w}{M_t}$

where ppm_w = parts per million by weight

M_w = molecular weight of water

M_t = molecular weight of carrier gas.

3.5.5 MASS SPECTROSCOPY

Mass spectroscopy was used to identify the carbon number groups in order to calibrate the gas chromatograph for liquid product analysis. This

was achieved by separating a liquid sample in a G.C.-mass spectrometer under nearly identical conditions (temperature programme, flow rates, column packing) to that being used for G.C. analysis of liquid product. Using a scanning method, molecular weights corresponding to individual signals could be assigned.

Mass spectroscopy was also used to obtain an indication of the presence of saturates in the product.

3.5.6 NUCLEAR MAGNETIC RESONANCE

High resolution NMR is a useful technique for the analysis of liquid fuel product enabling determination of the relative amounts of protons bonded to different carbon atoms. The principles of NMR spectrometry have been described elsewhere (Mathleson, 1967; Bovey, 1969).

The method proposed by Galya et al (1985) was used to interpret the NMR spectra. Due to uncertainty and problems with the carbon-13 NMR spectra, proton NMR was used extensively. Thus the actual volumes of aromatics, olefins and saturates present could not be determined. However, the relative intensities of the $-CH_3$, $-CH_2$ and CH NMR peaks were assumed to give a reasonably accurate measure of the degree of branching.

The degree of branching was determined by the following equation (Galya et al, 1985) :

$$\text{Ratio} = (\text{internal } CH_3) \;/\; (CH_2 + -CH + \text{ter}CH_3)$$

$$= \{1/3 \quad (D+B+H)\}/\{([E+A - H/3]/2 + F) + G/3\}$$

where A = integral intensity of $Ar-CH_2-R$ group

B = integral intensity of $Ar-CH_3$ group

D = integral intensity of $R-CH=CH-CH_3$ group

E = integral intensity of $R-CH-CH_2-CH=CH-CH_2-R$ group

F = integral intensity of $-CH_2-CH-R$ group

G = integral intensity due to terminal CH_3

H = integral intensity due to internal CH_3

A typical NMR spectrum is shown in Appendix 3.

3.5.7 THERMOGRAVIMETRIC ANALYSIS

Thermogravimetry (TG) is a technique whereby a sample is continuously weighed as it is heated at a constant rate. The resulting weight change versus temperature curve gives information concerning the thermal stability of the sample, the composition and the thermal stability of the intermediate compounds and the composition of the residue (Wendlandt, 1964; Webb, 1981). Differential thermal analysis is another useful method which can be used to determine enthalpic effects of the sample during heating. By observing temperature changes, enthalpy changes (endothermic and exothermic) can in principle be calculated. The results of the TG-DTA data are greatly influenced by the geometry of the furnace, the sample particle size and heating rate.

In this study the thermal analysis was used to determine :

1. the thermal stability of the fresh catalysts ;
2. the mass of physically absorbed water present on the fresh catalysts;
3. the mass losses (and temperatures at which they occur) due to dehydroxylation ;

4. the coke content on the spent catalyst, viz., reversibly adsorbed hydrocarbons and graphitic coke

20 mg of catalyst was used for TG and DTA studies on a Stanton-Redcroft STA 780 Simultaneous Analyzer. Alumina was used as a reference material. The analyses were carried out in nitrogen and air at a flow rate of 87 ml/min. All experiments were performed at atmospheric pressure, using a heating rate of 10 K/min to a maximum temperature of 1123 K. To characterize the fresh catalyst, only nitrogen was used.

To determine the coke content, the following procedure was employed :

1. The deactivated sample was subjected to heating (at 10 K/min) in flowing nitrogen up to 1023 K. (Nitrogen is an inert gas and serves to carry off the volatilized hydrocarbons). The quantity of long chain hydrocarbon could then be determined from the weight loss in this region.
2. At 1023 K, gas flow was switched to air which reacted with the graphitic coke on the catalyst sample. An exothermic peak was observed indicating combustion. The TG-DTA run was terminated at approximately 1123 K. Upon introduction of air, there was immediate reaction (and weight loss) which corresponded to graphitic coke being "burnt off" on spent catalyst.

A typical TG/DTA curve is shown in Appendix 3.

3.5.8 STANDARD FUEL TESTS

To maintain and control the quality of petroleum products, they are subjected to a series of tests at various stages of manufacturing, storage and distribution.

Firstly, there are those which are designed to control the quality of the product and, secondly, those which give an indication of its expected performance.

The majority of test methods used have been standardized and published either by the American Society for Testing of Materials (ASTM) or the British Institute of Petroleum (I.P.) (1981). Appendix 3.4 gives a list of the typical tests carried out on fuels.

4. RESULTS

4.1 Nickel Ion-Exchanged SMM (NiIXSMM)

The ammonium form of SMM obtained from the Filtrol corporation was used to prepare nickel ion-exchanged SMM. In order to determine whether there were any significant nickel losses during the decomposition of the catalyst for AA analysis, a mass balance over the system was performed. By analyzing the nickel content in the sample, initial and final solutions, it was found that nickel percentage loss was less than 3 %.

Wright et al (1972) showed that uncalcined SMM contained 175 meq NH_4^+/100 g on a dry basis. The theoretical maximum exchange capacity was determined on a wet basis $\{[(Al_4)^{OCTA}\ (Al_x\ Si_{8-x})^{TETRA}\ O_{20}\ (OH,F)_4]^{x-1} \times NH_4^+\ H_2O$ where x = 1.5$\}$ using a fluoride to silicon ratio of 0.1 (Wright et al, 1972). The degree of ion exchange was based on the theoretical value of 196 meq NH_4^+/100 g (196 meq Ni^{2+}/100 g). By degree of exchange, is meant the ratio of the mass Ni^{2+} present in the catalyst to the maximum possible weight Ni^{2+} (5.75 wt %) that could be retained by the catalyst.

It was found that the catalyst reached its equilibrium exchange capacity after 6 to 8 h. Using a 0.03 N nickel nitrate solution, the nickel ion content rose sharply at first then decreased slightly before reaching equilibrium, as given below :

Period of Exchange (h)	0.5	1	2	4	8
% Exchange	29	26	27	27.5	27

During each run the pH was monitored continuously. Partial hydrolysis ($\overline{NH_4}^+ + H_2O \rightarrow \overline{H}^+ + NH_4^+ + OH^-$ where $\overline{\ }$ represents catalyst) was found to be negligible with the pH remaining constant at 5.85. The degree of exchange increased with increasing initial concentration of the nickel nitrate solution, reaching a maximum at 0.04 N - 0.05 N as shown in Figure 4.1. Table 4.1 gives the numerical values of this plot plus the corresponding weight percent nickel.

CONCENTRATION OF SOLUTION (N)	% EXCHANGE	WEIGHT % Ni
0.00025	1.0	0.057
0.0005	3.4	0.196
0.001	7.9	0.46
0.0015	9.5	0.542
0.005	19.4	1.12
0.01	21.5	1.24
0.02	25.2	1.45
0.03	27.1	1.56
0.05	27.1	1.56

Table 4.1 Nickel Ion Exchanged SMM

In an attempt to achieve higher levels of exchange, repeated exchange was performed using fresh solutions in succession. However, using a 0.01 N Ni $(NO_3)_2$ solution the % exchange essentially reached a maximum after the first contact with Ni $(NO_3)_2$ solution, after which very little exchange occurred. Exchange levels obtained using a closed and heated system were compared. No significant changes were observed.

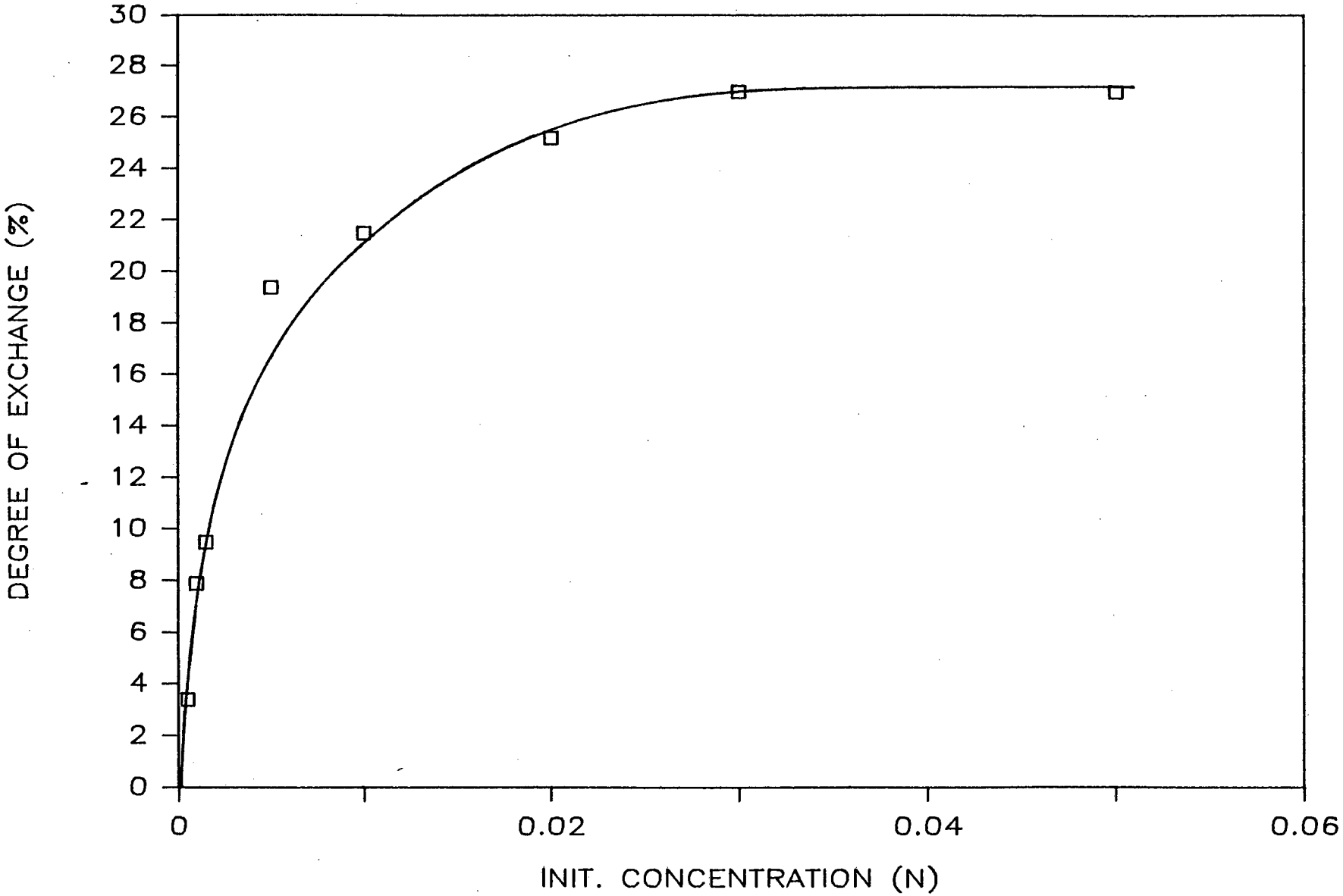

Figure 4.1 % Exchange vs initial solution concentration

CONC = Ø.Ø3 N	OPEN SYSTEM	CLOSED SYSTEM	T = 348 K
Degree of Exch. (%)	27	26	27.5

The exchange capacity determined using the method of Kunin and Myers (1970) was Ø.674 meq NH_4^+/ g which corresponds to a 34 % degree of exchange.

The exchanged catalyst samples will be referred to as x % nickel ion exchanged SMM (x% NiIXSMM) where x is the degree of exchange.

4.2 CATALYST CHARACTERIZATION

SMM, NiSMM and NiIXSMM were characterized using X-ray diffraction, surface area and fluorine content determinations and thermal analyses. 1 % and 9.5 % NiIXSMM were chosen as the two extremes for further experimental work.

4.2.1 X-RAY DIFFRACTION

Uncalcined samples were crushed to size fraction 106 to 212 micron and random XRD patterns were obtained using a standard Phillips diffractometer.

Samples of SMM and nickel ion-exchanged SMM were compared to determine the effect of ion exchange on the catalyst structure. From Figure 4.2 it can be seen that there is no significant difference in the XRD pattern (ØØ1 and ØØ2 reflections are shown). A similar XRD pattern was obtained for 7% NiSMM, although there was a slight difference in intensity at the ØØ2 reflection. Table 4.2 gives the average interlayer spacing of the catalysts.

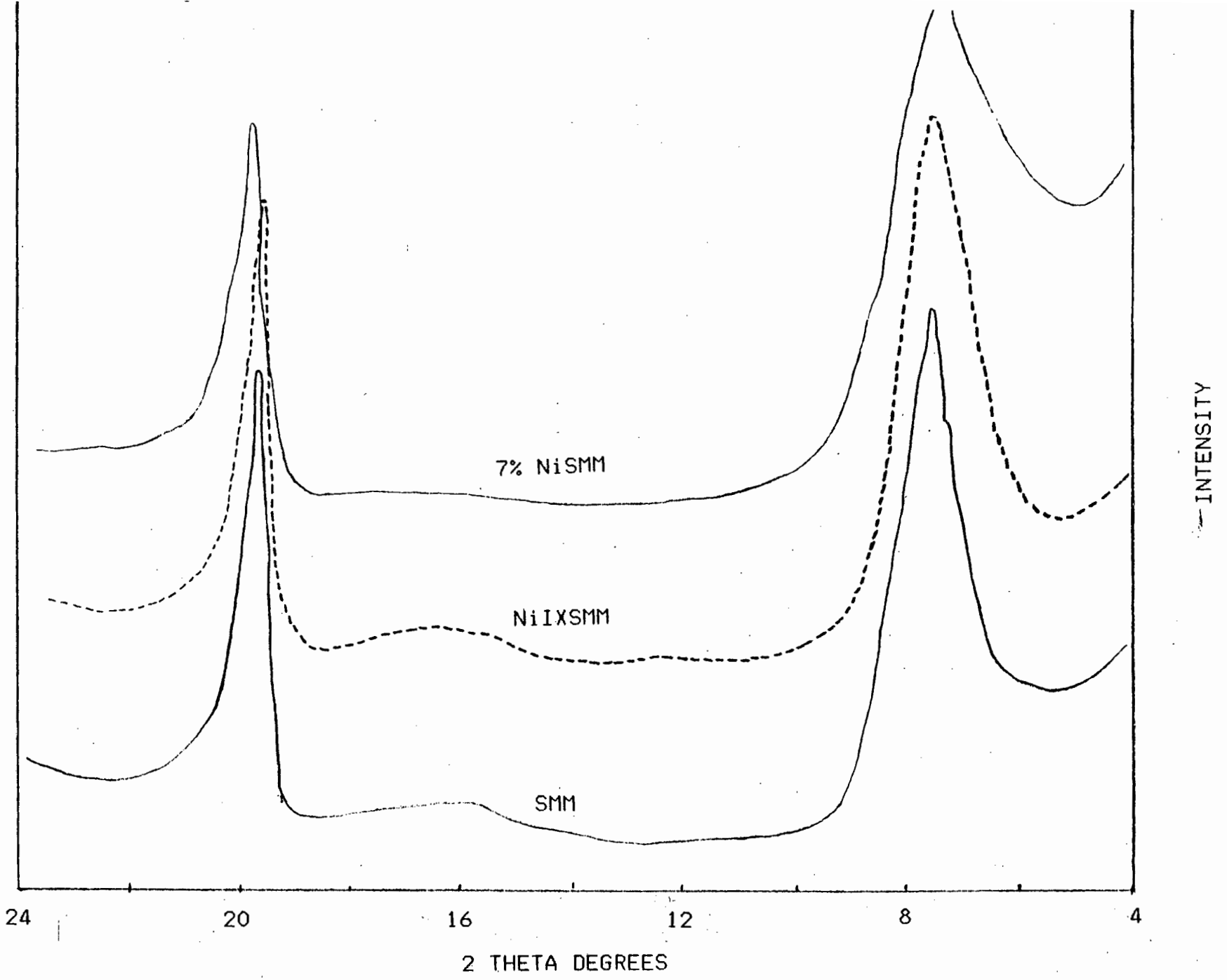

Figure 4.2 XRD Patterns

CATALYST	2 THETA (DEGREES)	d_{001} (A)
SMM	7.9	11.19
7% NiSMM	7.8	11.30
1% Exch. SMM	7.85	11.26
9.5% Exch. SMM	7.85	11.26

Table 4.2 Basal Spacings

The d_{001} values compare well with those obtained by Fletcher (1984) for SMM (11.08 A) and Black et al (1976) for NiSMM (11.32 A), indicating therefore that the catalyst samples obtained from Filtrol are structurally of a similar nature to those prepared by Granquist and Pollack (1967) and Granquist et al (1976).

4.2.2 SURFACE AREA

The results of the surface area determination of the calcined catalyst samples are shown in Table 4.3

CATALYST *	AVE SURFACE AREA (m^2/g)
7% NiSMM	204
SMM	107
1% Exch. SMM	108
9.5% Exch. SMM	106

Table 4.3 Surface Areas of Catalysts
* Calcined at 773 K for 4 h

The surface area of 7 % NiSMM is almost double that of SMM and nickel ion-exchanged SMM, and compares well to the value of 199 m^2/g for 6.75 % NiSMM reported by Black and Swift (1974). The surface area of SMM is similar to that obtained by Fletcher (1984) (114 m^2/g), but is lower than the 135 m^2/g reported by Wright et al (1972). It appears that after a low degree of ion exchange (< 10%) there is no significant change in surface area. However, Black and Swift (1974) reported that impregnating SMM (as opposed to ion exchanging) with nickel nitrate resulted in a decrease in surface area from 145 to 94 m^2/g.

4.2.3 FLUORINE CONTENT

Samples of NiSMM and SMM were analyzed for fluorine content. Since the fluoride ions are not present as exchangeable ions, the fluorine content of the nickel ion-exchanged SMM and SMM is expected to be the same.

CATALYST	F (wt %)
NiSMM	1.0
SMM	1.9
Nickel IX SMM	1.9

Table 4.4 Fluorine Content

From Table 4.4, it can be seen that NiSMM has a lower fluorine content than SMM. The fluorine content of synthetic catalysts may affect the activity of the catalyst (Becker et al, 1985) and the amount of water lost during dehydroxylation (Wright et al, 1972).

4.2.4 THERMAL ANALYSES

The TG-DTA curves for SMM, NiSMM and nickel ion-exchanged SMM (1 % and 9.5 %) are shown in Figures 4.3 to 4.6.

The DTA curve in Figure 4.3 shows an endothermic peak at 390 K, which is a result of the loss of physisorbed water. From the TG curve in Figure 4.3 the mass of physisorbed water is approximately 4.5 % of the mass of fresh SMM. Desorption of the physically adsorbed water is complete by 420 K. A broad exothermic peak occurs in the region 423 K to 673 K, followed by an endothermic peak at 753 K in the DTA trace in Figure 4.3. The exothermic band, during which there is about 2.5 % mass loss, is probably due to deammoniation. The endothermic peak is accompanied by a further mass loss of 6.5 % due to dehydroxylation which is complete by 1120 K.

The TG-DTA curve of 7% NiSMM shown in Figure 4.4 is slightly different to SMM. Physisorbed water is removed by 423 K, but accounts for about 7.5% of the mass of fresh NiSMM. An exothermic reaction occurs in the region 473 K to 1120 K. The TG curve shows a gradual mass loss (due to deammoniation and dehydroxylation) from 473 K to 1120 K. Approximately 12.5% of the mass of fresh NiSMM is 'lost' in this region. Thus the total weight loss is greater in the case of 7% NiSMM (19.8%) than SMM (13.5 %).

The TG-DTA curves of nickel ion-exchanged SMM (1 %, 9.5 %) shown in Figures 4.5 and 4.6 do not differ much from that of SMM (Figure 4.3). However, 9.5% ion exchanged SMM has a total mass loss of 14.5% of the mass of the fresh catalyst compared to the 13.5% weight loss for SMM and 1% ion-exchanged SMM. The DTA curves for SMM and nickel ion exchanged

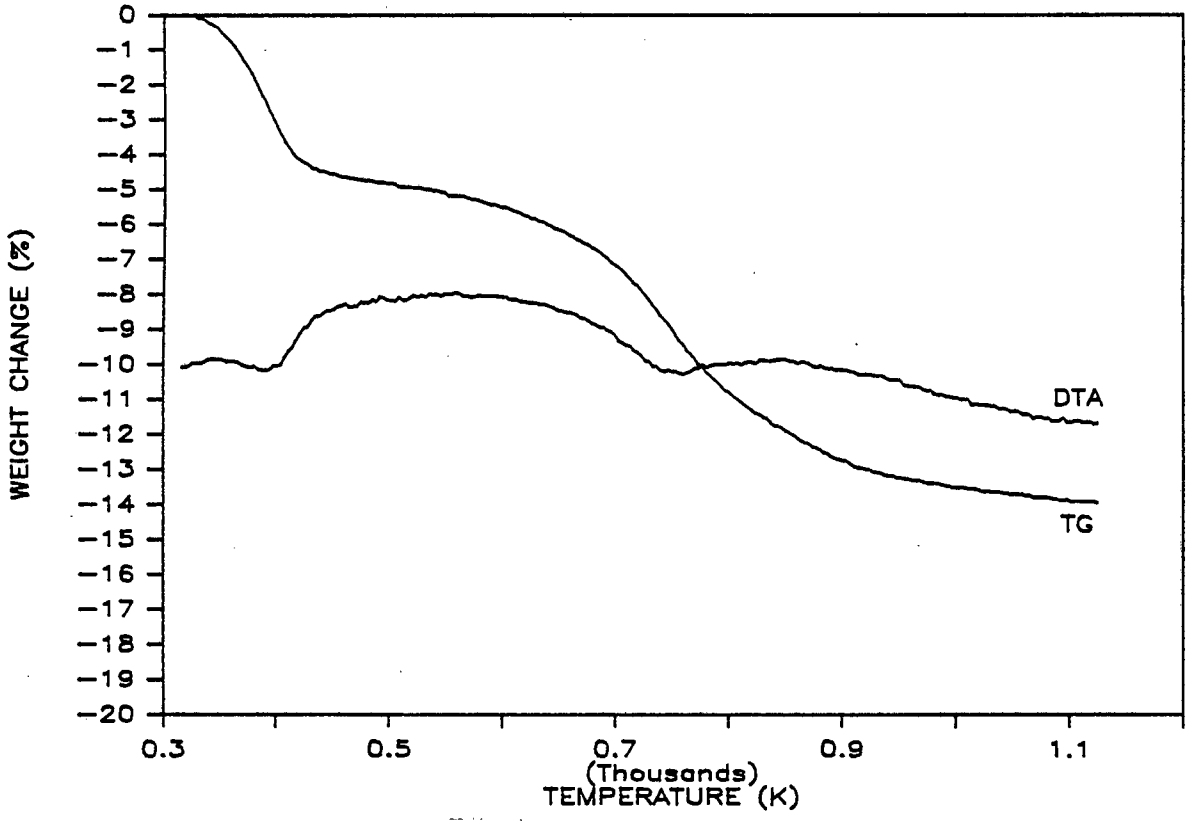

Figure 4.3 TG-DTA curve of SMM

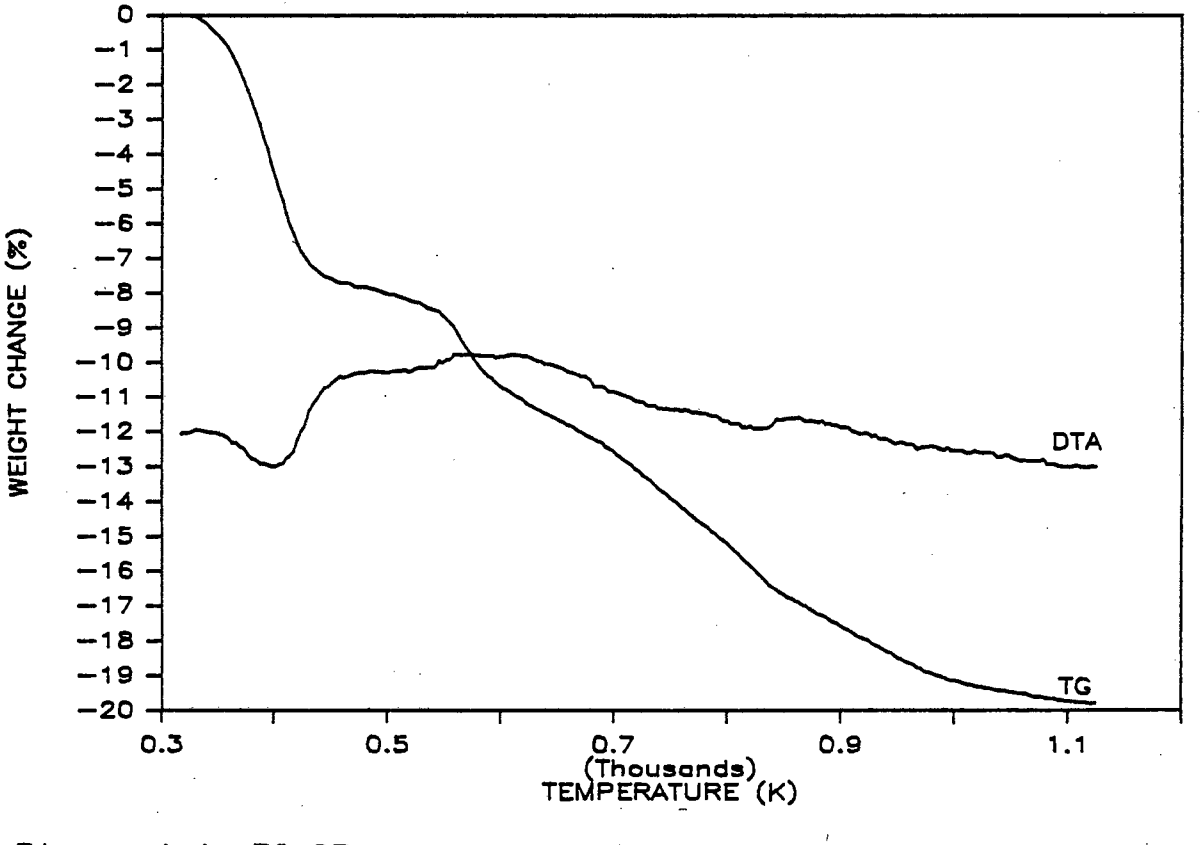

Figure 4.4 TG-DTA curve of 7% NiSMM

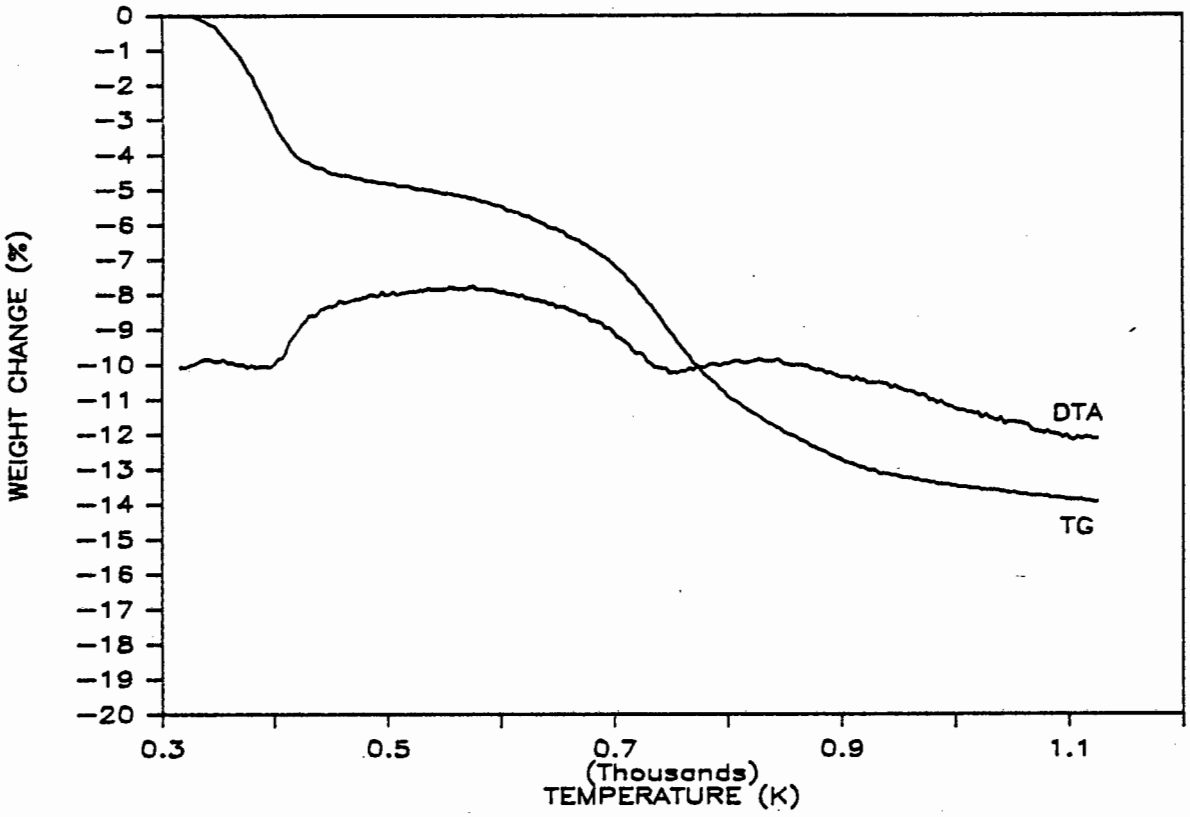

Figure 4.5 TG-DTA curve of 1% NiIXSMM

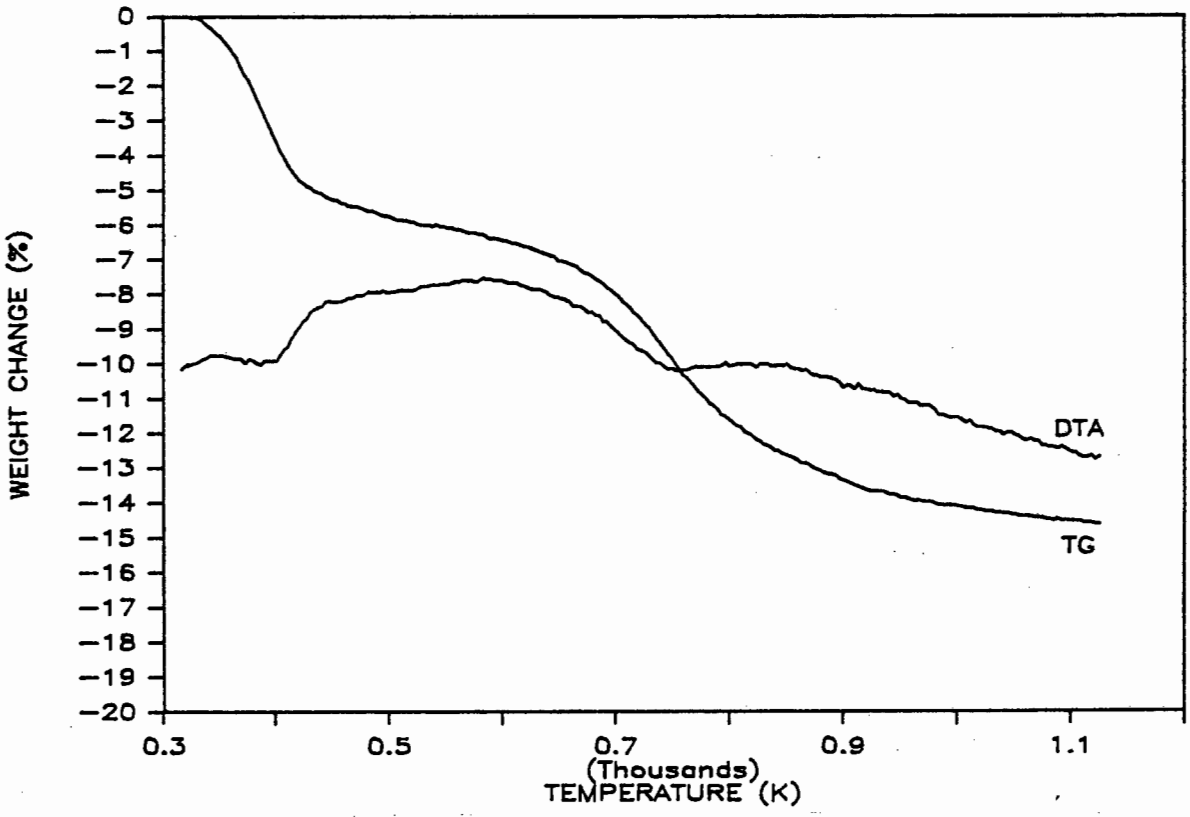

Figure 4.6 TG-DTA curve of 9.5% NiIXSMM

SMM samples are identical.

During a TG-DTA experiment, the temperature was held at 773 K for 4 h and it was found that this period was sufficient for complete dehydroxylation of the catalyst. The total weight loss was approximately 13% for a SMM catalyst sample.

4.3 ETHANE HYDROGENOLYSIS OVER 7 % NiSMM

As stated in Section 3.3, the specific activity of the metallic nickel is related to its dispersion on the acid catalyst support and the average crystallite size. Therefore by monitoring the activity, an indirect measure of the nickel dispersion is obtained. The results are presented as g moles ethane converted.hr^{-1}. $(g\ Ni)^{-1}$.

Reproducibility runs were performed on 7% NiSMM. The samples were reduced at 763 K. It is clear from Figure 4.7 that the results (log rate vs 1/T) obtained are reproducible (within 3%).

4.3.1 EFFECT OF CALCINATION TEMPERATURE

For this series of experiments, the calcination period was maintained at 4 h and the reduction temperature was kept constant at 763 K for 16 h. The ethane hydrogenolysis activity of the catalyst was monitored over a temperature range between 473 K to 573 K. Figure 4.8 illustrates the marked effect of calcination temperature on the activity of the reduced sample. The hydrogenolysis activity of reduced NiSMM was seen to increase as the calcination temperature increased. The rate of ethane hydrogenolysis / gram nickel was over 50-fold higher for the sample calcined at 773 K than when the catalyst was not calcined. It appears that the presence of water (both physisorbed and that resulting from

100% conv 0.64 − 0.45
10% 6.4×10⁻² − 2.7
1% − 5.05

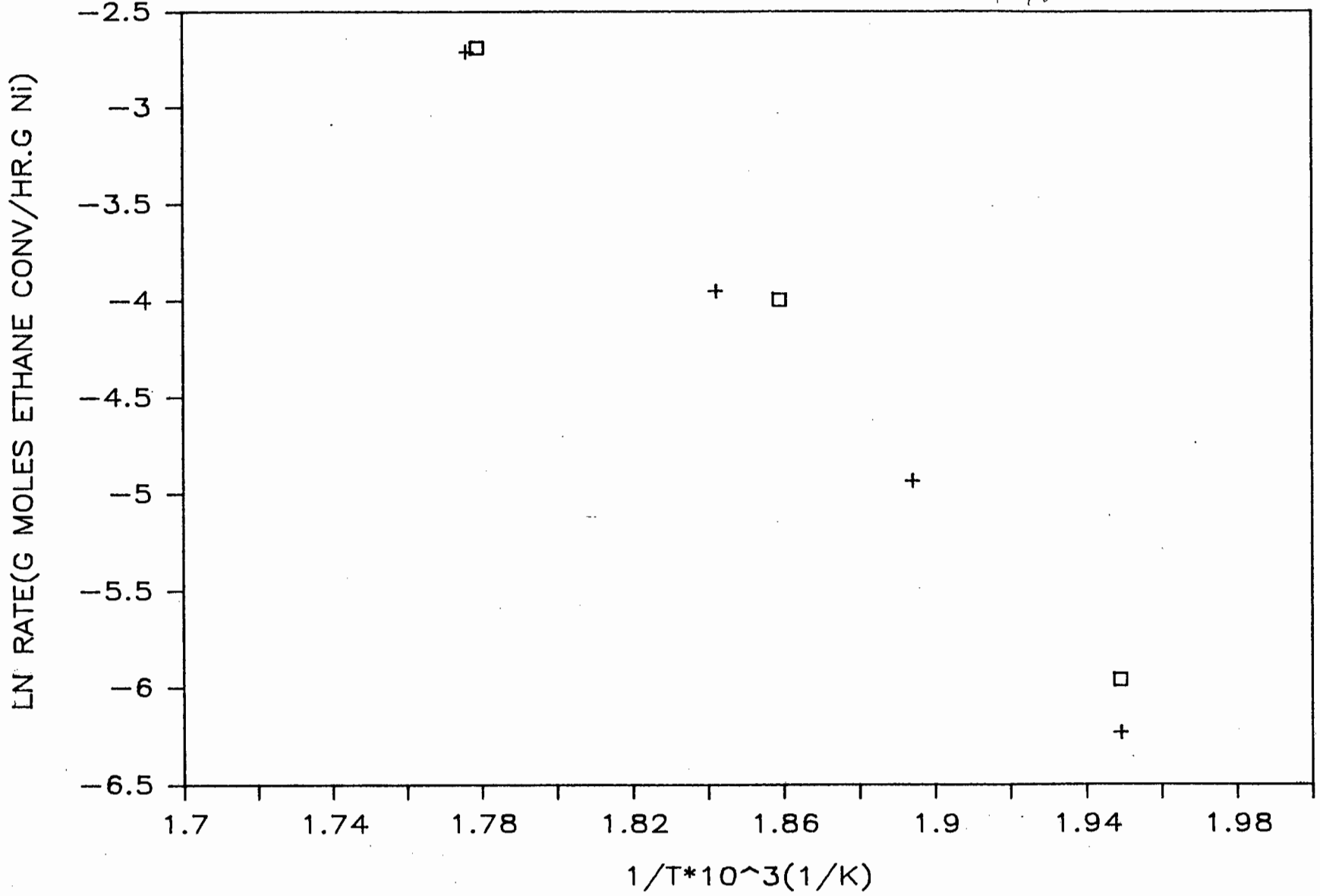

Figure 4.7 Reproducibility

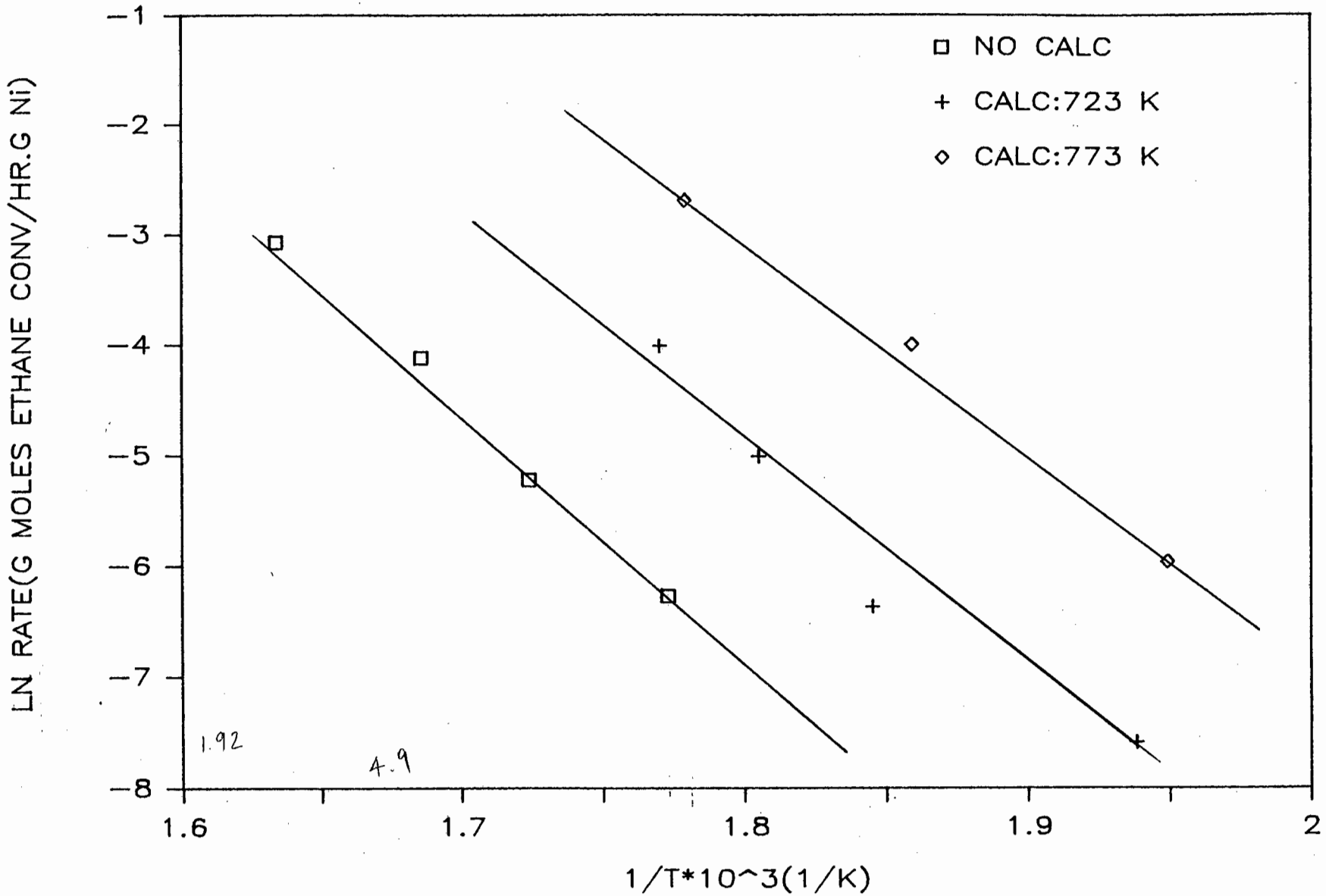

Figure 4.8 Effect of calcination temperature

(dehydroxylation) interfered with the nickel reduction process. The catalysts were thus calcined at 773 K before the reduction treatment.

4.3.2 EFFECT OF REDUCTION TEMPERATURE

Significant reduction of 7% NiSMM was found to occur at a reduction temperature of 723 K, in agreement with Heinerman et al (1983). At reduction temperatures below 723 K, NiSMM showed no ethane hydrogenolysis activity. The effect of reduction temperature is shown in Figure 4.9 (samples calcined at 773 K for 4 h and reduced for 16 h). The activity of reduced NiSMM increased upon increasing the reduction temperature from 723 K to 763 K. However, the activity dropped after reduction at temperatures above 763 K. Table 4.5 gives the rate of ethane hydrogenolysis as a function of reduction temperature at a reaction temperature of 540 K. From the slopes of the plots in Figure 4.9, the apparent activation energies were determined and are given in Table 4.5.

REDUCTION TEMPERATURE (K)	723	763	823
Rate (g moles $C_2H_6.h^{-1}$. (g Ni)$^{-1}$) @ 540 K	1 x 10-2	1.9 x 10-2	9 x 10-4
Apparent Activation Energy, E_a ($kJ.mol^{-1}$)	168	166	176

Table 4.5 Effect of Reduction Temperature (7% NiSMM)

The activity following reduction at 763 K was about twice that after reduction at 723 K, but approximately twenty times greater than for reduction at 823 K. The results suggest that the maximum activity is associated with an intermediate level of dispersion. There are small

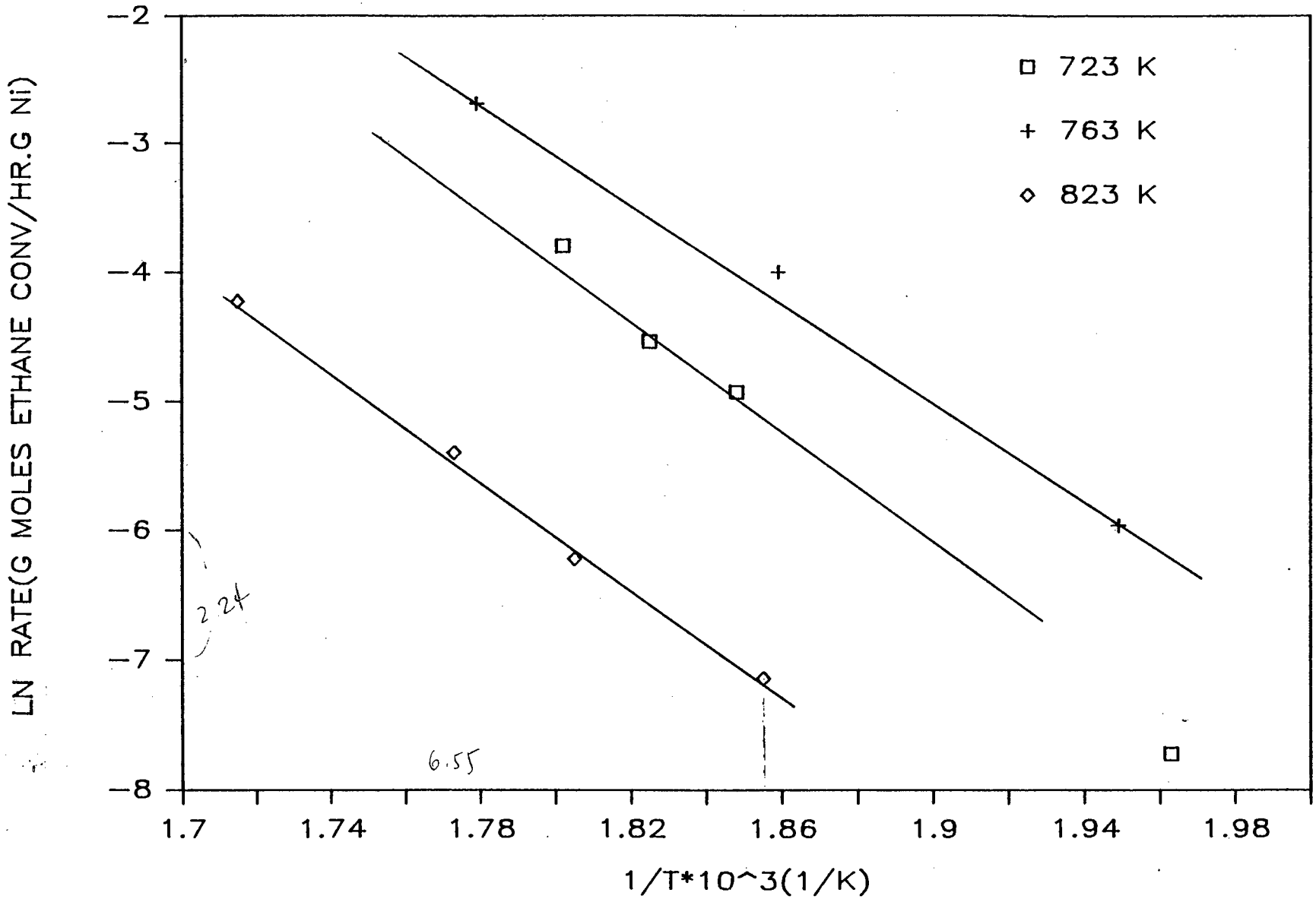

Figure 4.9 Effect of reduction temperature

differences in the apparent activation energies (E_a) listed in Table 4.5, with the average value approximately equal to 40 kcal. $mole^{-1}$ (168 kJ $mole^{-1}$).

4.3.3 EFFECT OF REDUCTION TIME

The catalyst samples for this series of experiments were calcined at 773 K for 4 h and reduced for varying times at a reduction temperature of 763 K. It can be seen from Figure 4.10 that the reduction of nickel occurred very rapidly during first 3 hours. However, reducing for longer periods (24 h) caused the activity to drop. Thus it appears that the optimum reduction time is 16 h. The activity was similar for a reduction period of 3 h and 24 h indicating that an even longer reduction period (48 h) would result in lower activity.

4.3.4 EFFECT OF NH_4^+ IONS

Richardson (1971) reported that the presence of ammonium ions inhibited nickel reduction on nickel zeolites. NH_4^+ ions in NiSMM were replaced by sodium ions by ion exchange. Both samples were pretreated under identical conditions : calcination at 773 K for 4 h, reduction at 763 K for 16 h. The presence of NH_4^+ ions did not affect the activity of the reduced catalyst to any significant extent as shown in Figure 4.11. The activity of NH_4^+ - NiSMM was in fact slightly higher than that of Na^+ - NiSMM.

The apparent activation energies for most of the Arrhenius-type plots ranged from 164 to 176 kJ mol^{-1} and was in agreement with values obtained by other workers (Taylor et al, 1964; Yates and Sinfelt, 1967). The optimum pretreatment conditions for 7% NiSMM are therefore :

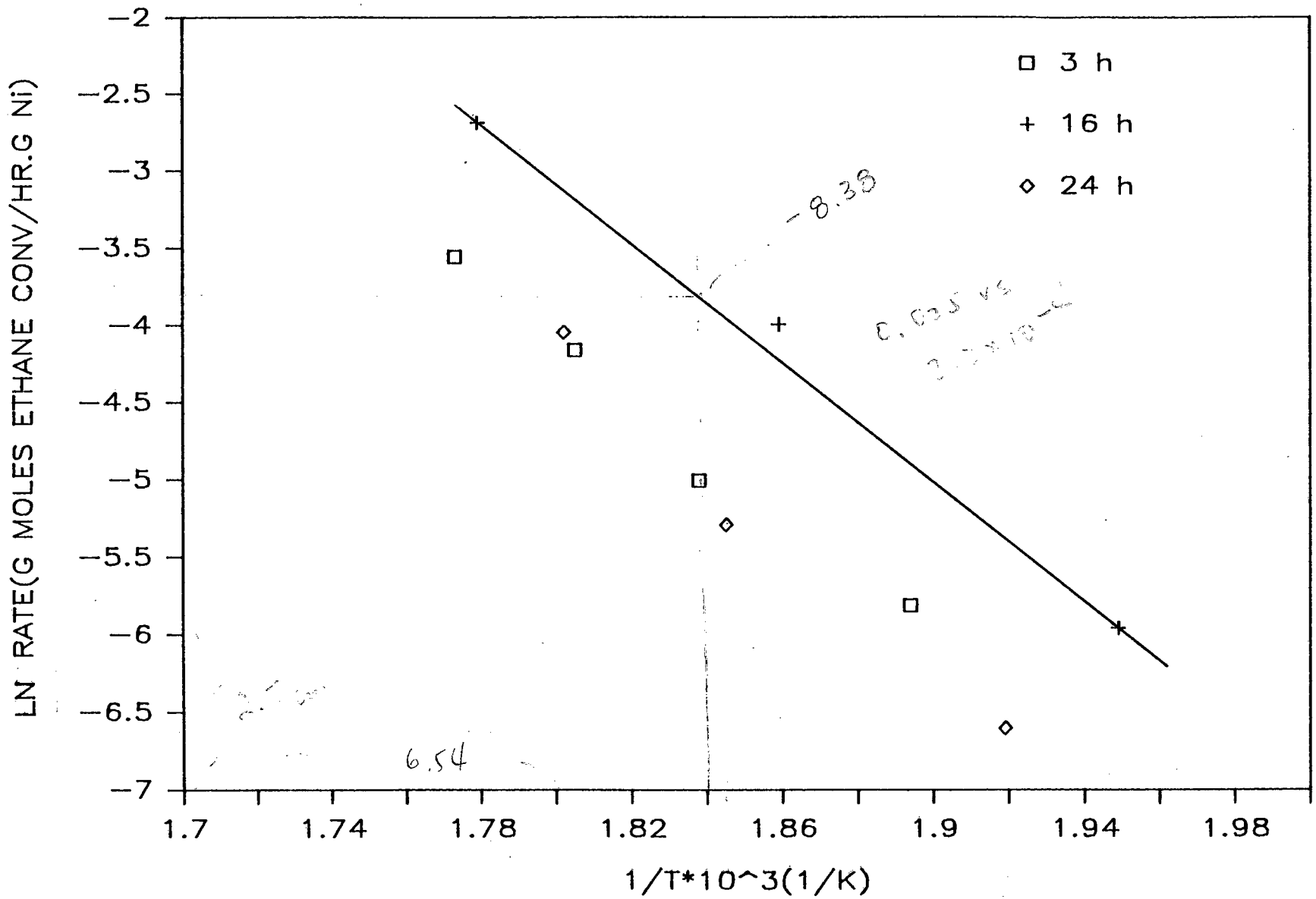

Figure 4.10 Effect of reduction time length

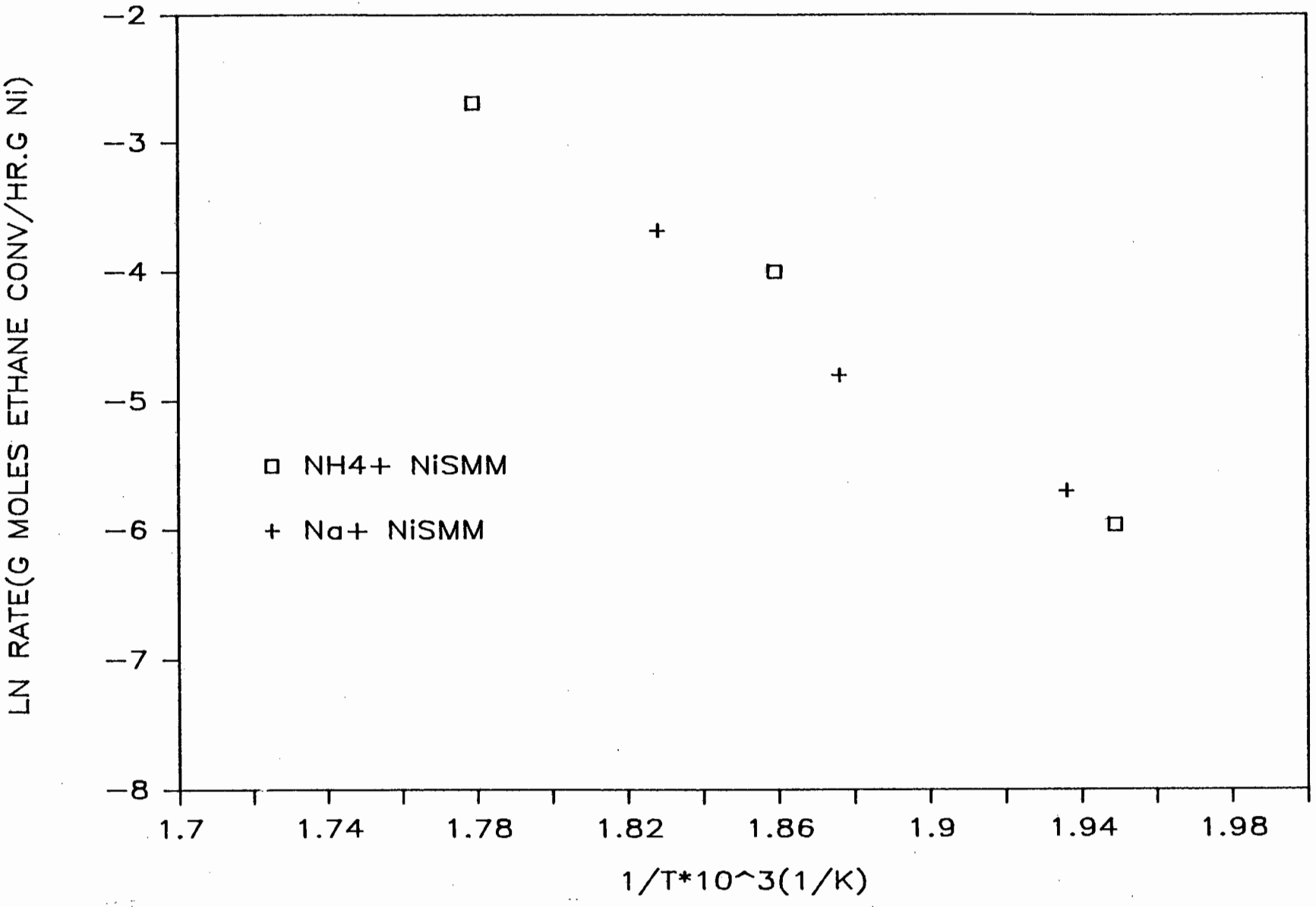

Figure 4.11 Effect of NH_4^+ ions in the interlayer spaces

- calcination at 773 K for 4 h in dry N_2
- reduction at 763 K for 16 h in flowing H_2

4.4 OLIGOMERIZATION OF PROPENE

This section of the work addresses the following questions with respect to the oligomerization of propene :

a) Does the incorporation of nickel in the matrix enhance catalytic activity and/or lifetime?

b) How do Ni^{2+} ions in the interlayer spaces affect lifetime and activity?

c) It has been reported in the literature (Robschlager et al, 1984) that upon reduction of the nickel in 20 wt% NiSMM, the number of Bronsted sites increases by nearly four-fold. How does this increase affect the oligomerization activity of reduced NiSMM?

d) What is the role of the metallic nickel?

e) What effect do other exchange cations have on catalyst performance?

The catalyst activity was compared using the liquid production rate (LPR) expressed in terms of grams of liquid product per gram catalyst per hour. The term selectivity was used to refer to the relative amounts of liquid product in a carbon number group range (oligomer fraction). Selectivity data was plotted excluding the monomer content. The abbreviation D, TR, TE, P, H, HEP^+ are used in the figures to represent dimer, trimer, tetramer, pentamer, hexamer, and heptamer and heavier products, respectively. The weight hourly space velocity (WHSV) was defined as the weight of the propene and propane mixture fed to the reactor system per hour per weight of catalyst.

For all experiments a mass balance was carried out. The mass loss in all cases was less than 5 %. A size fraction of 106 - 212 micron and reaction conditions of 5 MPa and 403 K, were used for the oligomerization experiments unless otherwise stated.

4.4.1 PRELIMINARY INVESTIGATIONS OF OLIGOMERIZATION REACTIONS OVER CATALYSTS

Since no previous work had been done on NiIXSMM, the average catalytic activity for propene oligomerization was monitored at three reaction temperatures, viz, 363 K, 403 K and 453 K in an attempt to find optimal conditions. 1% and 9.5% NiIXSMM were chosen as the two extremes. Table 4.6 tabulates these results which were obtained by monitoring the oligomerization activity at one reaction temperature for 4 - 6 h before slowly increasing to a new reaction temperature.

CATALYST	SMM	1 % NiIXSMM	9.5 % NiIXSMM
AVE CATALYTIC ACTIVITY (G LIQ/HR.G CAT) @ 363 K	0	2.3	2.1
403 K	1.9	1.70	2.2
453 K	2.3	1.80	2.23

Table 4.6 Activity vs Temperature

The above results gave an indication of the activity of the exchanged catalysts. The activity, in most cases, did not vary much with temperature, possibly because different reaction temperatures were tested in the same run and as the temperature was increased the catalyst was simultaneously undergoing deactivation. It was found that SMM is inactive at 363 K where feed is in the liquid phase, indicating that

Ni^{2+} ions play an important role in SMM.

Generally it was found that product distributions were the same for SMM and NiIXSMM at the same reaction temperature. However, there was a shift towards heavier oligomers with an increase in the reaction temperature. This was accompanied by an increase in the degree of branching as measured by NMR. Table 4.7 gives the liquid distribution for 9.5% NiIXSMM at similar conversion levels.

	Reaction Temperature		
Mass % Oligomer	363 K	403 K	453 K
Dimer	12	9	10
Trimer	50	26	24
Tetramer	24	26	22
Pentamer	10	16	14
Hexamer	3	11	11
Heptamer+	1	12	19
Conversion (%)	35.0	35.5	37.0
Degree of Branching	0.4	0.55	0.75

Table 4.7 Selectivity vs Reaction Temperature

It was decided to use a base reaction temperature of 400 - 410 K for all the catalysts since :

- At 363 K catalyst deactivation started after 5 h whereas a steady state activity was maintained for the reaction period of 6 h at 400 K.

- At the higher reaction temperatures the deactivation rate was more rapid than reaction at 363 K.
- No significant cracking occurred at 405 K compared to 453 K.

4.4.2 REPRODUCIBILITY

Propene oligomerization was carried out over two samples of 7% NiSMM of size fraction 106 - 212 micron under similar reaction conditions (reaction temperature = 403 K, WHSV = approx. 8 h^{-1}). The catalysts were subjected to the same pretreatment of calcination at 773 K for 4 h in dry nitrogen.

Figure 4.12 shows the LPR for each run as a function of time on stream. It was difficult to maintain the WHSV at exactly 8 h^{-1} for each experiment and therefore WHSV is indicated. The largest discrepancies in the 2 runs occur during the initial period (start up). However, after 2 - 4 h on stream the production rate is similar and catalyst deactivated at the same rate. Thus, from these results, reproducibility is acceptable.

A study of the variation of composition with time on stream for RUN 014 (7% NiSMM) is shown in Figure 4.13. The mass % oligomer in the liquid product did not vary much in the steady state region. There is a slight increase in the trimer fraction and decrease in heptamer fraction upon the deactivation of the catalyst. Unless the product spectrum varied radically over the reaction period for the forthcoming experiments, the oligomer fraction distribution of one steady state sample will be plotted. Figure 4.14 shows that the composition of the liquid product is reproducible. The similarity in the liquid fuel distribution is further indicated by ASTM distillation, the results of which are shown

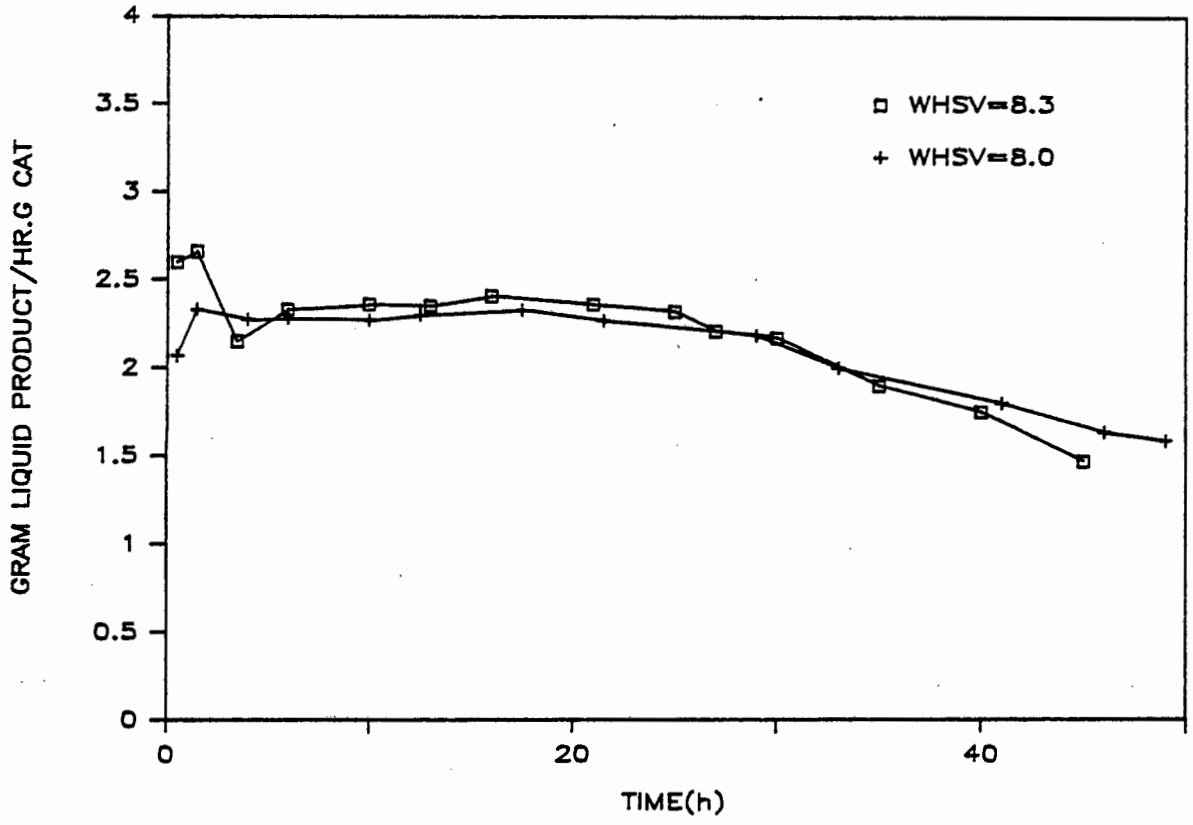

Figure 4.12 Reproducibility - activity

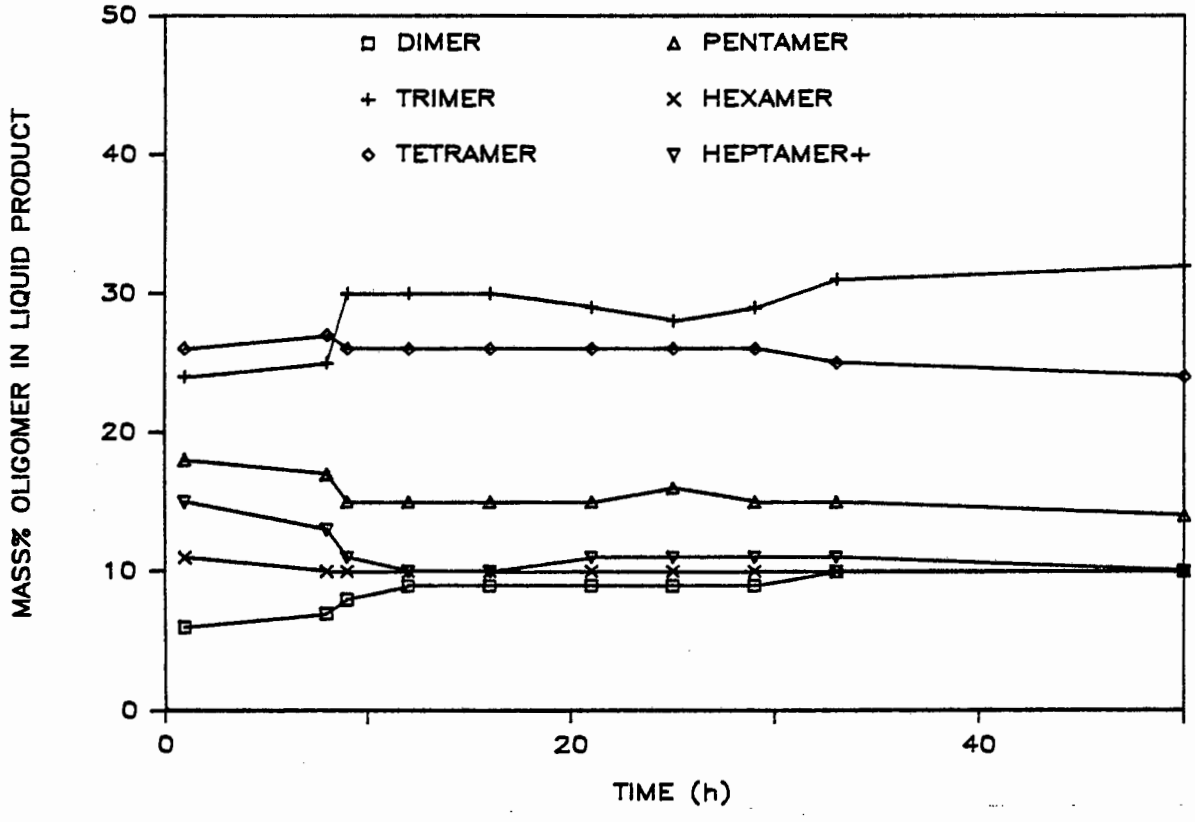

Figure 4.13 Liquid product compositon versus time

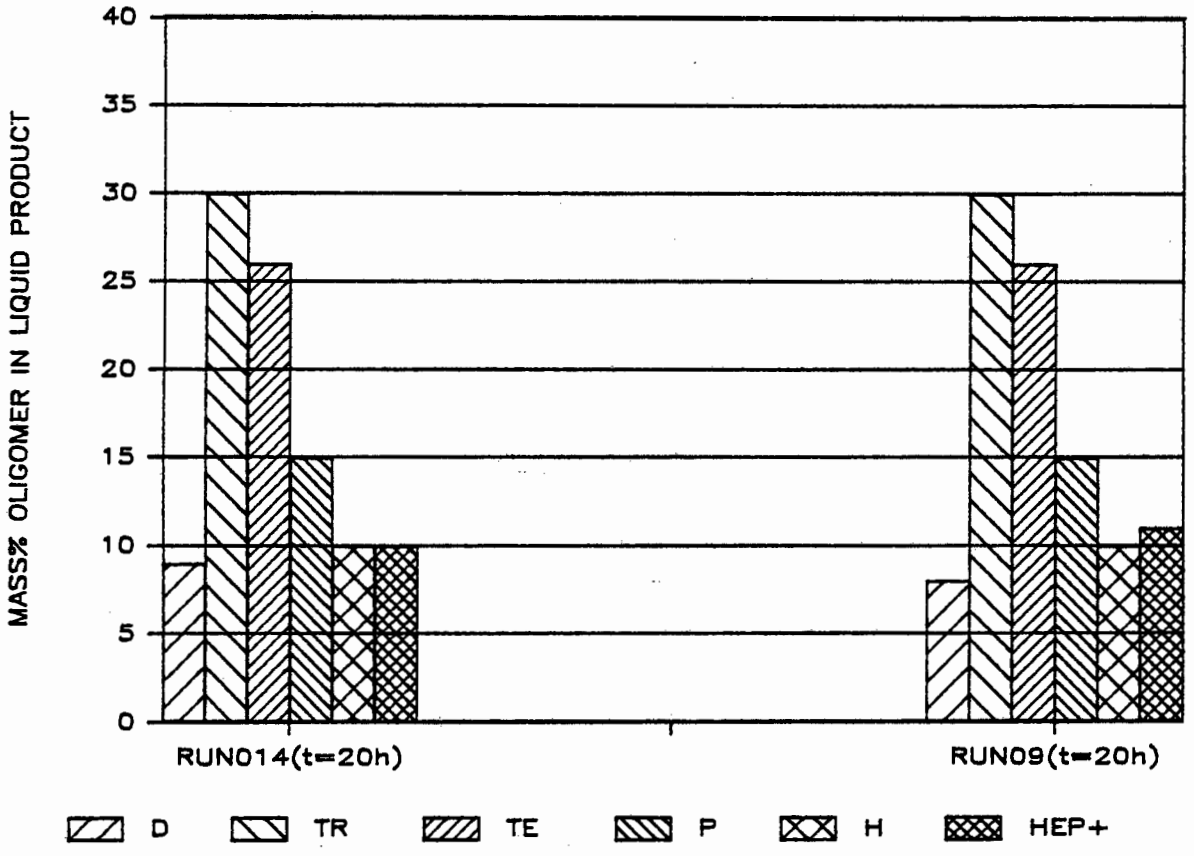

Figure 4.14 Reproducibiltity - selectivity

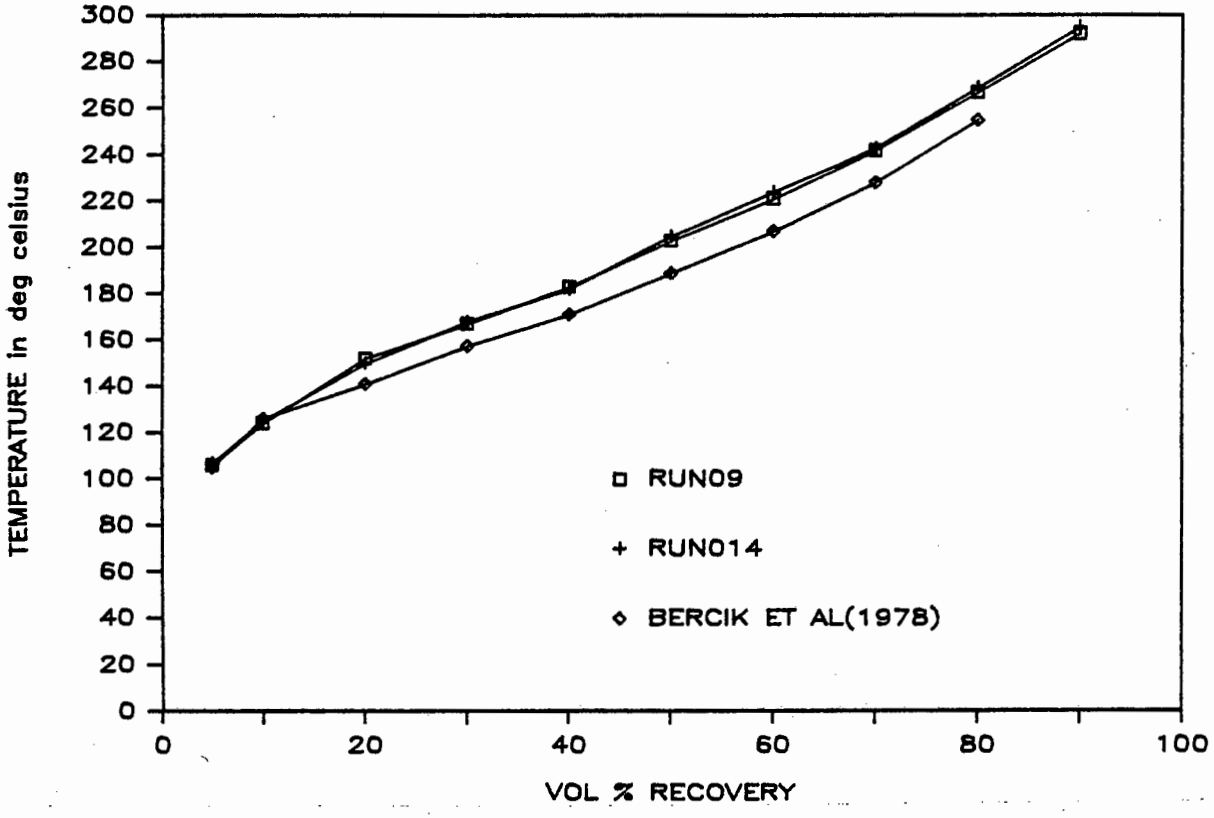

Figure 4.15 ASTM distillations

in Figure 4.15. The synthetic fuel produced is compared with that obtained by Bercik et al (1978) over sulphided NiSMM at a reaction temperature of 433 K and WHSV = 0.98 h^{-1}. The ASTM profiles produced in this study compares well with that obtained by these workers.

It is therefore concluded that adequate reproducibility, with respect to LPR and selectivity, is attained.

4.4.3 OLIGOMERIZATION USING FRAMEWORK NiSMM

In order to establish whether the nickel ion in the matrix improves the catalyst lifetime and activity, propene oligomerization reactions were carried out using 7 % NiSMM and SMM at a reaction temperature of 403 K and WHSV of approx. 8 h^{-1}. Figure 4.16 compares the liquid product formation rate versus time on stream for the two catalysts. It can be seen that NiSMM gives an improved catalyst performance reaching steady state within 2 hours, whereas SMM has a long induction period of 15 h. The reason for the induction period is not known. The run using SMM was repeated and a similar result was obtained. NiSMM with a surface area of 204 m^2g^{-1} shows a higher LPR than SMM (surface area of 107 m^2g^{-1}). However, for both catalysts deactivation occurred after 30 h.

There is no significant difference in selectivity as shown in Figures 4.17 and 4.18, with 60 % of oligomers boiling at over 453 K (diesel fraction). The product spectrum did not vary much over the reaction period. During the induction period product distribution was similar to the steady state sample.

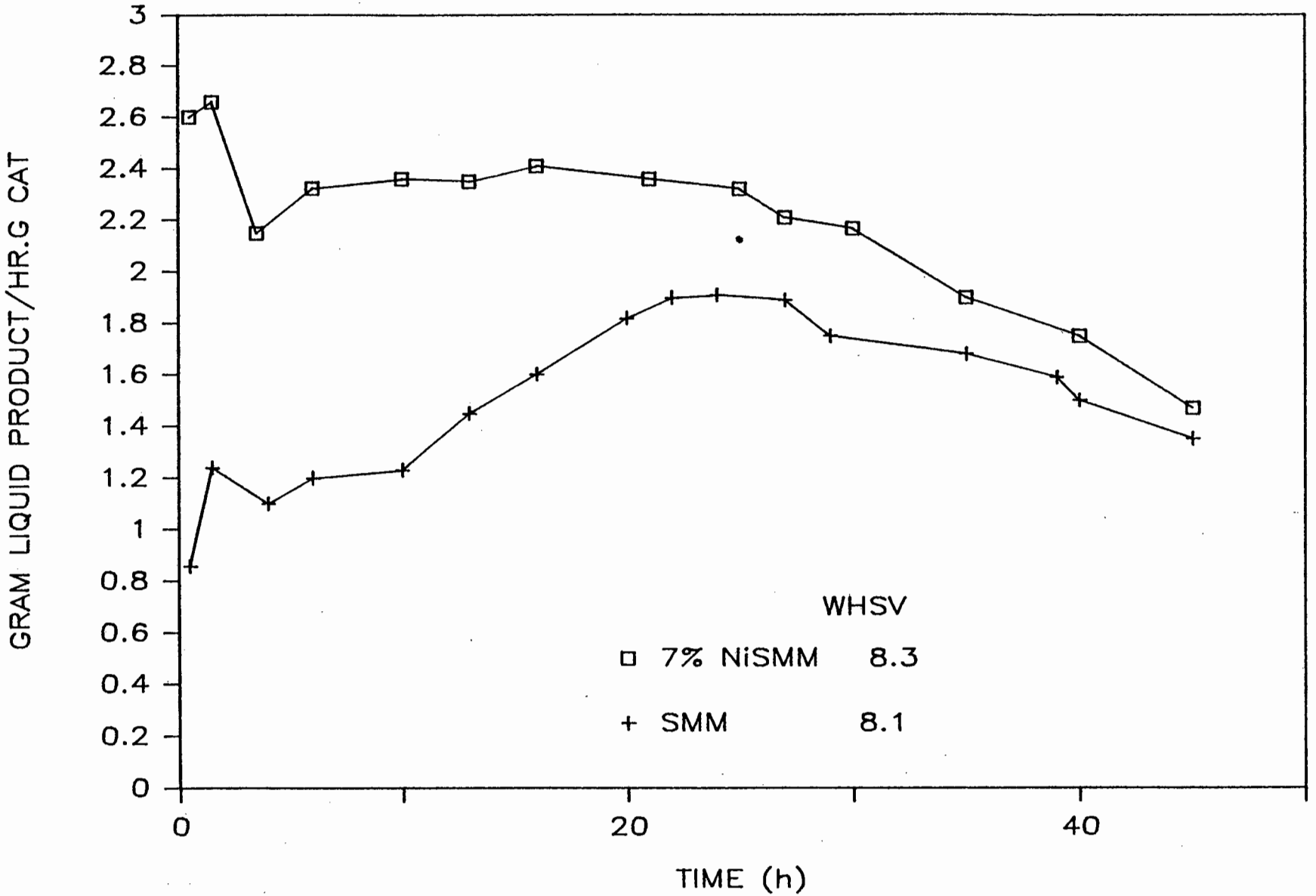

Figure 4.16 NiSMM vs SMM

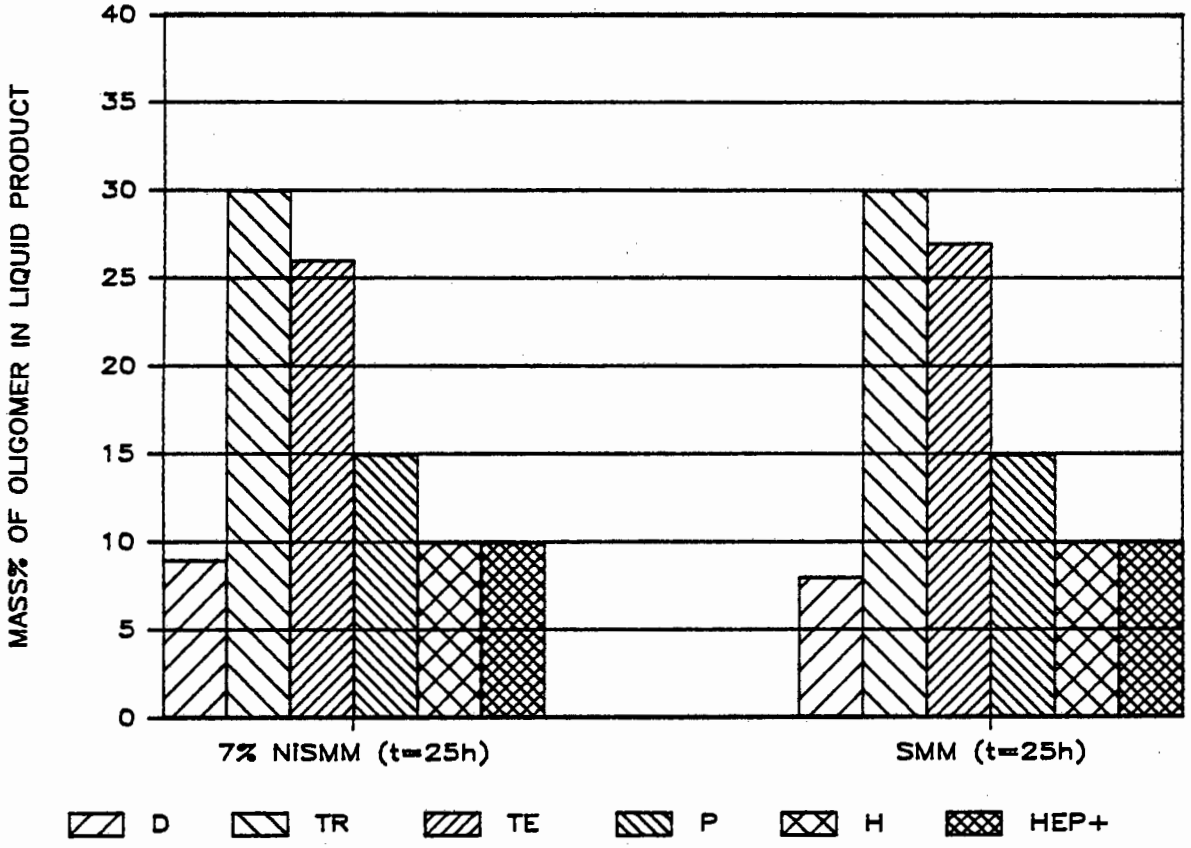

Figure 4.17 Effect of matrix nickel on selectivity

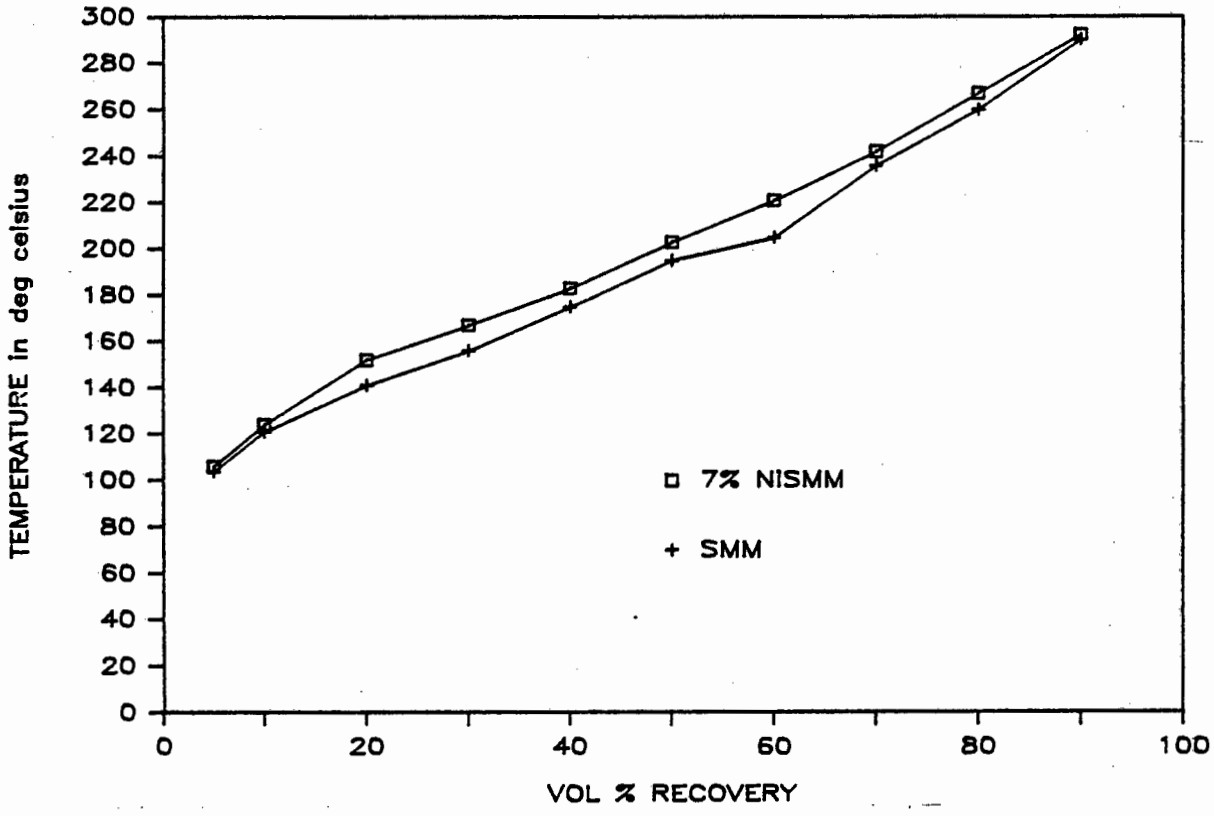

Figure 4.18 ASTM distillation - NiSMM vs SMM

4.4.3.1 EFFECT OF REACTION TEMPERATURE

Figures 4.19 and 4.20 shows the effect of reaction temperature on the performance of NiSMM and SMM, respectively. At reaction temperatures above 450 K, both catalysts deactivate almost immediately. SMM showed higher initial activity at 453 K than at 403 K. NiSMM which was reacted at a slightly higher reaction temperature (473 K) deactivated at a similar rate to SMM.

Figure 4.21 illustrates the effect of reaction temperature on selectivity. It can be seen that initially longer chain products are formed (increase in heptamer fraction). However, as the catalyst deactivates, the trimer fraction increases with corresponding decrease in heavy oligomers resulting in a product distribution similar to that produced over SMM and NiSMM at a reaction temperature of 403 K.

4.4.3.2 EFFECT OF MOISTURE IN THE FEED

Two experiments were conducted in which 7% NiSMM catalyst was calcined at 773 K in dry nitrogen for 4 h, and then exposed to a dry and a wet propene feed. The LPR versus time plots are shown in Figure 4.22. The feed passed over 3A molecular sieves at 24 g/h was found to be essentially water-free. The undried feed contained about 120 ppm_v (51 ppm_w) H_2O as calculated using a hygrometer.

From Figure 4.22 it can be seen that the presence of the water in the feed greatly reduced the catalyst lifetime even though initial activity was reasonably high. The catalyst was at half its initial activity after 8 hours on stream. No steady state period as with the dry feed run occurred. No temperature runaway occurred as was observed by

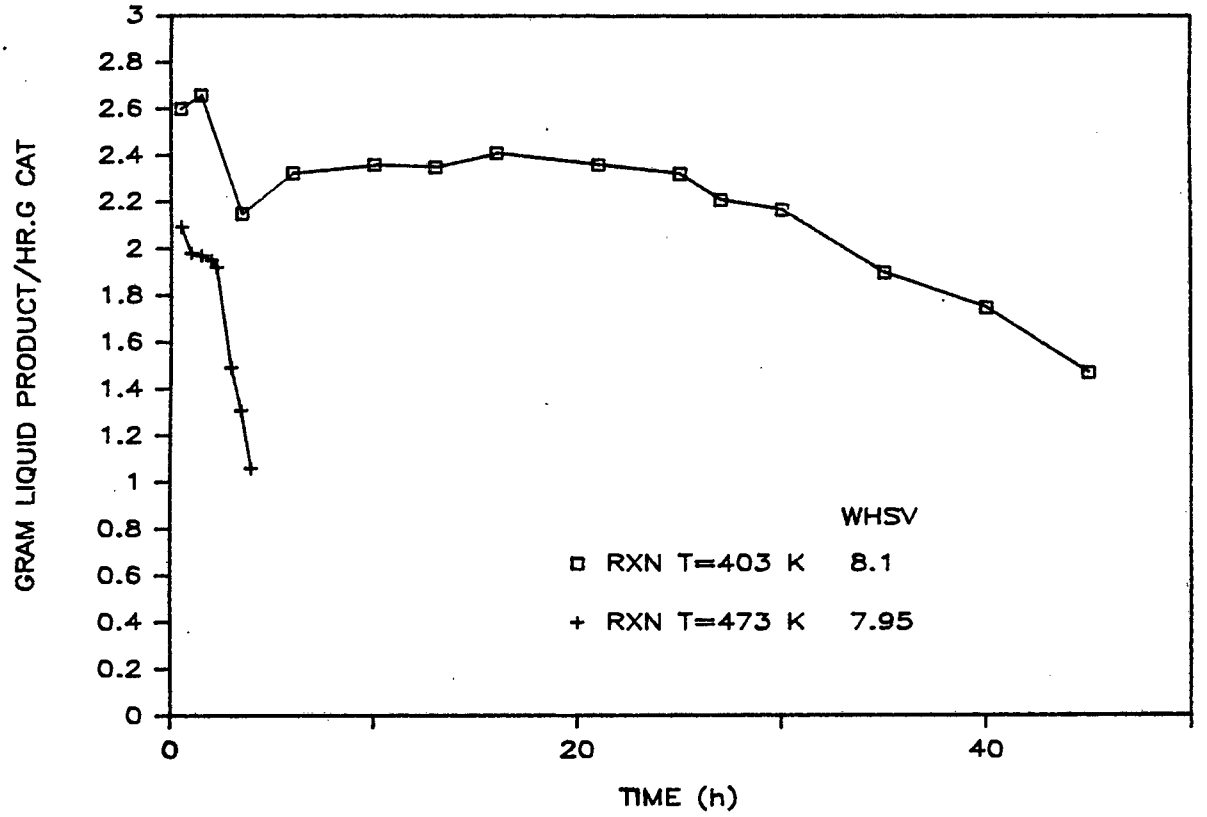

Figure 4.19 Effect of reaction temperature - 7% NiSMM

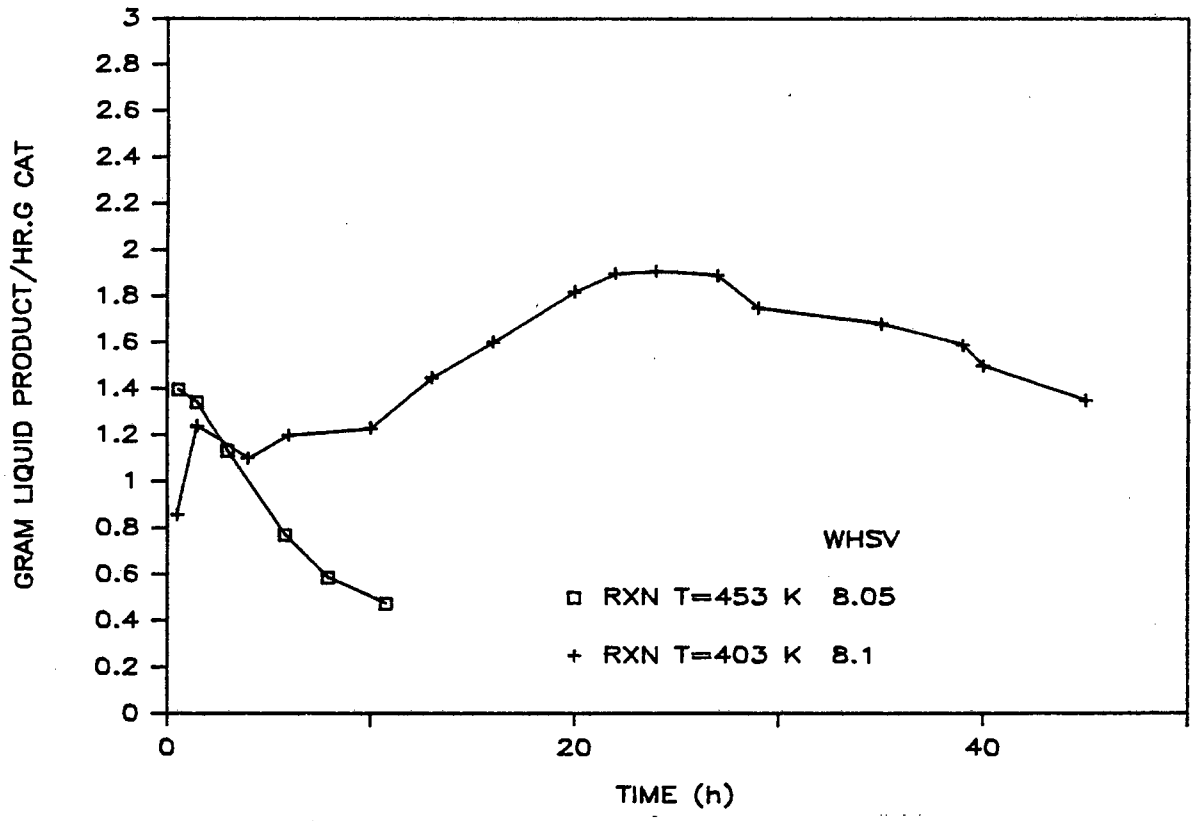

Figure 4.20 Effect of reaction temperature - SMM

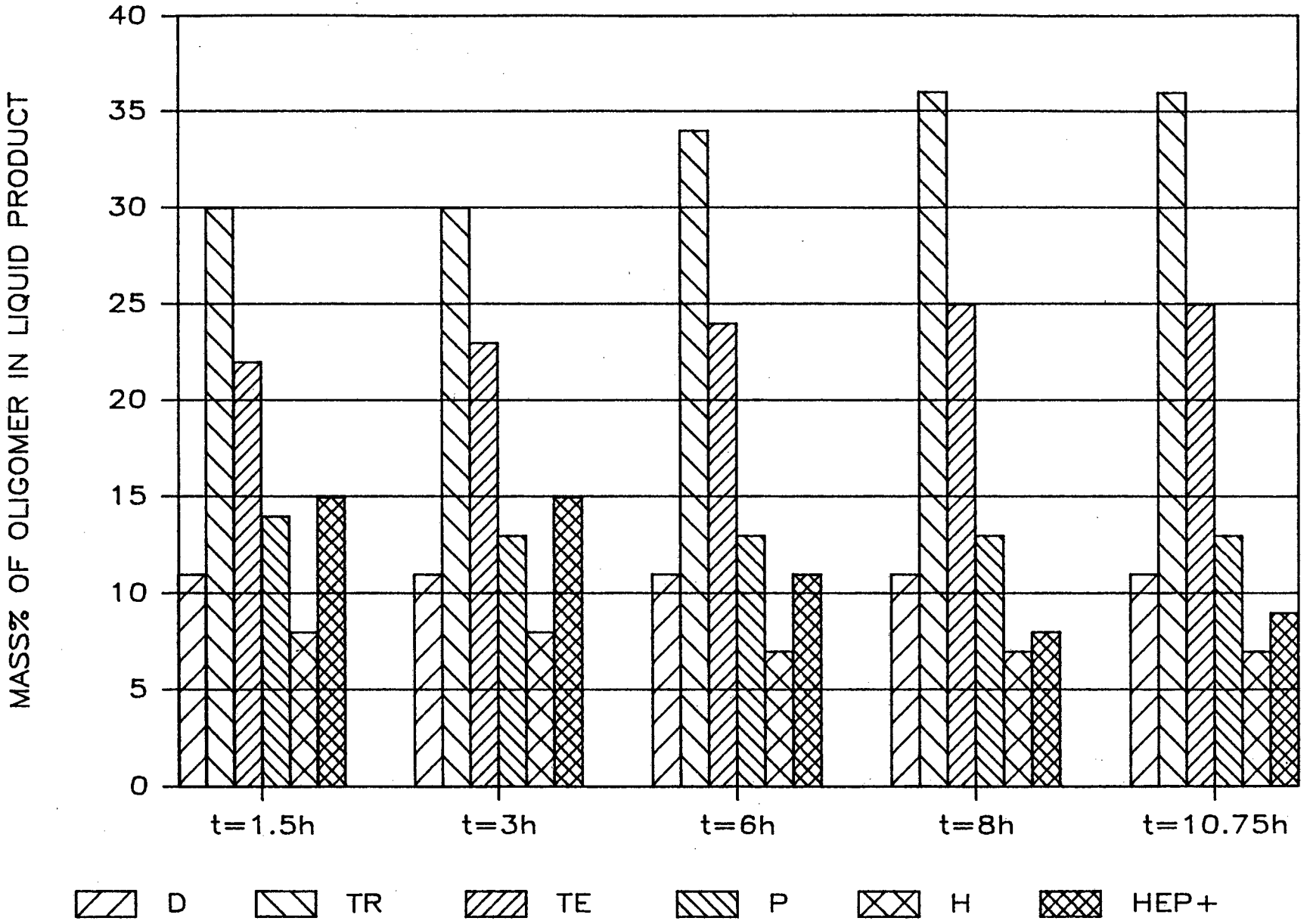

Figure 4.21 Effect of reaction temperature on selectivity

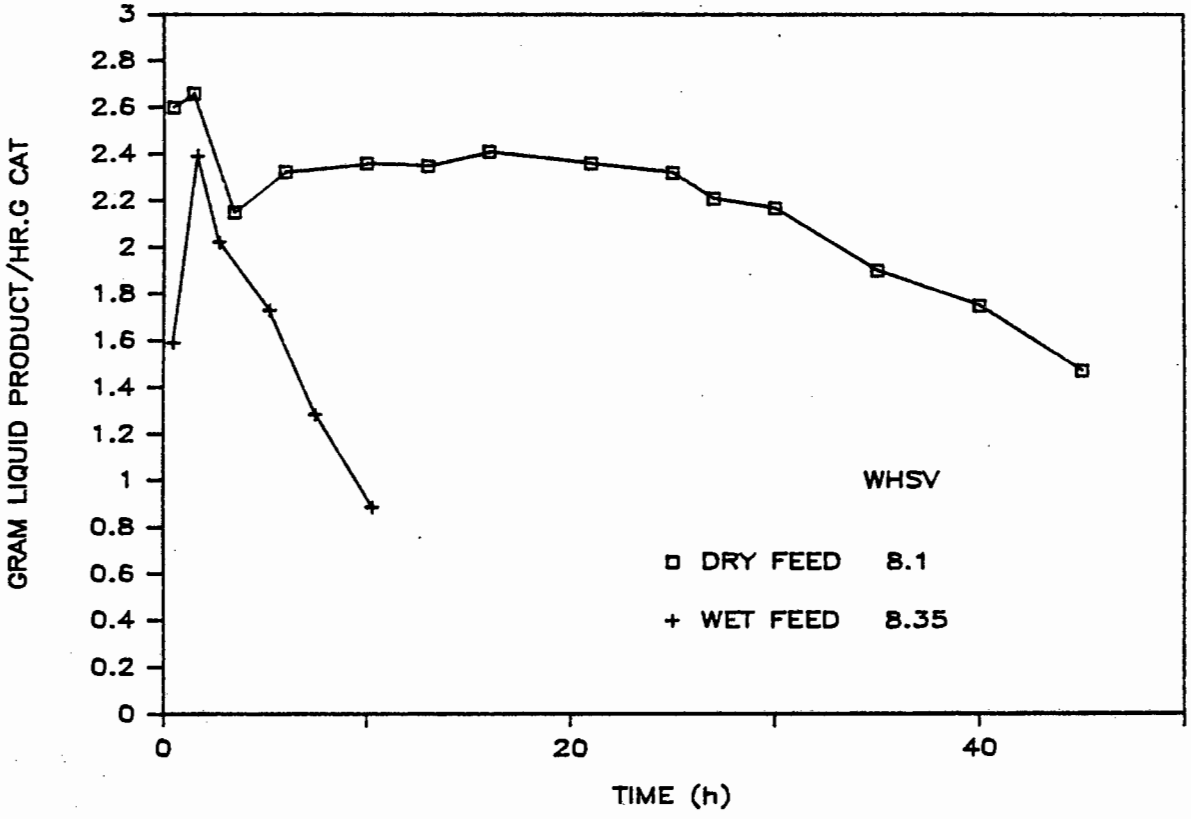

Figure 4.22 Effect of moisture in feed

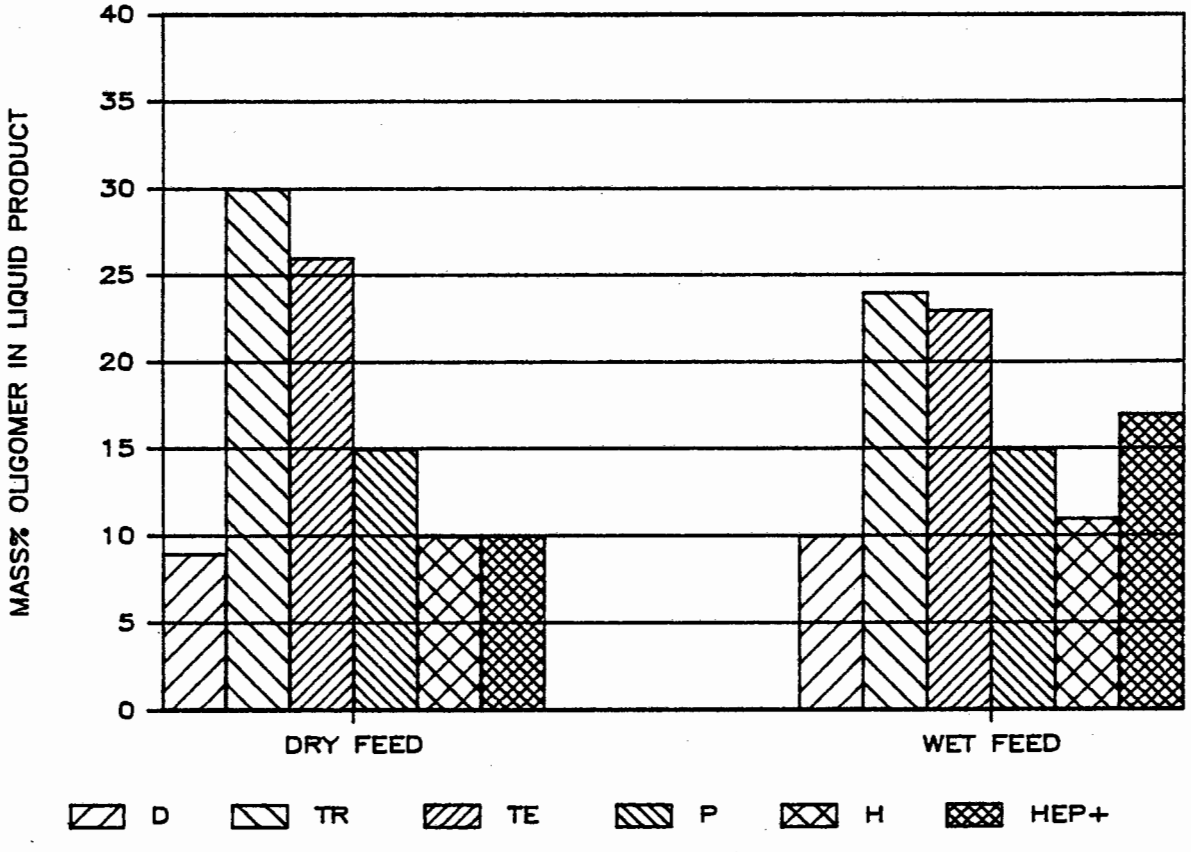

Figure 4.23 Selectivity: wet vs dry feed

Fletcher (1984) when he performed a similar experiment using SMM as catalyst (WHSV = 1.9 h^{-1}, reaction temp. = 440 K).

The product spectrum of the liquid samples for the wet feed run showed a marked shift towards longer chain products over the entire reaction period. The products of wet and dry feed runs are compared in Figure 4.23. A decrease in the trimer and tetramer fractions is observed for wet feed while there is an increase in hexamer and heptamer fractions.

4.4.3.3 LONG RUN AT TYPICAL INDUSTRIAL CONDITIONS

An experimental run was conducted at a lower WHSV (1.6 h^{-1}) using 1/16" extrudates of 7% NiSMM catalyst. The primary purpose of the run was to collect sufficient quantities of the liquid product to perform complete characterization of the gasoline (C_5 - C_{12}) and diesel (C_{13} - C_{18}^{+}) fractions. The catalyst, which was calcined at 773 K for 4 h, occupied a bed volume of 14 cm^3. The feed rate was held at 24 g/h.

A mass % conversion - time plot is shown in Figure 4.24. It can be seen that the catalyst reached a conversion of 90 % almost immediately and maintained this steady state conversion for 72 h. The deactivation of the extruded catalyst was fairly rapid. The mass % oligomer fraction over the reaction period is shown in Figure 4.25. The product spectrum remained the same over the entire steady state region and was similar to that obtained using the powder form of 7% NiSMM at WHSV of 8 h^{-1}, as shown in Table 4.8.

The liquid samples were treated with an antioxidant, Ethyl 733 to prevent possible deterioration during fuel characterization tests, the results of which are documented in Section 4.4.7.3.

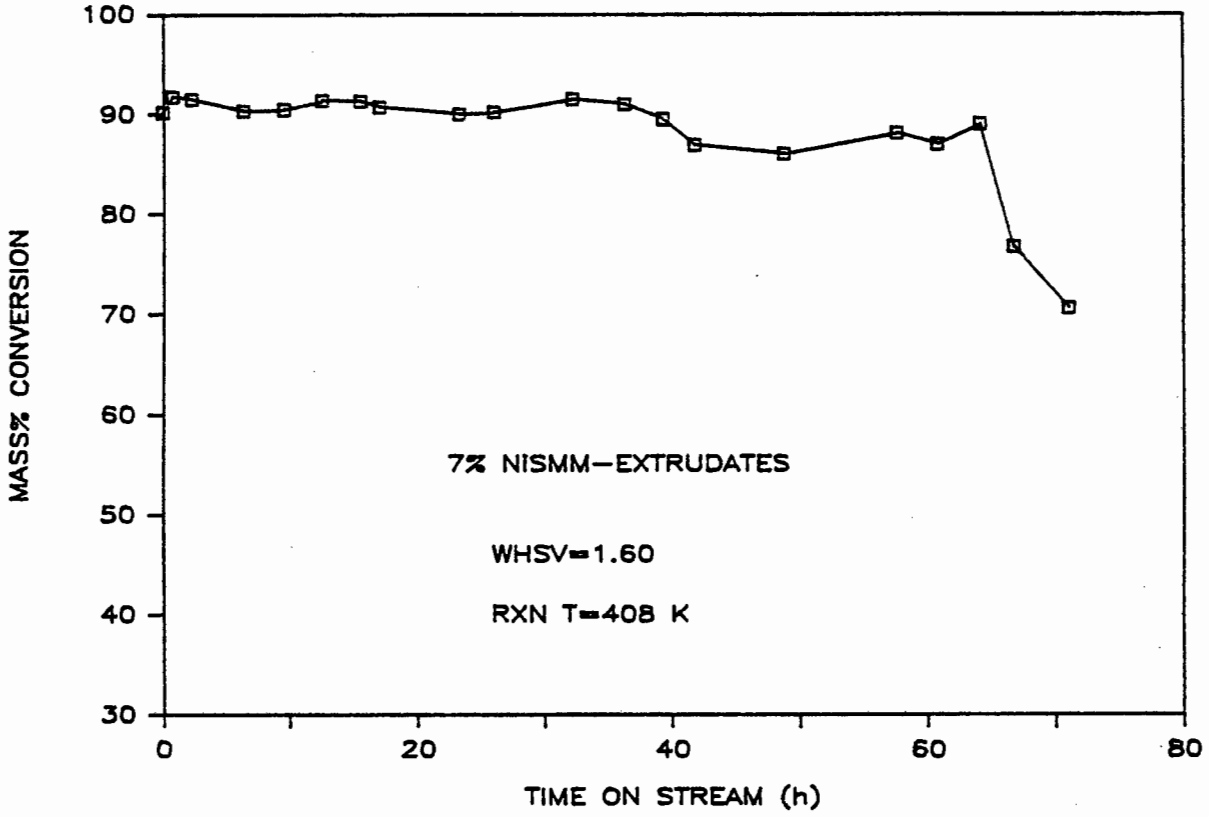

Figure 4.24 Long run at typical conditions

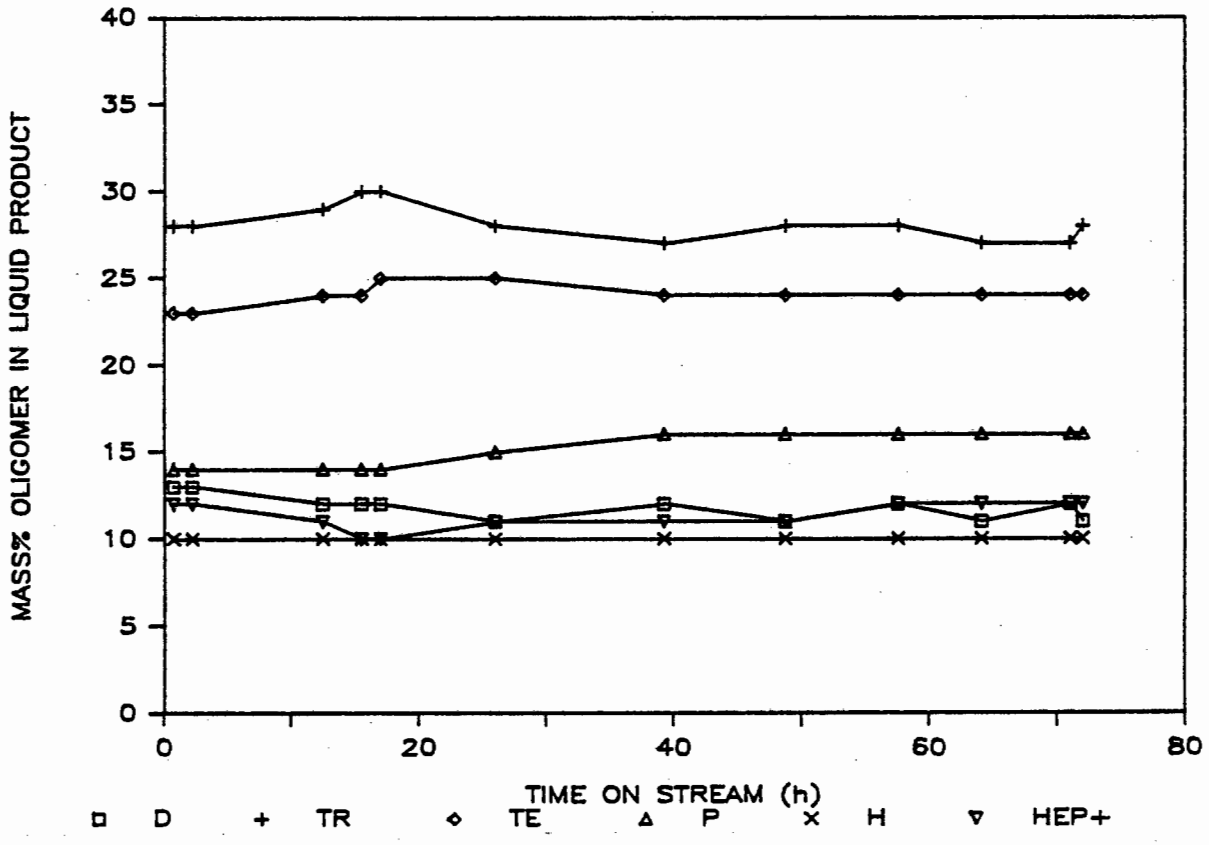

Figure 4.25 % Oligomer versus time

MASS % OLIGOMER	NiSMM (106 - 212 MICRON) WHSV = 8 h^{-1}	NiSMM (EXTRUDATES) WHSV = 1.6 h^{-1}
Dimer	9	11
Trimer	30	28
Tetramer	26	24
Pentamer	15	16
Hexamer	10	9
Heptamer+	10	12

Table 4.8 Extrudate Form vs Powder Form - Selectivity

4.4.4 OLIGOMERIZATION USING NICKEL ION EXCHANGED SMM (NiIXSMM)

It has been established that nickel ions cause appreciable activity of the catalyst at a reaction temperature of 363 K. The objective of these experiments was to investigate the nickel (2+) ion effect at 405 K. 1% NiIXSMM and 9.5% NiIXSMM contained 0.057 weight % nickel and 0.54 weight % Ni, respectively.

The effect of introducing Ni^{2+} ions in the interlayer spaces of SMM is shown in Figure 4.26. The 'induction' period which occurred with propene oligomerization over SMM was also observed for the nickel exchanged SMM catalysts. 1% NiIXSMM (0.057% Ni) gave higher oligomerizing activity. However, SMM and 1% NiIXSMM had similar lifetime characteristics. 9.5% NiIXSMM (0.54% Ni) gave a poorer performance than SMM and 1% NiIXSMM and had a shorter catalyst lifetime. It appears that there is an optimum nickel ion loading for propene oligomerization over the ion exchanged catalysts.

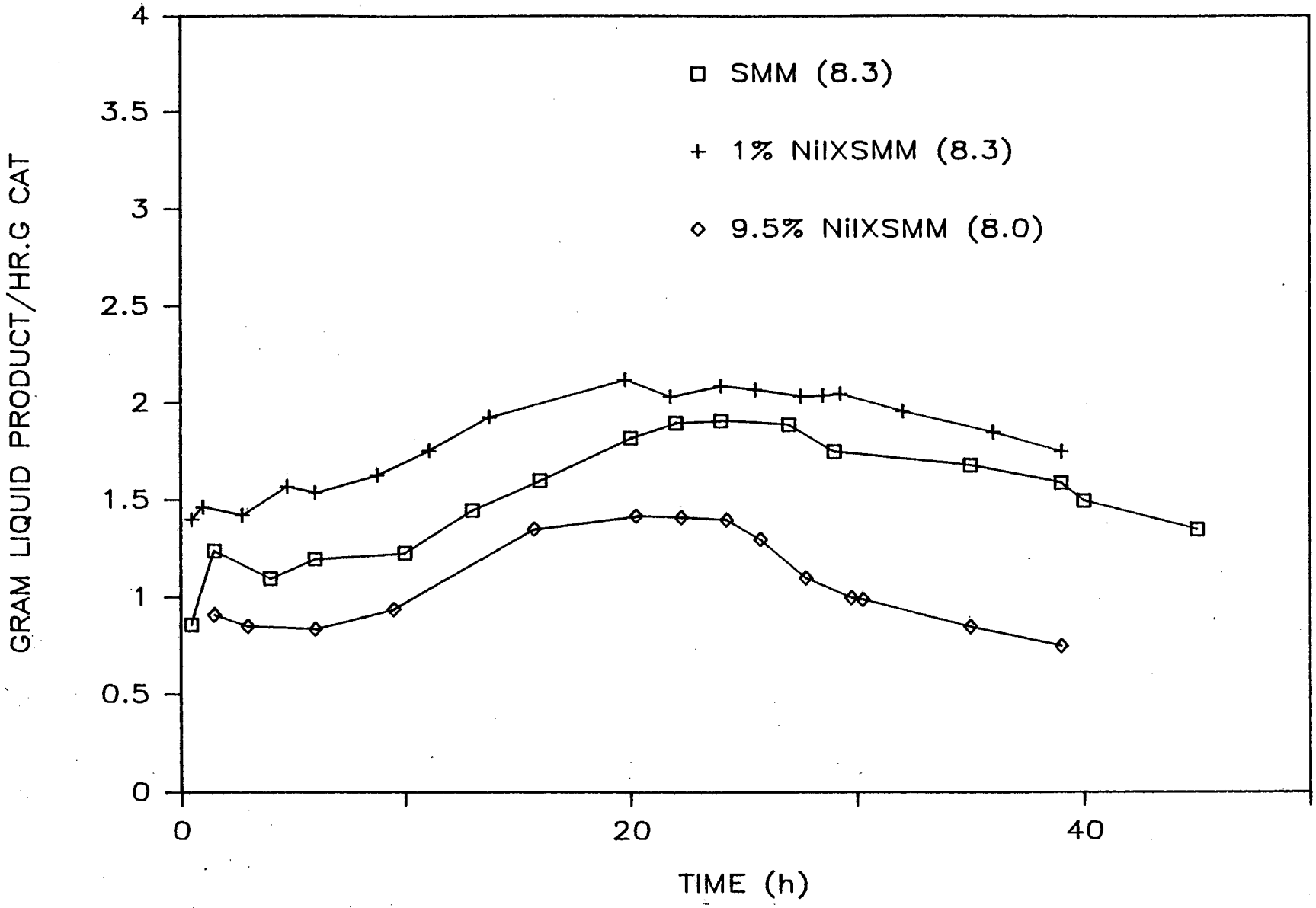

Figure 4.26 Effect of nickel(2+) ions on activity
* WHSV in brackets

The product distribution was found to be similar over the entire reaction period. Product selectivity for oligomerization over SMM, 1% NiIXSMM and 9.5% NiIXSMM is shown in Figure 4.27. There was no significant difference in the oligomer fractions of the liquid product for the three catalysts.

4.4.5 EFFECT OF REDUCTION

It has been reported that upon reduction of NiSMM, an improvement in the catalytic activity for hydroisomerization and hydrocracking was observed (Black and Swift, 1974). In this series of experiments, the effect of reducing the matrix nickel in NiSMM and the interlayer nickel ions in NiIXSMM on the propene oligomerization reaction is investigated.

4.4.5.1 7% NiSMM

The catalyst activity and lifetime for the oligomerization over 7% NiSMM, reduced at 723 K and 763 K, respectively, were compared to unreduced NiSMM. The catalysts were reduced for 16 h at their respective reduction temperatures. Figure 4.28 shows the effect of reducing the framework nickel on the activity and lifetime. Reaction over both the reduced catalysts resulted in a shorter catalyst lifetime, although they showed high initial activity. 7% NiSMM which was reduced at 723 K, gave a more steady performance than that reduced at 763 K where the onset of deactivation was almost immediate. It should be noted that the 7% NiSMM, reduced at 763 K, gave an optimum nickel dispersion as determined by ethane hydrogenolysis reactions (Section 4.3). It appears from these results that the more severe the reduction

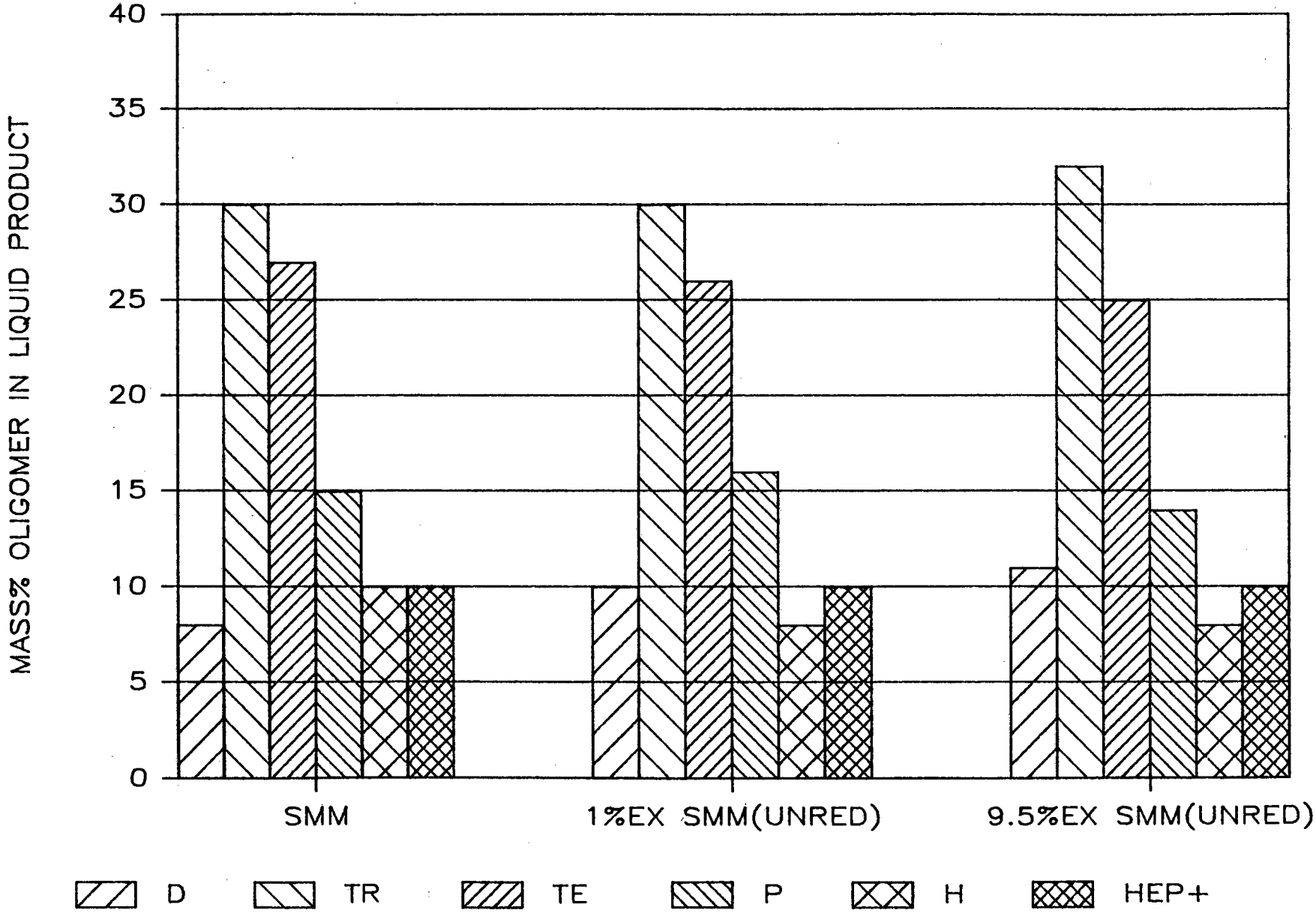

Figure 4.27 Selectivity:effect of Ni^{2+} ions

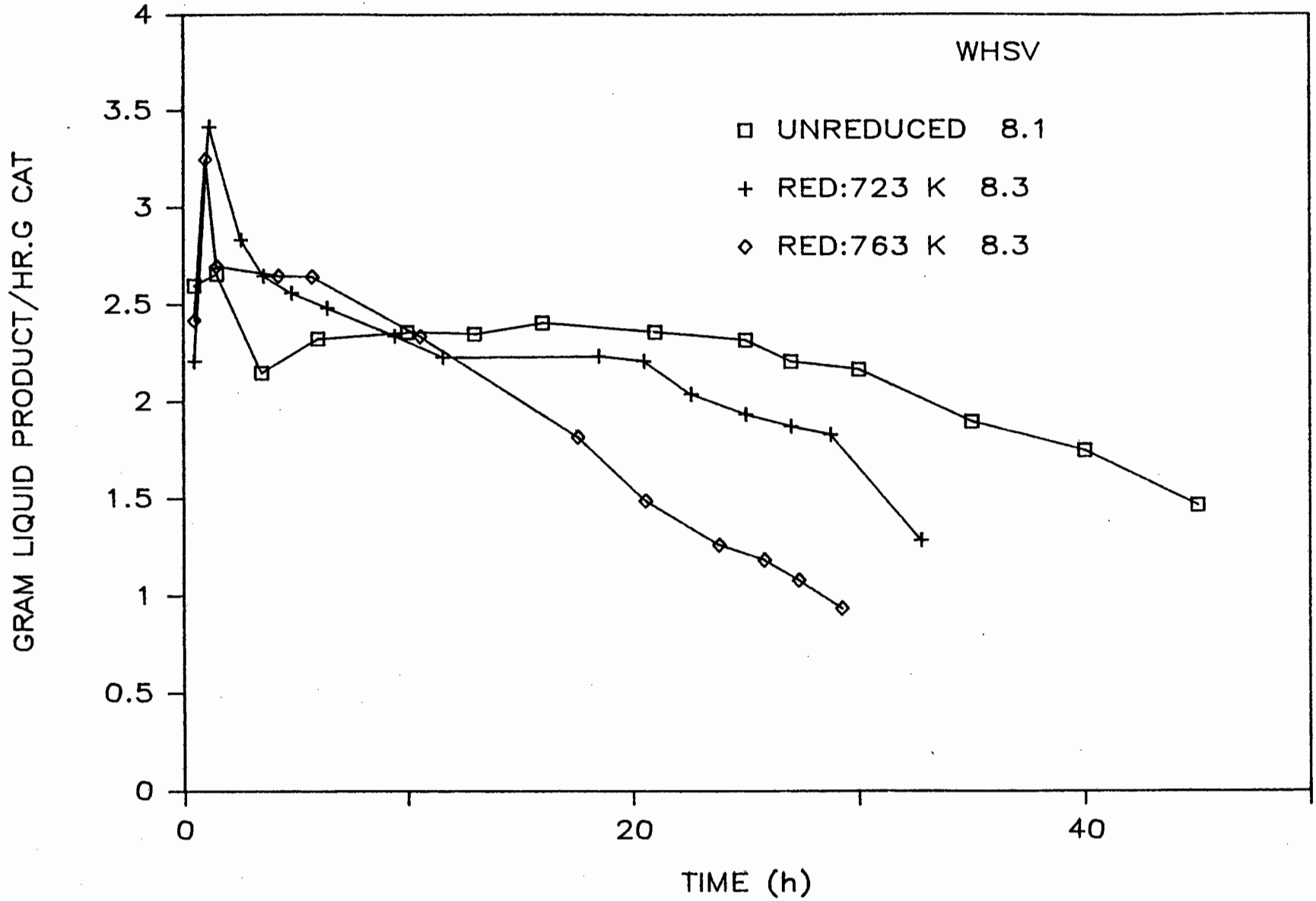

Figure 4.28 Reduction of 7% NiSMM

treatment the poorer the catalyst performance.

A comparison of the liquid product distribution is given in Figure 4.29. It can be seen that during the initial period of high activity (reduced 7% NiSMM) long chain products were formed as was observed when reacting at high temperature (453 K). However, there was an increase in trimer and tetramer fraction with time resulting in a similar product to that of the steady state liquid sample of unreduced NiSMM.

4.4.5.2 NICKEL ION-EXCHANGED SMM (NiIXSMM)

Figures 4.30 and 4.31 illustrate the effect of reducing the interlayer Ni^{2+} ions for propene oligomerization over 1% NiIXSMM (0.057% Ni) and 9.5% NiIXSMM (0.54% Ni), respectively. The exchanged catalysts were calcined at 773 K for 4 h and reduced at 723 K for 16 h. A marked improvement in the catalyst performance can be seen with the disappearance of the induction period, characteristic of the unreduced NiIXSMM, upon the reduction of the interlayer Ni^{2+} ions. 1% NiIXSMM showed a high LPR, but deactivated more rapidly than the unreduced form. However, the cumulative liquid recovery in 30 h for the reduced 1% NiIXSMM was about 1.3 times that of unreduced 1% NiIXSMM. The reduced 9.5% NiIXSMM was a much more active catalyst and its activity remained higher than the unreduced form. 1% NiIXSMM was more active than 9.5% NiIXSMM, but its deactivation rate was higher.

The product spectrum of the liquid samples resulting from reaction over reduced NiIXSMM was similar to that of the unreduced form throughout the reaction period, as shown in Figure 4.32. During initial reaction there was no shift to heavy oligomers as was the case upon the reduction of 7% NiSMM.

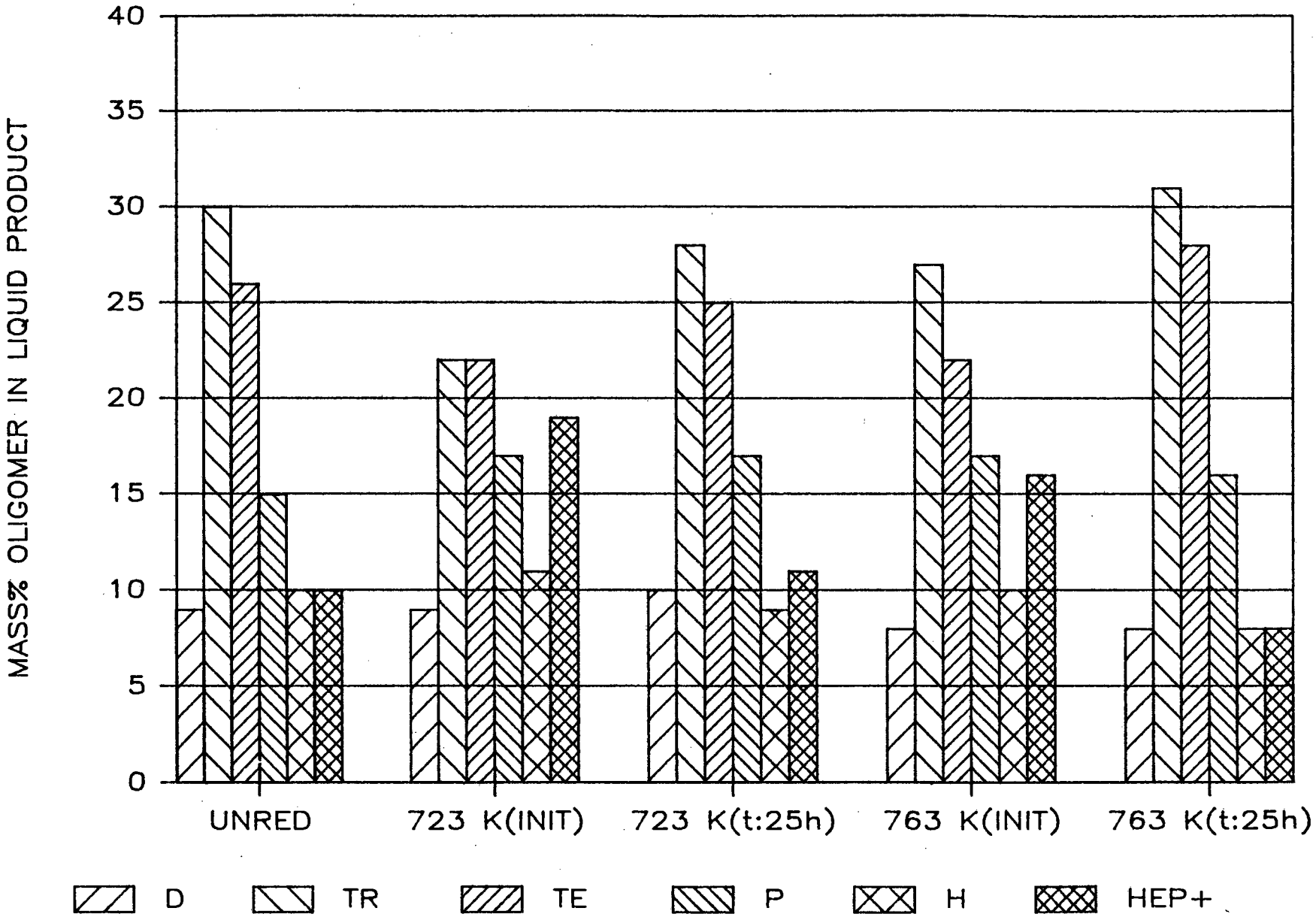

Figure 4.29 Selectivity:effect of reduction - 7%NiSMM

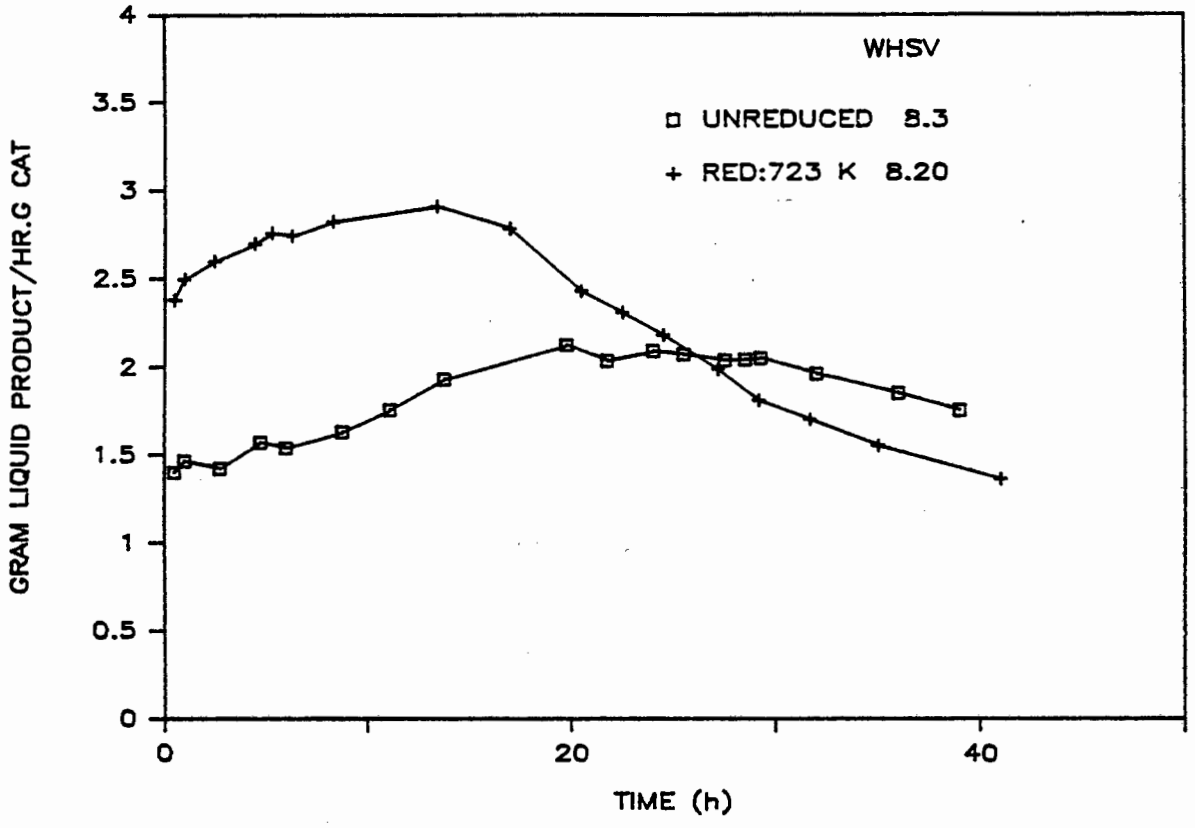

Figure 4.30 1% NiIXSMM - effect of reduction

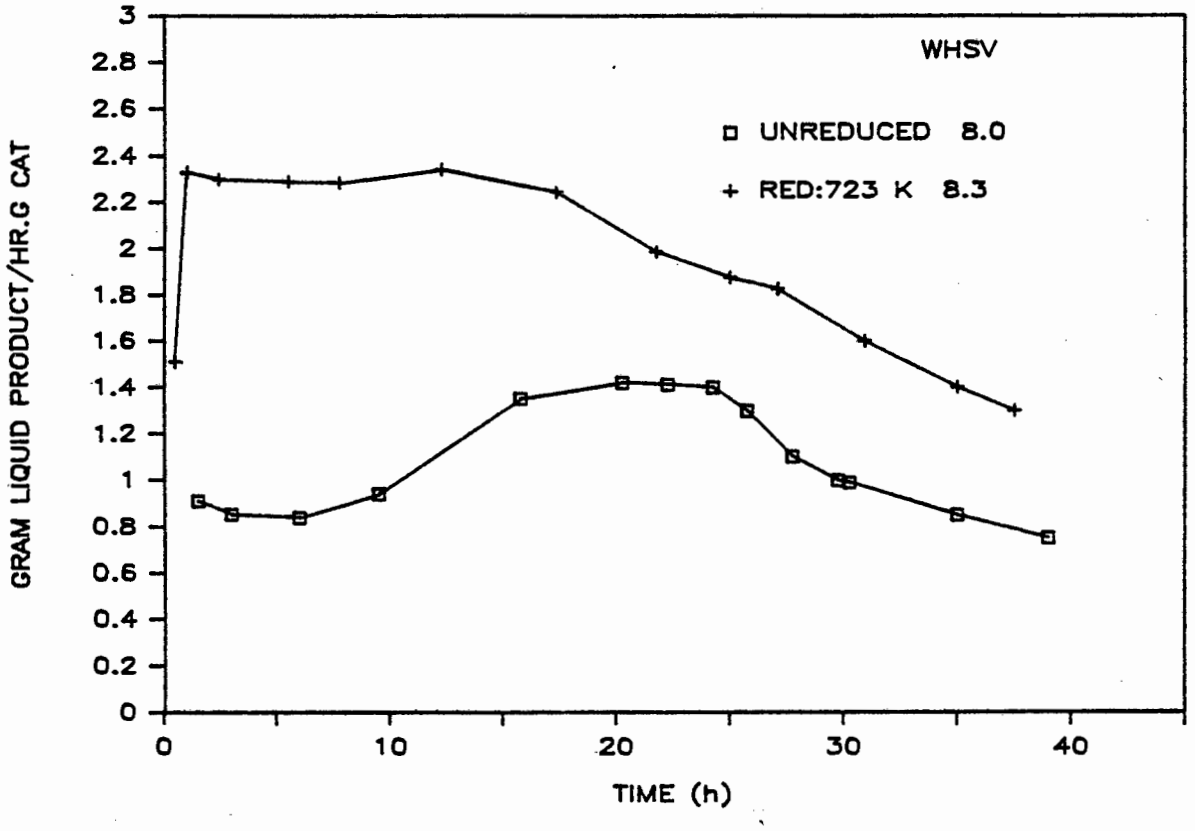

Figure 4.31 9.5% NiIXSMM - effect of reduction

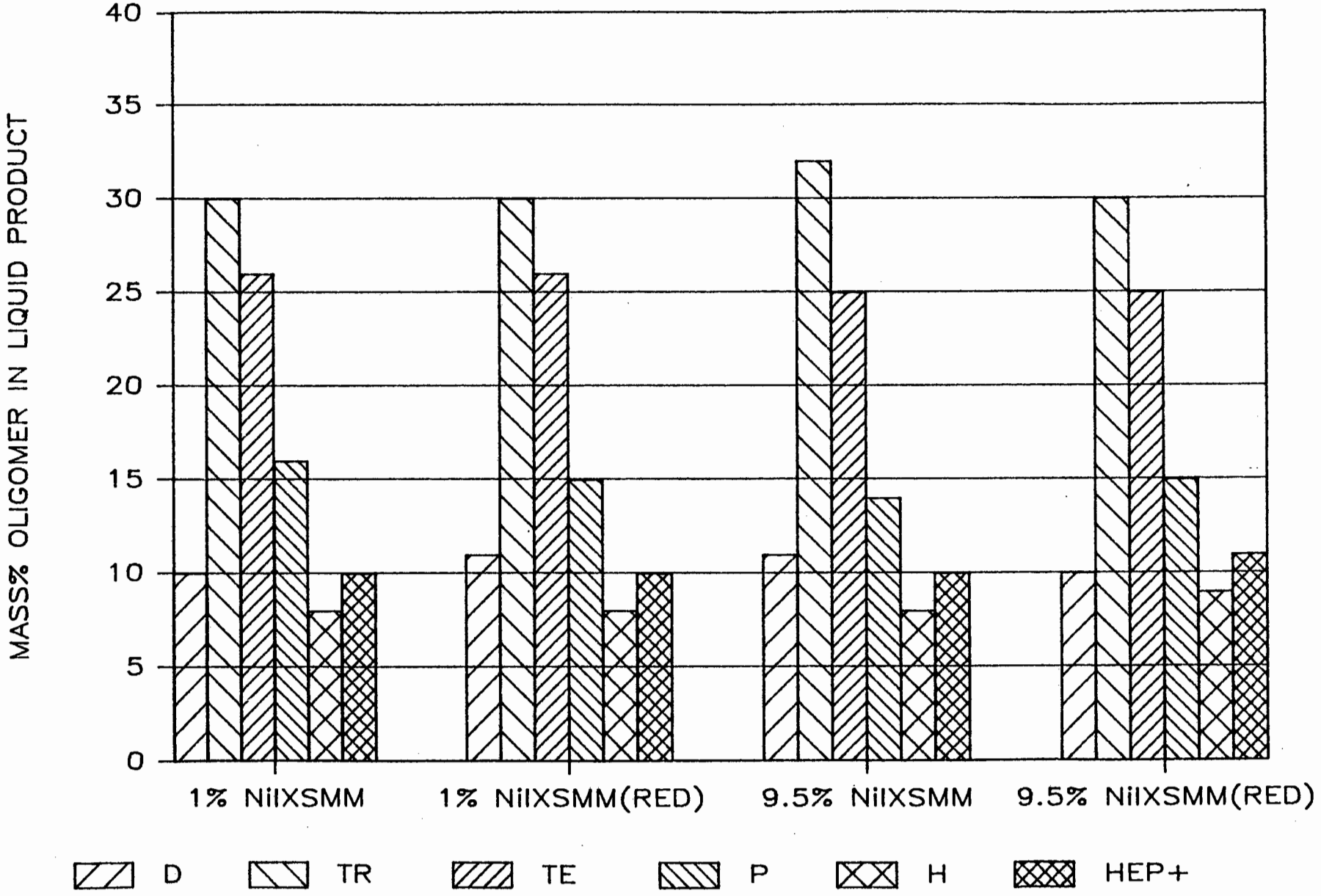

Figure 4.32 Selectivity:reduction of interlayer Ni ions

4.4.5.3 CARBON MONOXIDE TREATMENT OF REDUCED NiSMM

In order to establish the significance of the metallic nickel formed on reduced NiSMM, the reduced samples were subjected to CO treament at 413 K. The metallic nickel is removed as Ni $(CO)_4$ gas. 7% NiSMM samples were calcined at 773 K for 4 h and reduced at 763 K for 16 h. The catalysts were then treated with CO for :

- 5 h, which resulted in 17% removal of the nickel present as determined by AA analysis of the nitric acid solution;
- 24 h, which resulted in 31% removal of the nickel present.

Figure 4.33 shows the effect of the CO treatment of reduced NiSMM. The CO-treated catalyst gave higher activity than the reduced NiSMM. Although the 5 h CO treated NiSMM had a higher activity during first 15 h, it deactivated rapidly. The 24 h CO treated sample had a lower activity than the 5 h CO treated catalyst but exhibited longer lifetime. From these results it is clear that the metallic nickel affects the catalyst performance since the acidic sites remain constant for all three runs. The results again suggest that there is an optimum metallic nickel loading.

Selectivity data for the CO treated NiSMM are plotted in Figure 4.34 and 4.35. The liquid product spectra resulting from reaction over the 5 h CO treated NiSMM showed a similar trend to that of reduced NiSMM, with the formation of heavy oligomers initially. There was an increase in lower chain products with time on stream. However, in the case of 24 h CO treated NiSMM, a more constant product spectrum were observed. It should be noted that there was a shift to long chain oligomers initially as shown in Figure 4.35.

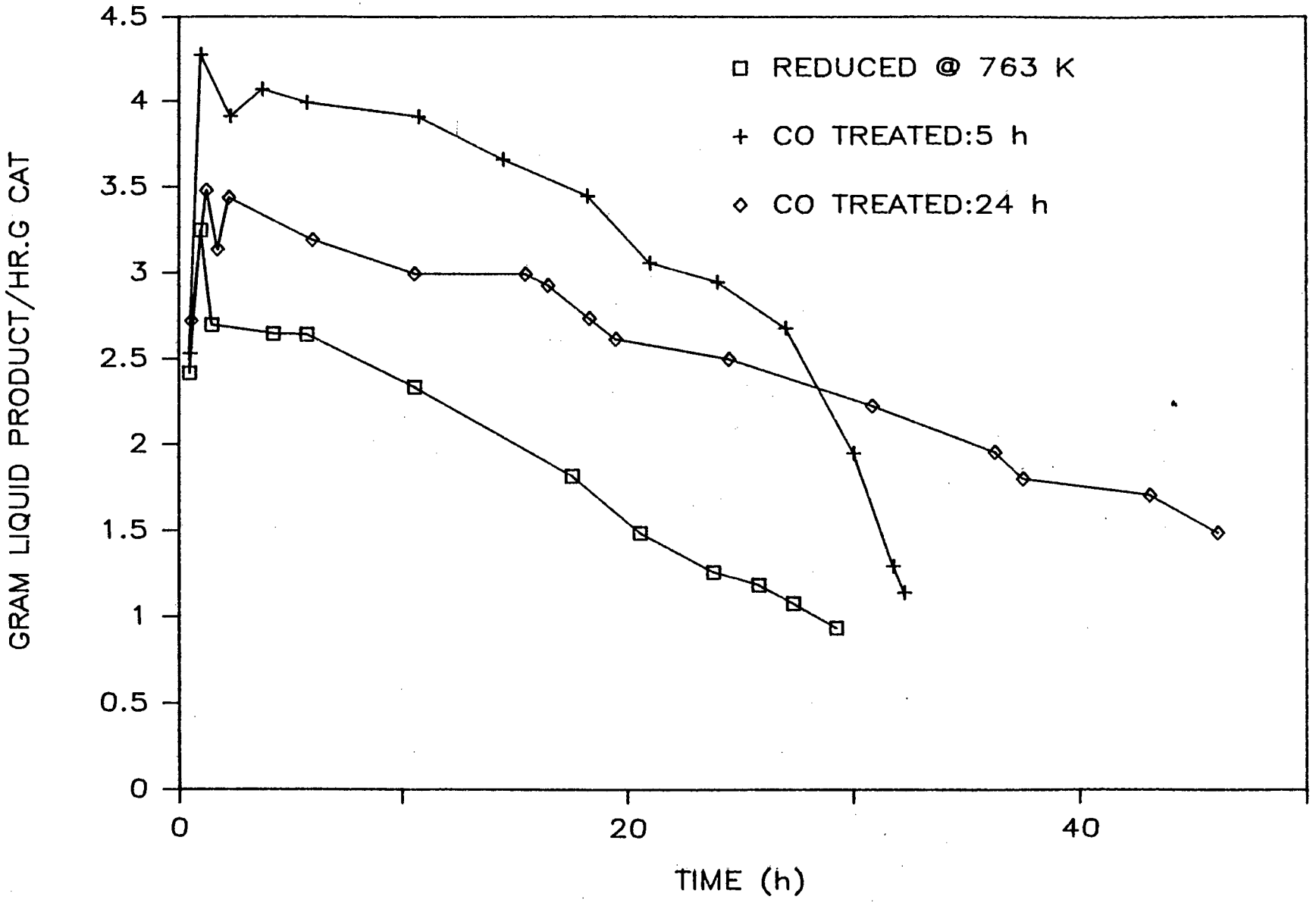

Figure 4.33 CO treatment of reduced 7% NiSMM

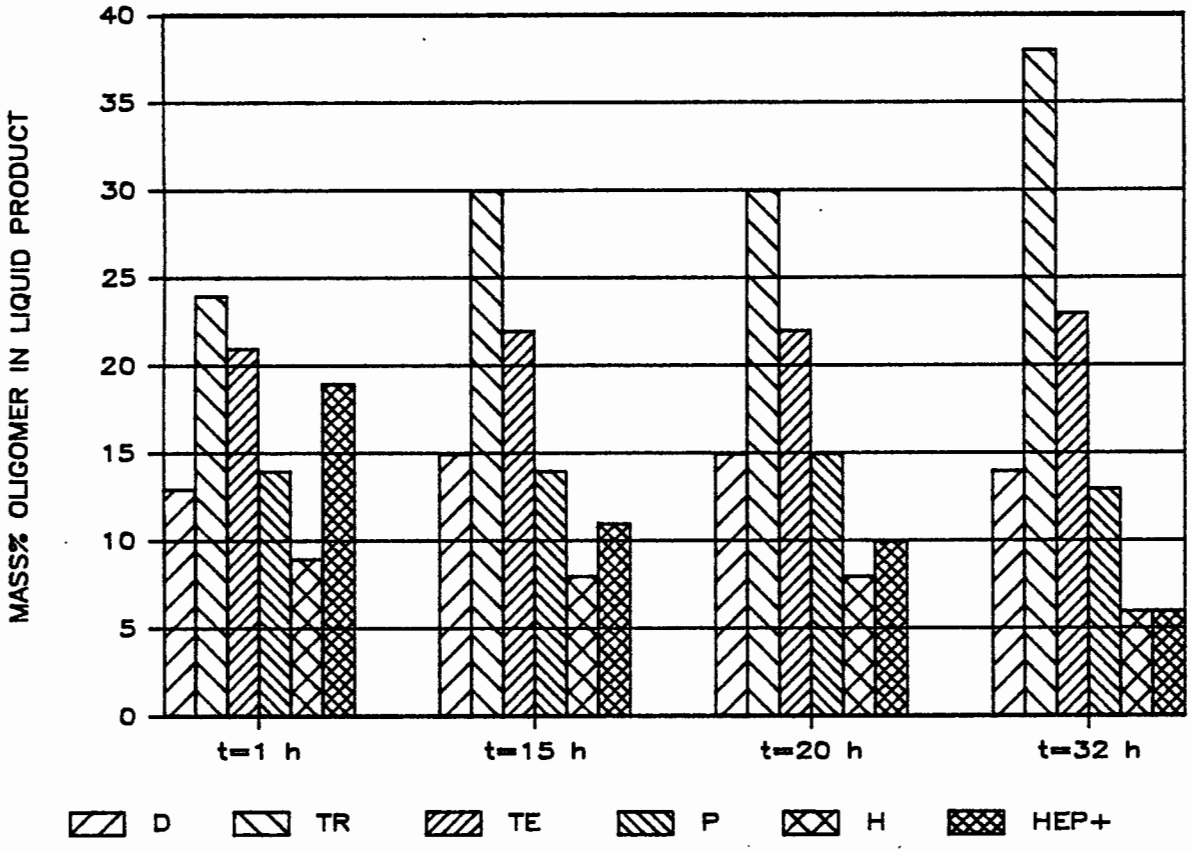

Figure 4.34 % Oligomer versus time (CO treatment:5 h)

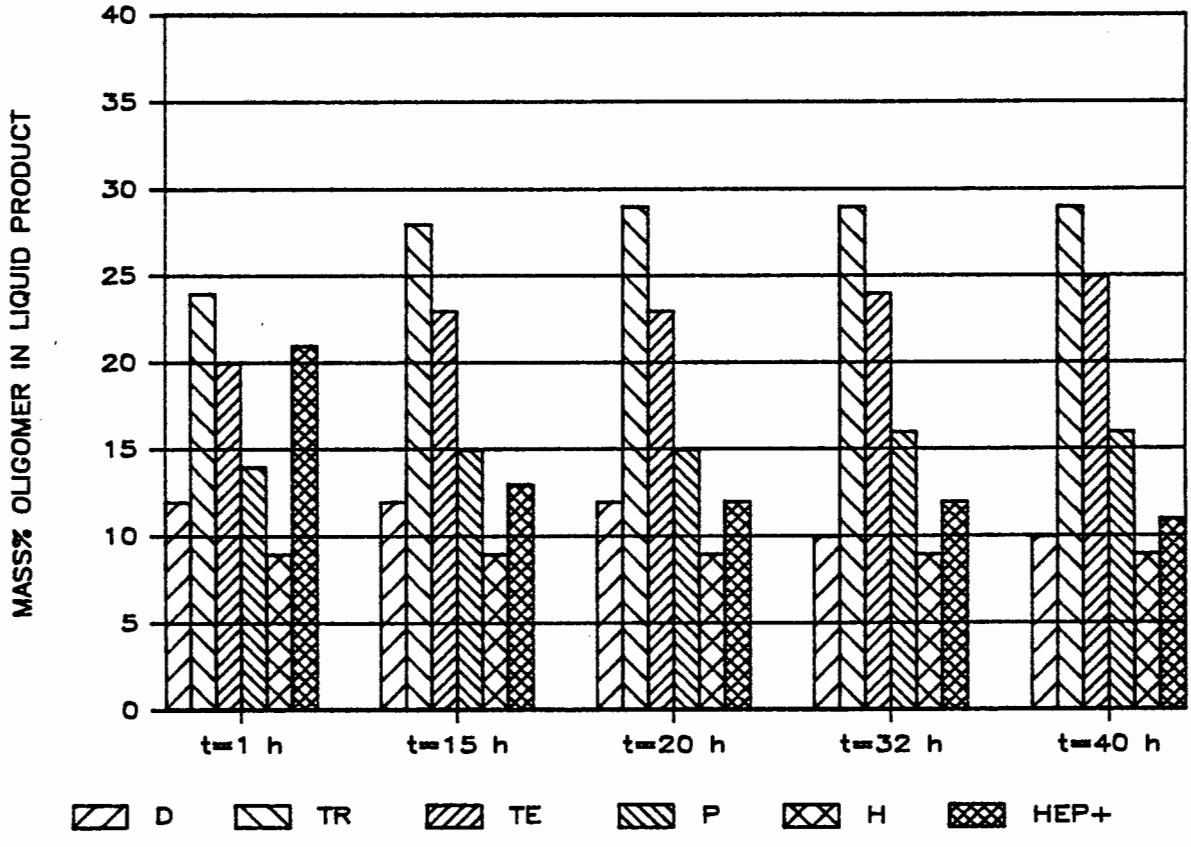

Figure 4.35 % Oligomer versus time (CO treatment:24 h)

Figure 4.36 compares the different forms of 7% NiSMM viz, unreduced, reduced at 763 K and 24 h CO treated. The CO treated NiSMM had a similar catalyst lifetime to the unreduced NiSMM. However, it produced more liquid fuel during first 20 h. Both the CO treated and reduced NiSMM showed appreciable initial activity.

4.4.6 THE INTRODUCTION OF OTHER EXCHANGE TRANSITION METAL IONS IN THE SMM STRUCTURE

The introduction of low concentrations of nickel ions (0.05 wt %) improved the activity of SMM. The effects of introducing the transition metal ions, cobalt and zinc, were investigated. Approximately 0.05 weight % of the particular ion was incorporated as described in Section 4.1. The catalysts were calcined at 773 K for 4 h and the reaction temperature was 405 K. As can be seen from Figure 4.37, the metal ion present affected the catalyst performance in significantly different ways.

CoIXSMM gave on appreciable initial activity, followed by immediate deactivation. The oligomerization run using ZnIXSMM showed a similar induction as in the case of reaction over SMM and NiIXSMM. However, the catalyst was far more active and had a lifetime similar to that of NiIXSMM.

The product distribution as shown in Figure 4.38 and 4.39 for CoIXSMM and ZnIXSMM, respectively, was not markedly different from that of reaction over NiIXSMM. However, there was an increase in the trimer and tetramer fractions with corresponding decrease in heavier fraction with time. In the case of ZnIXSMM, the product distribution was similar over the entire reaction period.

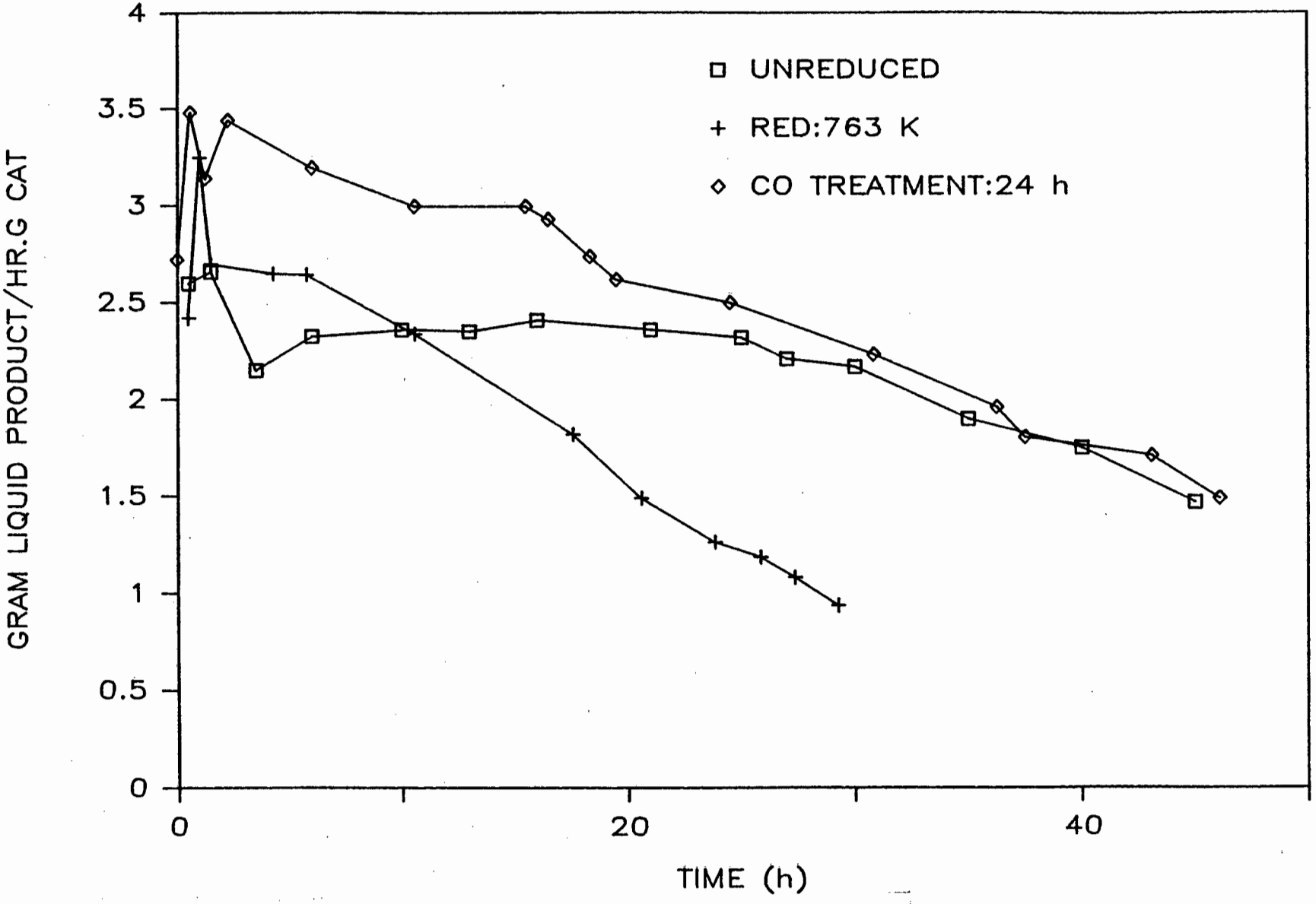

Figure 4.36 Catalytic activity:different forms of 7% NiSMM

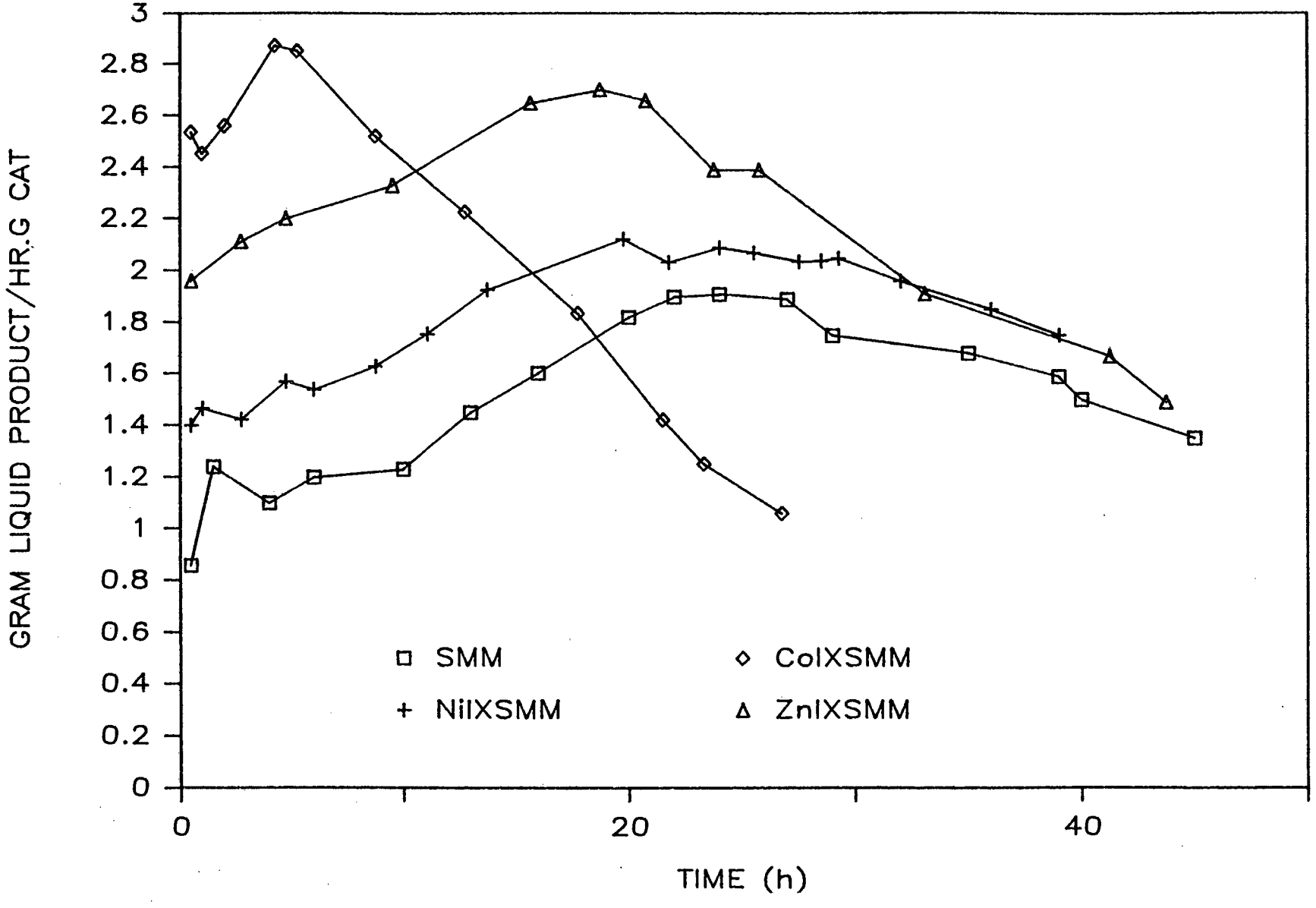

Figure 4.37 Effect of other metal ions(Co,Zn) in the interlayer spaces of SMM

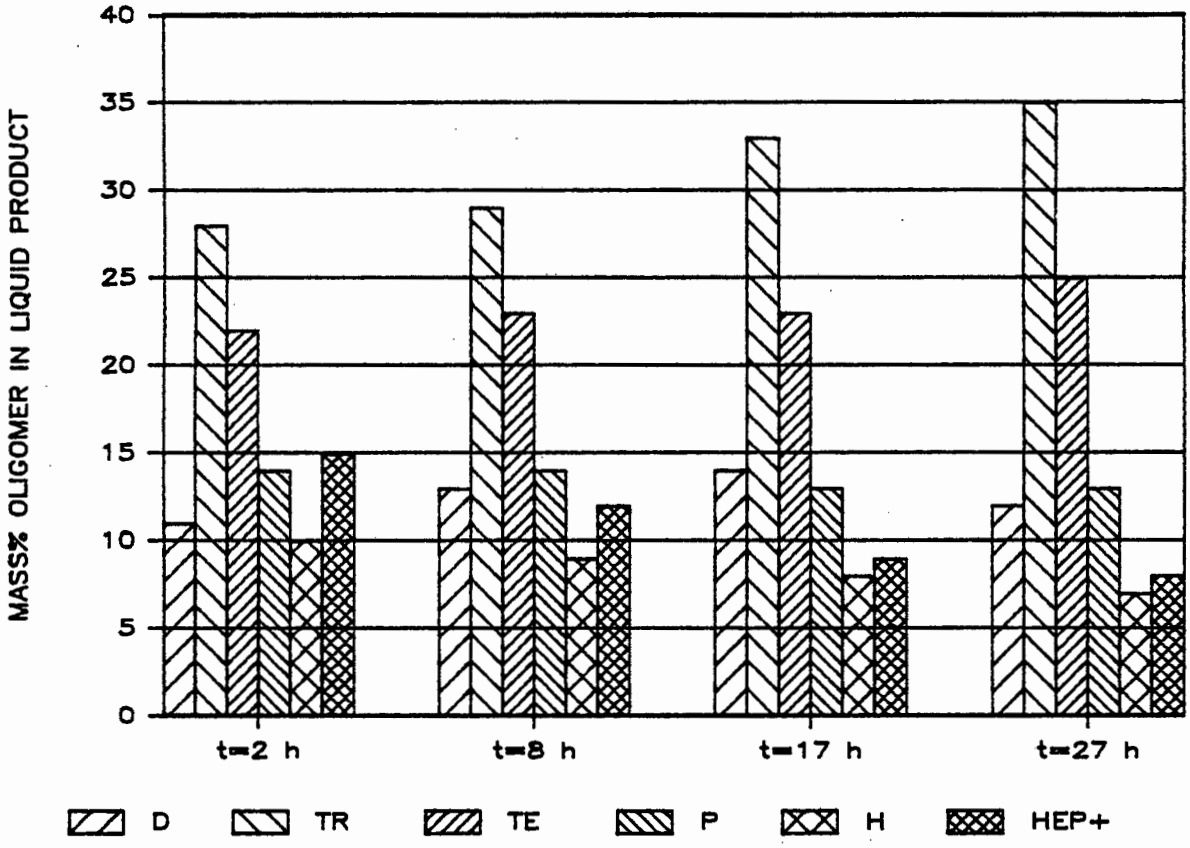

Figure 4.38 Selectivity versus time - CoIXSMM

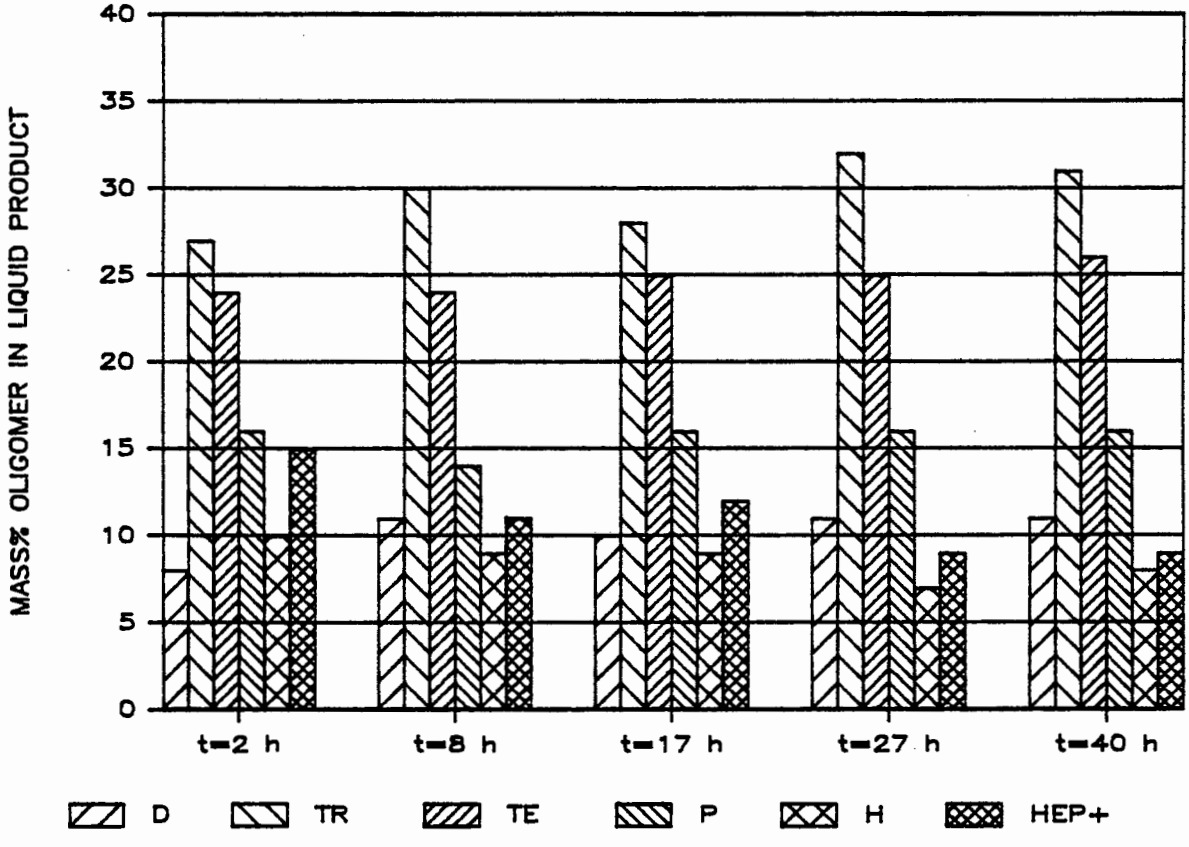

Figure 4.39 Selectivity versus time - ZnIXSMM

4.4.7 PRODUCT CHARACTERIZATION

4.4.7.1 MASS SPECTROSCOPY

A typical mass spectrum of the liquid product is shown in Figure 4.40. This was obtained using a GC-mass spectrometer unit. The molecular masses of the compounds responsible for the peaks are assigned in the figure. The relative intensities of the compounds were determined by means of the total ion current (T.I.C.). From Figure 4.40, the molecular masses of compounds other than that of the corresponding propene polymers (i.e. C_6, C_9, C_{12}, etc.) are also identified. This gives further evidence of the presence of conjunct polymers formed as a result of reaction processes such as cracking and co-polymerization. As a comparison to the GC - mass spectrometer plot of the liquid product, a chromatogram of the liquid fuel obtained from the Varian liquid GC is shown in Figure 4.41. The retention times of the GC - mass spectrometer system could not be correlated to the retention times obtained with the GC system since the former system operated at near vacuum conditions. However, the two spectra are similar and therefore it is possible to compare and identify peaks since both GC systems used a 3% OV-101 on Chromosorb W-HP column at nearly identical operating conditions. The liquid products are grouped into 'oligomer' fractions as shown in Figures 4.40 and 4.41.

The main observations of this study were as follows :

- Separation up to C_{15} was adequate using the above column.
- Traces of C_{25}^{+} were present in the liquid samples but in insignificant quantities. This was deduced by changing the sensitivity of the detector of the mass spectrometer at the point where heavier compounds eluted (> 523 K).

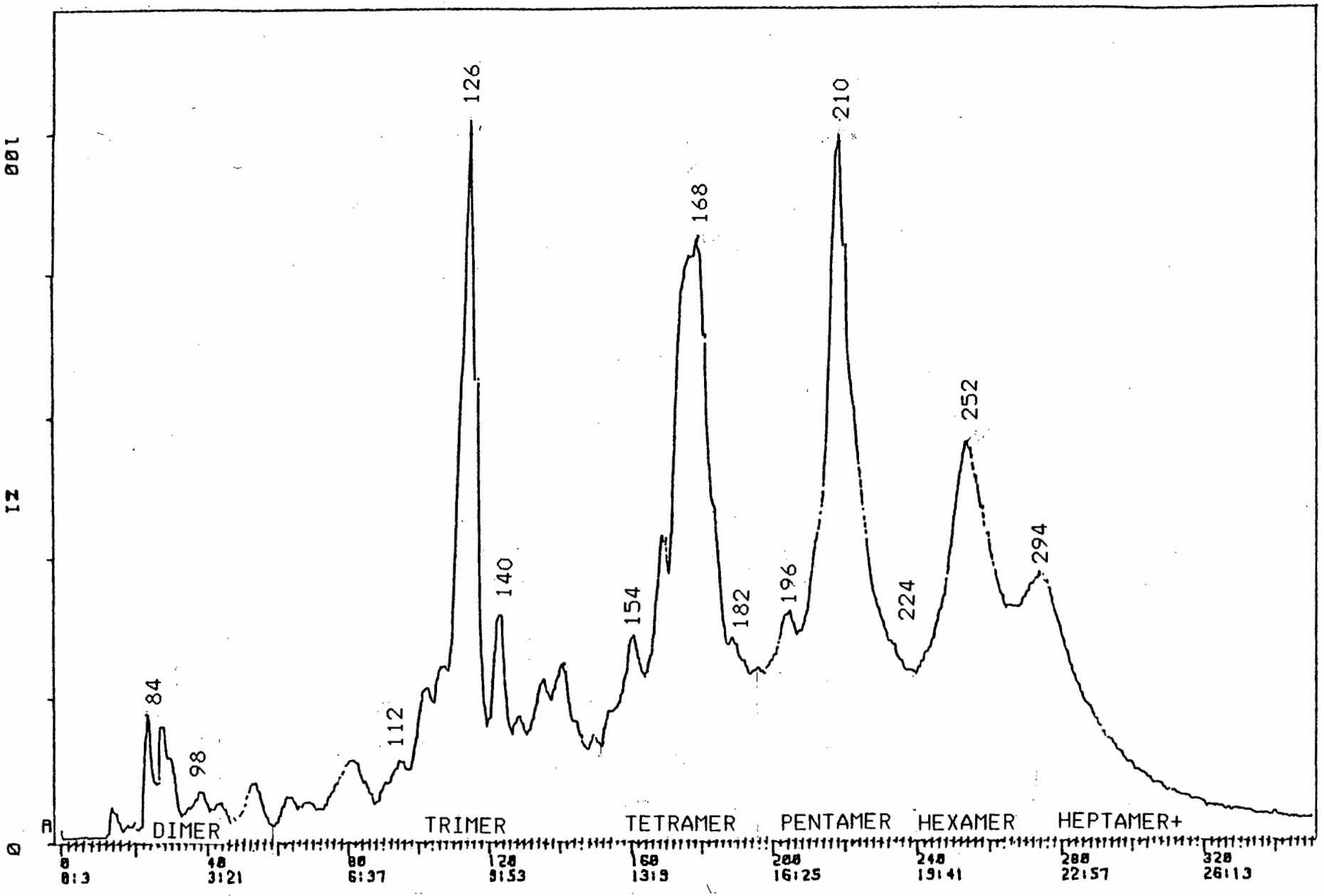

Figure 4.40 Mass spectrometer trace of a typical liquid sample

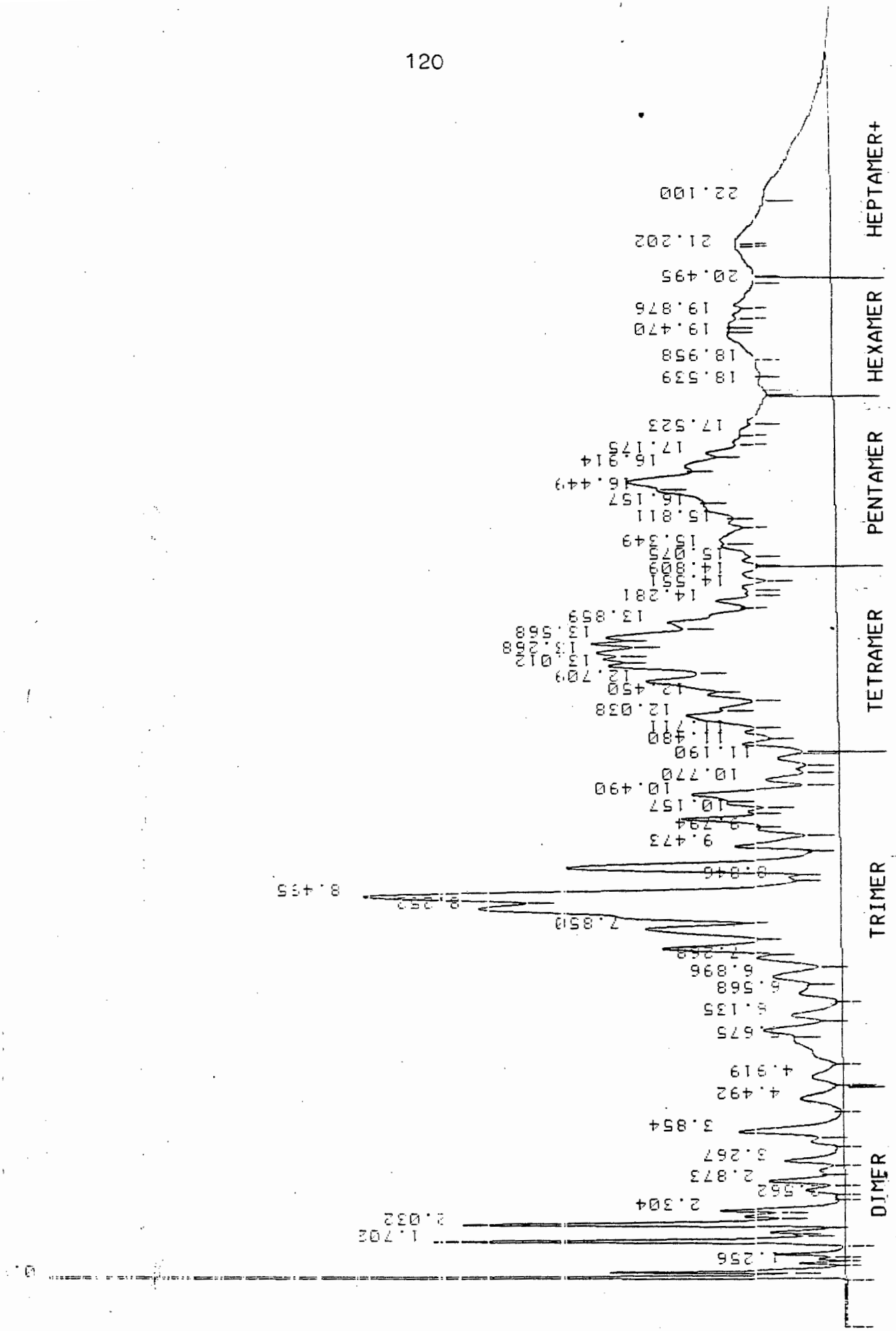

Figure 4.41 GC Chromatogram of a typical liquid sample

- Saturates, α-olefins, β-olefins were present in the liquid samples.
- Above C_{16}, a greater degree of overlap of compounds of different carbon numbers occurred.

4.4.7.2 NMR RESULTS

For a quantitative analysis of the chemical structure of the liquid fuel it is necessary to obtain carbon-13 and proton NMR spectra. However, the degree of branching could be measured using ^1H NMR by monitoring the CH_3/CH_2 ratio. It should be noted that high octane number petrol (C_6 to C_{12}) consists of highly branched hydrocarbons whereas high cetane number diesel (C_{13} to C_{18}) should have minimal branching. Since the liquid fuel produced is a synthetic product, the average degree of branching was determined over the entire range of hydrocarbons (C_6 to C_{20}^+) present.

A typical NMR spectrum of the liquid product is shown in Appendix 3.3. NMR spectra of the liquid fuel sample were monitored over a reaction period of 40 h for propene oligomerization over 7% NiSMM. No significant differences in the degree of branching was observed during this period. It was also observed that no aromatics, which resonate between 6.5 and 7.3 ppm (Galya, 1985), were present in the product at any stage during the run.

The NMR results of the fuels are given in Table 4.9. The relevant catalysts, reaction and pretreatment conditions are also indicated. The degree of branching varies between 0.45 and 0.75. At a reaction temperature of 408 K, the product obtained over SMM and the unreduced

CATALYST	REACTION TEMP.(K)	PRETREATMENT CONDNS*	DEGREE OF BRANCHING
SMM	403	—	0.53
SMM	443	—	0.76
7% NiSMM	403	UNREDUCED	0.55
7% NiSMM	405	WET FEED	0.64
7% NiSMM	408	WHSV = 1.6	0.45
1% NiIXSMM	405	—	0.49
9.5% NiIXSMM	404	—	0.53
7% NiSMM	405	REDUCED AT 763 K	0.49
7% NiSMM	403	REDUCED AT 723 K	0.46
1% NiIXSMM	403	REDUCED AT 723 K	0.70
9.5% NiIXSMM	404	REDUCED AT 723 K	0.62
7% NiSMM	403	REDUCED, CO TREATED: 5 h	0.58
7% NiSMM	403	REDUCED, CO TREATED: 24 h	0.64
1% CoIXSMM	402	—	0.50
1% ZnIXSMM	403	—	0.63

Table 4.9 NMR RESULTS

* ALL CATALYSTS CALCINED AT 773 K FOR 4 h

NiSMM and NiIXSMM showed similar branching (Ø.5 - Ø.55). However, upon reduction a more branched fuel was formed for the ion exchanged samples. The product of the propene reaction over reduced NiSMM samples showed similar branching to the product resulting from the unreduced form of NiSMM. At a higher reaction temperature of 443 K the degree of branching increased to Ø.76. A similar result was obtained when wet feed was used in propene oligomerization over 7% NiSMM. In both these cases, longer chain products were formed during the reaction period as discussed earlier (Section 4.4).

At a lower space velocity, the degree of branching decreased. The liquid fuel obtained from the oligomerization reaction over the carbon monoxide treated catalysts gave slightly more branched products.

The product from reaction over CoIXSMM was similar to that resulting from NiIXSMM. However, the fuel obtained using ZnIXSMM showed a significant increase in the degree of branching.

4.4.7.3 ASTM FUEL TESTS

The liquid product from the propene oligomerization reaction at typical reaction conditions (7% NiSMM extrudates) was subjected to ASTM fuel tests. The product was split into a petrol (< 45Ø K) and diesel (> 45Ø K) fraction. The diesel fraction was hydrogenated in an autoclave over a sulphided Co/Mo catalyst at 598 K and 15Ø atm for 9 h. The results, which include the GC simulation ASTM data on the fractions, are shown in Tables 4.1Ø and 4.11.

PROPERTY	PETROL FRACTION (UNHYDROGENATED)	SABS SPECIFICATIONS
Distillation		
10% (V/V) Evap., Deg C	96	65 (max)
50% (V/V) Evap., Deg C	144	77 - 115
90% (V/V) Evap., Deg C	153	185 (max)
End point, Deg C	187	215 (max)
RON	94.5	87, 93, 98
Density @ 20 Deg C	0.7277	
Acidity, mg KOH/g	0.01	0.03 (max)
Br number, g Br/100g	126.6	

Table 4.10 Results of Standard Petrol Tests

PROPERTY	DIESEL FRACTION (HYDROGENATED)	SABS SPECIFICATIONS
Distillation		
10% (V/V) Evap., Deg C	182	
50% (V/V) Evap., Deg C	215	
90% (V/V) Evap., Deg C	299	360 (max)
End Point, Deg C	369	385 (max)
Density @ 20 Deg C	0.7842	
Viscosity @ 40 Deg C	1.93	1.65 - 5.3
Cloud Point (Deg C)	< -20	
Br number, g Br/100 g	0.17	
Cetane No.	< 35	45

Table 4.11 Results of Standard Diesel Tests

4.4.8 TG-DTA STUDIES

Coke formation on acid catalysts for various hydrocarbon reactions have been investigated using different analytical techniques including infrared spectroscopy (Eisenbach and Gallei, 1979), carbon 13 NMR (Galya et al, 1985) and volumetric methods (Langner, 1981). In this study, the coke build-up on the catalyst during the oligomerization of propene was investigated by means of thermogravimetry (TG).

The TG curve of coked 7% NiSMM in flowing air is shown in Figure 4.42. From the DTA curve in Figure 4.42 two exothermic peaks at 673 K and 873 K, respectively, can be seen. It is clear therefore that two forms of coke deposits are present on the catalyst. The first peak is attributed to the combustion of long chain hydrocarbons which adsorb to the catalyst whereas the second exothermic peak is due to carbonaceous deposits ("graphitic" coke). Since both forms of coke combust in the presence of air, the relative amounts of each coke type could not be determined as there was no clear transition cut-point. Figure 4.43 shows a TG-DTA curve of the same coked catalyst. In this case nitrogen was passed over the catalyst up to a temperature of 1023 K, at which point the gas was switched to air. In this way, the long chain hydrocarbons were 'evaporated' from the catalyst surface until the weight became constant. The introduction of air resulted in the combustion of the 'graphitic' coke with a subsequent mass loss. The DTA curve of Figure 4.43 shows a broad slightly exothermic peak during the volatolization of the hydrocarbons, after which a sharp exothermic peak is observed upon the introduction of air to 1023 K. It should be noted that the total weight loss of about 15 % is the same for the two methods use. Therefore comparing the two curves gave us an indication of the

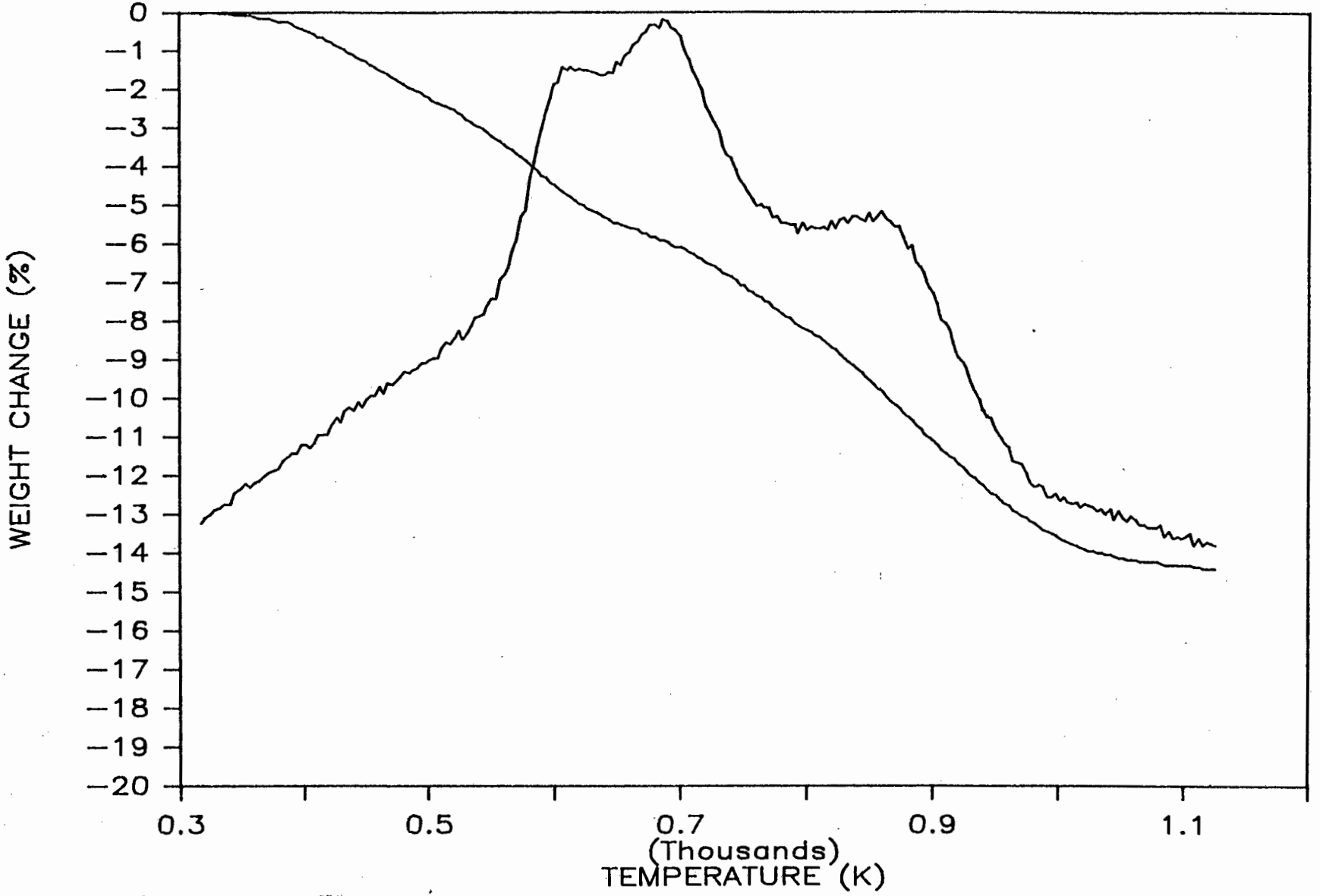

Figure 4.42 TG-DTA curve of coked 7% NiSMM

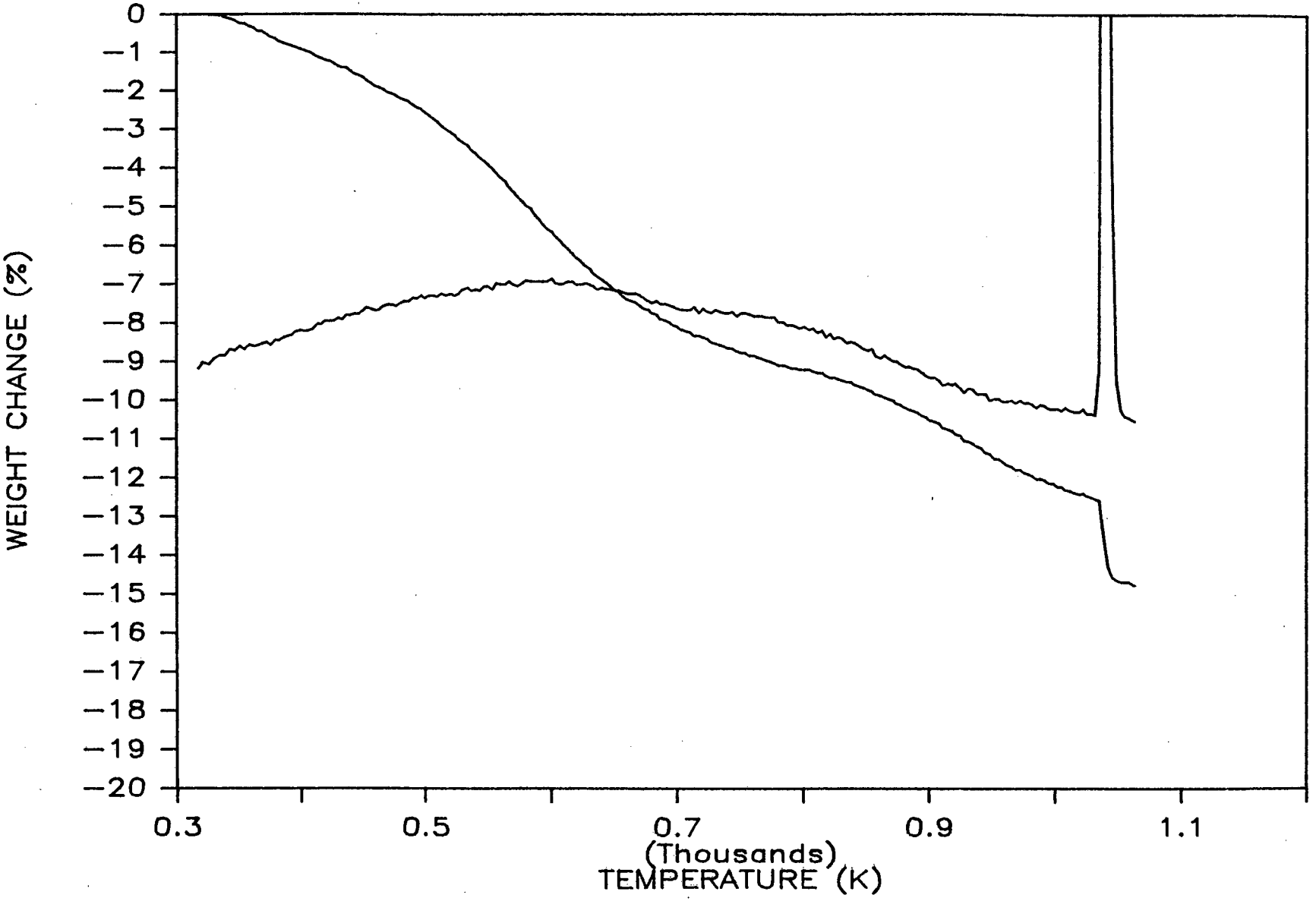

Figure 4.43 Coke determination curve

reproducibility of the technique. Similar plots are shown in Figures 4.44 and 4.45 for coked 7% NiSMM using a wet propene feed for the oligomerization reaction. Since most oligomerization reactions were performed at 403 K, the weight loss between room temperature and 403 K was attributed to physisorbed water adsorbed when removing the catalyst from the reactor and transferring to the thermo balance.

The coke analyses for the different catalysts are shown in Table 4.12. The catalyst changed from black to a light grey after oxidation was completed. For all the above catalysts the ratio of long chain hydrocarbons to 'graphitic' coke varied between 6 and 11. It is interesting to note that although SMM and NiIXSMM have layered structures as opposed to the cagelike structure of the zeolites there is still a large hydrocarbon build-up. The result may imply that there is a strong adsorption of these hydrocarbons to the active sites of the catalyst.

It appears that a total coke content of above 10 % results in the deactivation of the catalysts. At higher reaction temperatures (443 K) the hydrocarbon and graphitic coke build-up was rapid causing immediate deactivation. The coke content after 10 h was 16 %, whereas when SMM was reacted at lower temperature of 403 K the coke build-up was 12 % after 45 h on stream. Using the wet propene feed, the catalyst deactivated after 10 h with a coke content of 15%.

Comparing NiSMM and SMM catalyst which have similar catalyst lifetime for the oligomerization reaction, it can be seen that the NiSMM coke content is slightly higher than that of SMM. This is expected since NiSMM is the more active catalyst. It should also be noted that the graphitic coke content of NiSMM is double that of SMM. The reduced

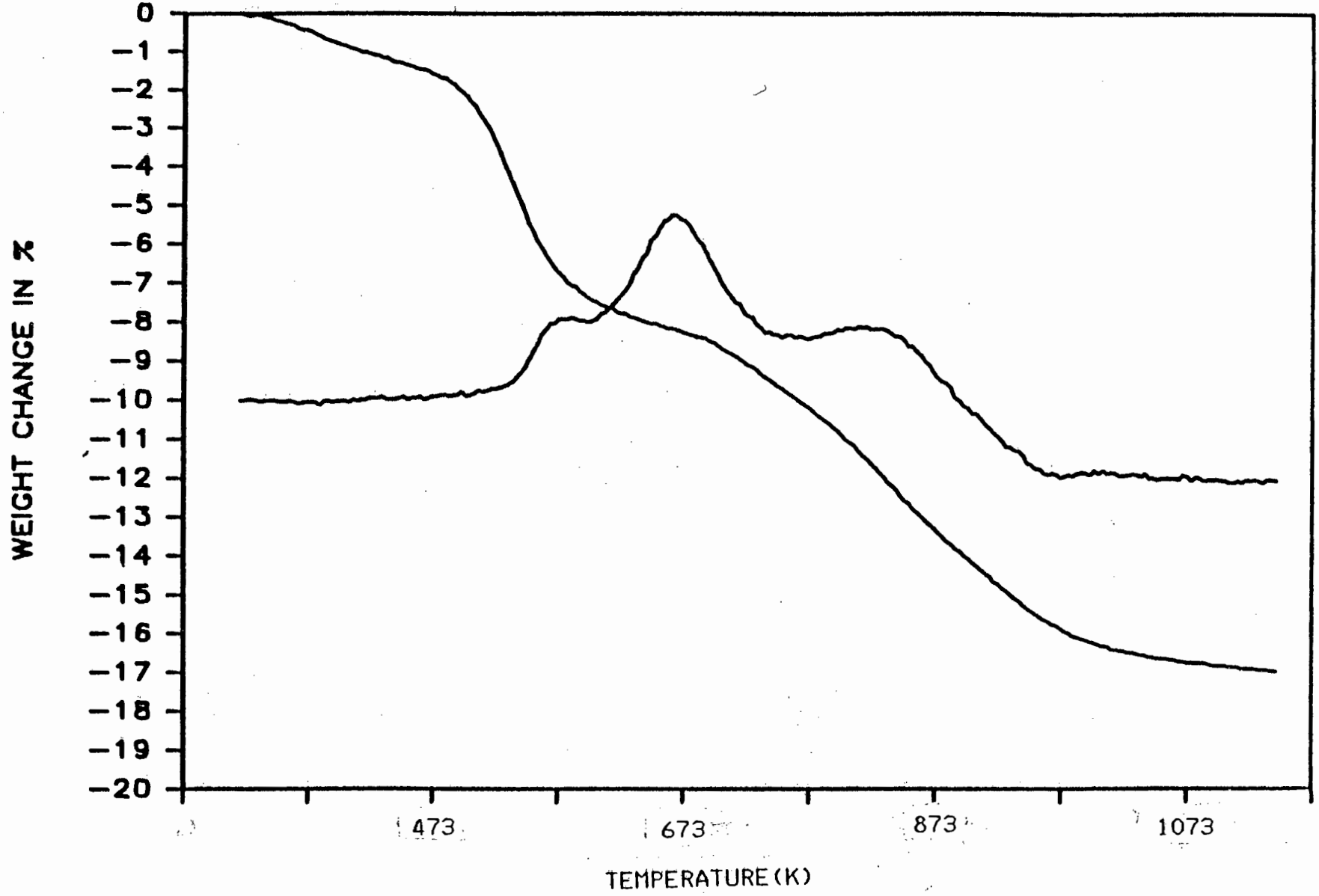

Figure 4.44 Coke combustion using air

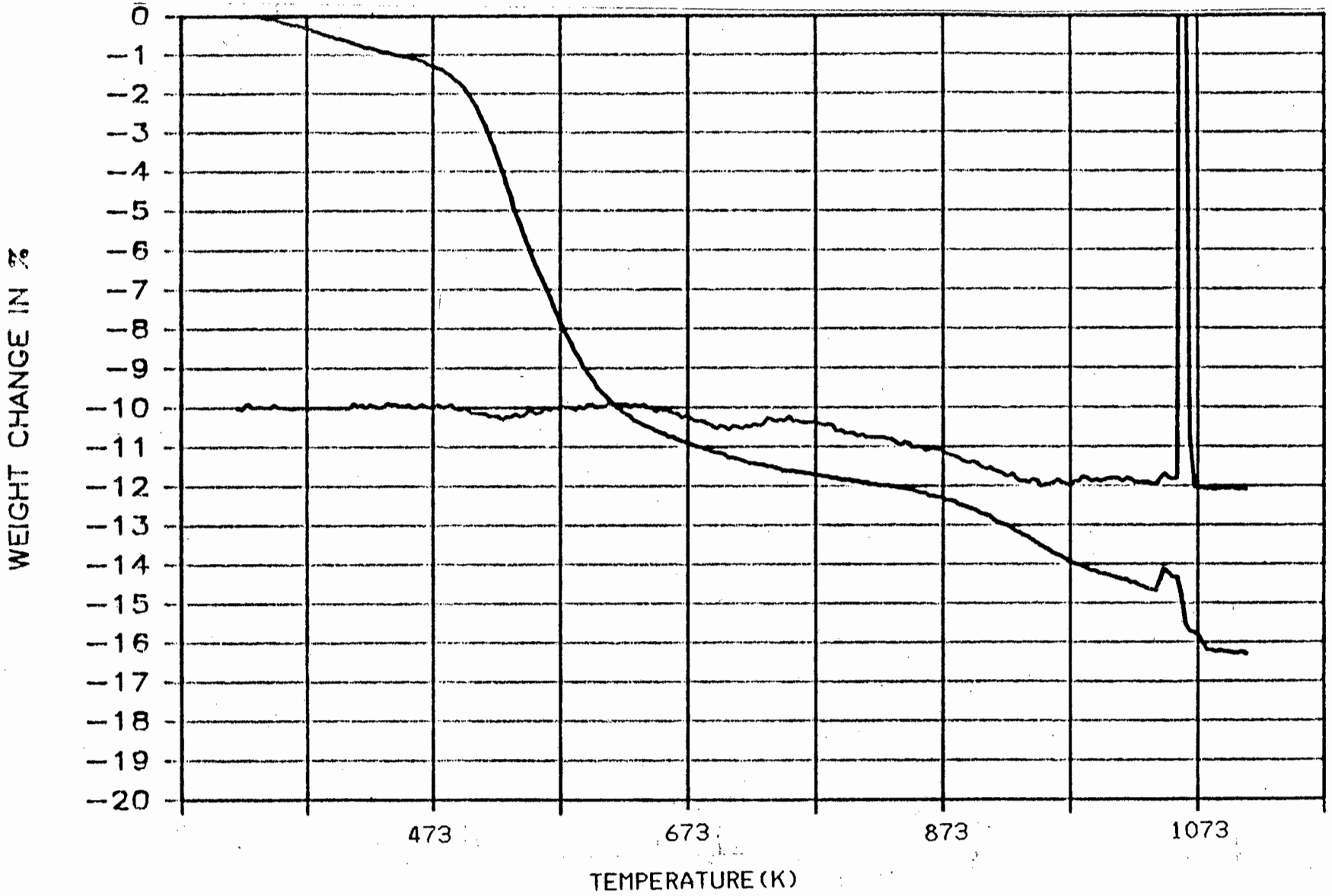

Figure 4.45 Coke determination curve

CATALYST	PRETREATMENT*	RXN T (K)	RXN TIME (h)	WEIGHT LOSS (%)		
				GRAPHITIC COKE	HYDRO-CARBONS	TOTAL
SMM	-	403	45	1.0	11.3	12.3
SMM	-	443	10	1.2	14.3	15.5
NiSMM	UNREDUCED	403	45	2.0	11.5	13.5
NiSMM	WET FEED	405	10	1.85	13.5	15.4
NiSMM	WHSV = 1.6	408	72	2.0	11.5	13.5
1% NiIXSMM	-	405	35	2	10.0	12.0
9.5% NiIXSMM	-	404	30	1.6	12.3	13.9
NiSMM	REDUCED @ 763 K	405	30	2.8	14.0	16.8
NiSMM	REDUCED @ 723 K	403	33	2.5	12.6	15.1
1% NiIXSMM	REDUCED @ 723 K	403	32	2.0	11.5	13.5
9.5% NiIXSMM	REDUCED @ 723 K	404	31	1.9	11.0	12.9
NiSMM	RED, CO TREATED: 5 h	403	32	1.5	12.5	14.0
NiSMM	RED, CO TREATED; 24 h	403	46	1.7	15.0	16.7
CoIXSMM	-	402	27	1.25	11	12.3
ZnIXSMM	-	403	44	1.3	13.0	14.3

Table 4.12 Coke Content of Deactivated Samples

* All catalyst calcined at 773 K for 4 h

NiSMM samples had a higher graphitic coke content which may have resulted in a more rapid deactivation rate. The reduced NiIXSMM samples have a surprisingly lower coke content although they were much more

active than their corresponding unreduced forms. The coke content of CoIXSMM which was on stream for 27 h was similar to the coked SMM catalyst. The amount of 'graphitic' coke present in the exchanged samples decreased in the following order NiIXSMM > ZnIXSMM > CoIXSMM.

The CO treated (24 h) reduced NiSMM, which showed similar catalyst lifetime to SMM and unreduced NiSMM, had a higher coke content since it was the more active catalyst. Thus coke build-up is related to the activity of the catalyst.

At lower WHSV coke formation rate was slower as shown by the fact that deactivation occurred after 70 h. Coke content, at this point, was 1.9% graphitic coke and 13.5 % long chain hydrocarbons.

The thermal treatment of the coked catalyst in air at high temperatures results in the complete removal of long chain hydrocarbons and coke thus the catalyst is expected to be regenerable.

5. DISCUSSION

NiIXSMM catalysts, prepared by a direct ion exchange procedure (Section 3.1.2.1), showed a maximum degree of exchange equal to approximately 27% (based on a theoretical maximum capacity of 196 meq NH_4^+/100 g catalyst. The actual exchange capacity was 67.4 meq NH_4^+/100 g cat which corresponded to a 34% degree of exchange. However, the actual nickel content (weight %) was of more importance than the degree of exchange. The fact that only part of the NH_4^+ ions in SMM can be removed indicates the micaceous character of the catalyst. It has been shown that the ability of a clay or clay catalyst to undergo ion exchange decreases as the mica layer content increases (Kerns and Mankin, 1968). This is due to the fact that the mica layers are non-swellable and therefore prevent the complete removal of the exchangeable NH_4^+ cations. This is to be expected in the case of SMM since the average unit charge of SMM has been shown to be approximately 1.5 (Wright et al, 1972; Heinerman et al, 1983). This is similar to the average unit charge of a micaceous layer clay which is about 2 (Brindley, 1964).

SMM, NiIXSMM and 7% NiSMM gave similar XRD patterns (Figure 4.1). These patterns were indicative of mixed layering. The average d_{001} values for the catalysts (Table 4.2) compared well with those obtained by other workers (Black et al, 1976; Fletcher, 1984). It was concluded that the catalysts used were similar in structure to those prepared by these workers.

The surface area of 7% NiSMM (204 m^2/g) was double that of SMM and NiIXSMM (108 m^2/g). Black and Swift (1974) found that the surface

area of SMM was 145 m^2/g and of 36 wt % NiSMM was 330 m^2/g. However, a decrease in surface area was observed upon the incorporation of zinc into the SMM matrix. Although ZnSMM had a lower surface area, a more crystalline structure was formed. The incorporation of Co in the matrix results in an increase in surface area of the catalyst but this was not as significant as when nickel was incorporated. It appears that the catalyst surface area and crystallinity is affected by the metal salt used in the synthesis procedure.

The fluorine content of SMM (1.9 wt %) was almost double that of 7% NiSMM (1.0 wt %). The fluorine content of a clay catalyst influences mainly the degree of dehydroxylation (Wright et al, 1972). It is suggested that the loss of an (OH, F) pair from the octahedral layer is more difficult than the loss of an (OH, OH) pair since the loss of a proton or hydroxyl group from the former pair would result in a charged species.

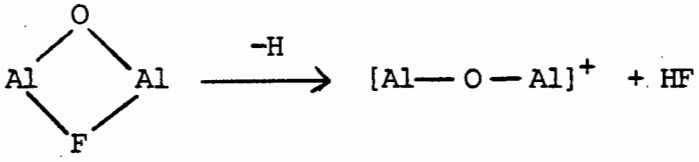

The dehydroxylation loss for an (OH, OH) pair results in the formation of a neutral species thereby maintaining the unit cell charge. Thus 7% NiSMM with a lower fluorine content should show a greater degree of dehydroxylation than SMM.

SMM and NiIXSMM (Figures 4.3, 4.5 and 4.6) show the same weight loss characteristics. The presence of nickel ions (< 10% exchange) in the interlayer spaces do not affect the loss of physisorbed water, deammoniation and dehydroxylation to any significant extent. However, 7%

NiSMM shows a different TG-DTA curve. In the case of NiSMM (7.5 wt %), physisorbed water accounted for a weight loss of about 3.5% more than for SMM (4 wt %). It is known that the ability of a clay to retain physisorbed water increases as the montmorillonite layer content of the clay increases since these layers are able to swell and therefore are able to hold more water molecules (Grim, 1968). Thus it appears that NiSMM has a higher ratio of montmorillonite to mica layer. The results also suggest that NiSMM has a lower average unit charge than SMM (1.5) since the unit charge of clay catalysts is related to the distribution of the layers (i.e. mica, montmorillonite) present. The TG-DTA curves also give a rough estimate of the number of acid sites on the catalyst. In a study of zeolite Y, Ward (1967) showed that the degree of dehydroxylation/deammoniation is related to the total acidity of the catalyst. He found that an increased weight loss due to dehydroxylation resulted in an increase in the catalyst acidity. In the case of NiSMM and SMM, the acidity of the catalyst is partly associated with the trigonal aluminium at the edge of the tetrahedral layers (Wright et al, 1972). Since only a fraction of the aluminium present would have trigonal configuration, acidity is not dependent on the degree of dehydroxylation only. However, the extent of dehydroxylation still gives an indication of the generation of Lewis sites. One cannot differentiate between deammoniation and dehydroxylation from the TG-DTA curves since Wright et al (1972) and Fletcher (1986) found the two processes to occur simultaneously. At temperatures above 800 K, the acidity of SMM was almost entirely of the Lewis type (Fletcher, 1986). From Figures 4.3 and 4.4, it can be seen that the weight loss due to dehydroxylation/deammoniation for NiSMM (12.5%) is greater than for SMM

(8.0%) indicating that NiSMM may have a higher total acidity than SMM. The higher weight loss due to dehydroxylation for NiSMM, with 1% F, confirms the postulate that the lower the fluorine content, the higher the degree of dehydroxylation. The basic structures of SMM, NiIXSMM, NiSMM are thermally stable up to 1100 K. It should be noted that the weight loss rate increases sharply after the appearance of the broad exothermic band on the DTA curves. Wright et al (1972) suggested that dehydroxylation is proton catalyzed since metal cation clays showed greater thermal stability than ammonium clays. The TG-DTA curves for NiIXSMM and NH_4^+-SMM were identical, but may differ for higher weight percent nickel in the interlayer spaces. It was observed that the dehydroxylation/deammoniation weight loss of the catalysts were complete after maintaining the calcination temperature at 773 K for 4 h and thus this procedure was used for the oligomerization experiments.

Ethane hydrogenolysis was used as a probe reaction to monitor the activity of the reduced nickel on NiSMM. The main objective of this work was to gain some information regarding the metal dispersion on 7% NiSMM after reduction in flowing hydrogen. Since the ethane hydrogenolysis activity is related to the degree of reduction and the metal dispersion on the catalyst surface (Yates and Sinfelt, 1967), the results obtained gave a reasonable indication of the formation of metal crystallite and dispersion on the catalyst. As expected, the unreduced NiSMM gave no ethane hydrogenolysis activity.

Water was shown to have an inhibiting effect on the reduction of NiSMM (Figure 4.8). The activity of the reduced NiSMM increased over 50-fold upon calcination. It appears that both physisorbed water and the water loss during dehydroxylation has a strong retarding effect on the

reduction process. Lawson and Rase (1970) and Coenen (1978) found that the water content of nickel exchanged zeolite Y and NiO silica alumina before reduction affected the metal activity. As the water content was increased, there was a decline in the ethane hydrogenolysis activity. In the case of NiO silica alumina, water is expected to affect the reduction process since a considerable amount of water is formed upon the reduction of NiO. However, similar results were obtained for nickel exchanged zeolite Y and NiSMM suggesting that without calcination the reduction process may result in nickel crystallite agglomeration. There is also the possibility that the extent of reduction is reduced due to the simultaneous dehydroxylation of the catalyst at this reduction temperature. It has been established that the reduction of NiSMM is a function of both the reduction temperature and reduction time length. In agreement with the observation by Heinerman et al (1983), there was no indication of nickel reduction below a reduction temperature of 723 K. The activity of NiSMM doubled upon increasing the reduction temperature from 723 K to 763 K (Figure 4.9). However, a decrease in the hydrogenolysis activity was observed upon reduction at a temperature of 823 K. This decrease in activity (and hence dispersion) is probably due to sintering of the metallic nickel at this high temperature. Nickel reduction was almost complete after 3 h as observed by Heinerman et al (1983). Reducing for longer periods (>18 h) at reduction temperatures above 723 K may cause crystallite agglomeration. Maximum ethane hydrogenolysis activity is thus associated with an optimum level of dispersion of the metal and occurs after calcination at 773 K (4 h) and reduction at 763 K (16 h).

No significant differences in apparent activation energies were observed and hence the mechanism of hydrogenolysis is probably the same. The value obtained of 170 $kJ.mol^{-1}$ is in agreement with values obtained by other workers (Yates and Sinfelt, 1967). Richardson (1971) found that NH_4^+ ions present in NiY prevented the reduction of nickel and ascribed this to the formation of Ni^+ or Ni-H species. However, the presence of NH_4^+ ions in NiSMM did not affect the nickel reduction process to any significant extent.

The optimum reduction treatment conditions allow for the removal of both physisorbed water and water resulting from dehydroxylation before reduction. The catalyst is then reduced at a reduction temperature of 763 K for 16 h resulting in an optimum nickel crystallite size and therefore optimum metal dispersion.

The main purpose of this work was to examine the effect of nickel, in the unreduced and reduced form, on the oligomerization activity of the NiSMM catalyst. Considerable work was done in developing an appropriate start up procedure since the catalyst was very sensitive to water present in the feed. The introduction of a bypass line and better control of the feed flow rate ensured that the feed was adequately dried.

Preliminary studies of propene oligomerization over NiIXSMM indicated that Ni^{2+} ions play a role in the oligomerization activity of SMM. SMM was shown to be inactive at 363K (propene feed in liquid phase), whereas both NiIXSMM catalysts (1% and 9.5% exchanged) had an average catalytic activity of 2.2 g liquid/h.g cat. However, at this low temperature NiIXSMM deactivated after 6 h. As the reaction temperature was

increased to 403 K, NiIXSMM regained their original activity and SMM became active. The product distribution showed a shift to heavier oligomer fractions upon increasing the reaction temperature. The results above seem to indicate that at the lower reaction temperature the higher boiling point oligomers formed may remain adsorbed to the surface acid sites causing the deactivation of the catalysts. Upon raising the reaction temperature to 410 K these oligomers desorb and therefore re-expose the acid sites thereby enhancing catalyst lifetime. This effect may also be accompanied by an increase in the intrinsic activity of the catalyst. The effect of Ni^{2+} ions on the activity of SMM will be discussed later. A reaction temperature of 400 - 410 K was chosen since in this temperature range the catalysts showed good lifetime (50 h) and activity (2 g liq/h.g cat) characteristics. A WHSV of 8 to 9 h^{-1} was used so that differences in catalyst activity could be observed since at lower space velocities conversion is almost 100%.

Figure 4.12 showed that adequate reproducibility was obtained. The mass balances for the oligomerization experiments were accurate to within 5%. Figure 4.14 showed that there was little variation in selectivity once steady state was reached. The liquid product was expressed as oligomer fractions and was shown in Figures 4.40 and 4.41. Mass spectroscopy studies indicated that side reactions such as cracking and co-polymerization occurred resulting in the presence of compounds other than propene oligomers (i.e. C_6, C_9, C_{12}, etc). It was observed that upon deactivation of the catalyst there was an increase in the trimer fraction and decrease in the heptamer$^+$ fraction. It should be noted that if oligomers were formed simultaneously, upon deactivation, the product composition would remain unchanged. It is therefore suggested

that the mechanism of oligomerization is probably the continual addition of monomer to an adsorbed oligomer via a carbonium ion mechanism. It is also possible that the strongest sites are those which deactivate first and as time on stream increases the weaker sites, which are only able to sustain dimerization /trimerization reactions, are more predominant.

The introduction of nickel into the matrix of SMM increases the propene oligomerization activity of the catalyst (Figure 4.16). Over NiSMM (2.4 g liq/h.g cat), an increase in activity of approximately 1.3 times that over SMM (1.85 g liq/h.g cat) was observed. When expressing these results in terms of surface area the comparitive values are Ø.Ø336 (SMM) and Ø.Ø353 (NiSMM) g liq / $h.m^2$. Swift and Black (1974) found that the increase in the rate of hexane hydrocracking for NiSMM could not be attributed to the surface area change. However, these workers reduced the NiSMM catalyst resulting in a dramatic increase in the number of Bronsted sites which are active for the hydrocracking reaction (Heinerman et al, 1983). Kojima et al (1986) have shown in TPD studies that only 1Ø% of the potential external sites on SMM are detected by pyridine adsorption, and therefore only part of the surface area is catalytically active. It is thus invalid to compare activities based on total surface area. Robschlager et al (1984) found that NiSMM and SMM had similar acid site distributions. However, the TG-DTA curve of 7% NiSMM (Figure 4.4) showed a greater weight loss due to dehydroxylation/ deammoniation and therefore, as discussed earlier, may result in an increase in the acidity. It is also possible that the increased surface area is associated with smaller platelets thus having more exposed edge sites (trigonal Al). This increase in edge sites may result in the higher oligomerizing activity of NiSMM. Upon the introduction of nickel

into the matrix, the SiO_2/Al_2O_3 ratio increases from 2.36 to 2.9 which may influence the acidity and therefore the activity of the catalyst.

The most significant difference in the behaviour of SMM and NiSMM is the presence of a long induction period. The reason why the incorporation of nickel into the matrix removes the induction period is not clear. It is possible that the nickel increases the surface acidity of the catalyst and this serves to remove the induction period.

No significant differences in selectivity (Figures 4.17 and 4.19) were observed indicating that the same reaction mechanism and acid sites are probably involved for propene oligomerization over NiSMM and SMM. The liquid product showed a degree of branching of 0.55 with 60% of the oligomers boiling at above 453 K. A comparison of the coke build up showed that NiSMM had a greater quantity of "graphitic" coke than SMM (Table 4.12). It has been shown that there is increased coke formation on more acidic catalysts (Blakmond et al, 1982; Ghosh and Kydd, 1986) for propene oligomerization. The higher coke build up on NiSMM is again a result of NiSMM having more acidity than SMM.

Reaction temperature has a marked effect on both the catalyst lifetime and product selectivity. After approximately 10 h on stream at a reaction temperature between 453 and 473 K, the catalysts were virtually inactive. The reaction temperature has a marked effect on both the catalyst lifetime and product selectivity. Initially long chain products were formed (increased heptamer$^+$ formation) and an increase in the degree of branching was observed (0.76 at a reaction temperature of 453 K as opposed to 0.55 at 403 K). The coke build up (1.2%) in the high reaction temperature run was rapid, achieving after 10 h a similar

carbon level to reaction at 403 K for 50 h. The results indicate that the rate of coking is favoured by higher reaction temperatures since the same carbon content level was obtained in a much shorter time. An increase in the coke formation rate with increasing reaction temperature is expected since this reaction is endothermic. NMR showed that no aromatics were present in the liquid product. The rapid deactivation of the catalyst is probably due to the high initial rate of oligomer formation resulting in rapid coke deposition. The presence of water in the feed greatly reduced the catalyst lifetime (Figure 4.22). The dry feed run resulted in a catalyst lifetime of 50 h whereas the catalyst reached half its activity after 8 h upon introduction of wet feed. Fletcher (1984) proposed that the deactivation of SMM, upon the introduction of the wet propene feed, was due to the initial high temperatures experienced during start up. However, no temperature runaway was observed when performing the same experiment with feed water content of 120 ppm_v. It is known that upon introducing water into the system the Lewis sites present on the catalysts are converted to Bronsted sites. The apparent shift in oligomers to longer chain product is further evidence that the acidity of the catalyst has changed. The increased Bronsted acidity therefore results in an increase in the coke formation rate since the amount of coke deposited on NiSMM (1.9%) during the wet feed run after 8 h on stream is similar to that for the dry feed run after 50 h on stream. An increase in the degree of branching to 0.64 was observed. The NMR data indicated that an increase in the coke formation rates coincide with the presence of more branched products.

The incorporation of Ni^{2+} ions in the interlayer spaces of SMM increases the activity at a reaction temperature of 403 K slightly in the case of

1% NiIXSMM (2 g liq/h.g cat) and decreases it in the case of 9.5% NiIXSMM (1.25 g liq/h.g cat). The above results cannot be explained in terms of surface area since this parameter did not vary much upon the introduction of these ions. The NiIXSMM samples showed a similar induction period to SMM (Figure 4.26). However, at a lower reaction temperature of 363 K no induction period was observed. It is often proposed that the mechanism of olefin oligomerization in the case of heterogeneously supported catalysts is similar to that of homogeneous Ni^{2+} catalysts (Cross et al, 1971). The latter involves a mechanism of insertion into the Ni-H bond. It may be that the nickel ions in SMM enhance the catalytic activity by enabling the formation of the nickel-hydride complex. The fact that SMM is inactive at 363 K indicates that the nickel ions influence the acidity of the catalyst or that the effect of the nickel ions is more significant at 363 K by virtue of a possible Ni-H mechanism. As the reaction temperature increases acidic sites similar to those of SMM become operative since the product spectra for SMM and NiIXSMM are similar with respect to selectivity and degree of branching. The fact that 9.5% NiIXSMM is less active than SMM suggests that there is an optimum nickel ion loading for improving propene oligomerization over the exchanged samples. These results were compared to 1% CoIXSMM and 1% ZnIXSMM. At a reaction temperature of 403 K (Figure 4.37), ZnIXSMM showed an activity of 2.5 g liq/h.g cat, whereas CoIXSMM gave appreciable initial activity (2.9 g liq/h.g cat) followed by rapid deactivation. At this reaction temperature the cations present seem to influence the acidity of the catalyst. Product selectivity did not vary much, although an initial shift to longer chain oligomers was observed for CoIXSMM. Lapidus et al (1973) showed that both activity and acidity were influenced by the metal cations present in Zeolite

Y. They observed that the introduction of Ni^{2+} ions in NaY resulted in a marked increase in i-butene oligomerization activity. The catalyst's acidity and activity changed upon incorporation of the divalent cations. Richardson (1967) proposed a model of the acid site in which the bond strengths of the acidic hydroxyl groups (Bronsted sites) are perturbed by the polarizing effects of the neighbouring cations. The ionization potentials of Co^{2+}, Zn^{2+} and Ni^{2+} are 17.05, 17.96 and 18.15 eV respectively, which suggests that the lower the polarizing power of the cation present in the catalyst, the higher the initial activity of the catalyst. The coke build up in the case of CoIXSMM is rapid (1.3 wt %) in a reaction period of 27 h again indicating that the coke formation rate is related to the activity of the catalyst.

Reducing the interlayer Ni^{2+} ions in 1% and 9.5% exchanged samples results in a dramatic improvement in the oligomerizing activity and the disappearance of the induction period. The activity increases from 2.0 to 2.8 g liq/h.g cat and from 1.25 to 2.3 g liq/h.g cat for 1% and 9.5% NiIXSMM, respectively. It is assumed that all the nickel ions in the interlayer spaces are reduced to metallic nickel since it is easier to reduce cations in the interlayer spaces than it is to reduce matrix nickel (Richardson, 1971). The formation of metallic nickel results in the generation of Bronsted sites by the reaction $Ni^{2+} + H_2 \rightarrow Ni^{o} + 2H^{+}$. However, the total amount of acidity should remain the same since on exchange, one Ni^{2+} ion replaces $2NH_4^{+}$ ions. The improvement in activity must therefore be associated with the zero valent nickel. It is also possible that the new Bronsted sites are stronger.

The reduction of 7% NiSMM results in high initial activity (3.4 g liq/h.g cat) followed by a fairly rapid deactivation (1.5 g liq/h.g cat after 20 h on stream). Long chain oligomer formation occurs during this high initial activity. Figure 4.28 shows that the more severe the reduction treatment, the poorer the catalyst lifetime. This is probably due to the increased Bronsted acidity which arises upon reduction of the catalyst (Robschlager et al, 1984; Heinerman et al, 1983). Heinerman et al (1983) found that upon reduction of NiSMM at 723 K, the Bronsted acidity doubled whilst the Lewis acidity remained constant. The catalyst showed a poorer oligomerizing performance at the optimum nickel dispersion level (Ethane hydrogenolysis study). However, at this reduction condition a greater number of Bronsted sites are formed (Robschlager et al, 1984). In order to discriminate between the function of the metallic nickel and the increased acidity, part of the reduced nickel was removed by carbon monoxide leaching. The carbon monoxide leaching would not have removed all the reduced nickel since Heinerman et al (1983) found that after 48 h the nickel was only partly removed. They also observed that after CO leaching the number of acid sites was unchanged. The CO-treated catalysts gave higher activity (3 g liq/h.g cat) than reduced NiSMM. Although more active, the 5 h CO treated sample (17% of nickel removed) still showed relatively early deactivation. However, upon removing 31% of the nickel present, the deactivation rate decreased and the catalysts showed a similar lifetime to unreduced NiSMM. It is clear from these observations that the activity and lifetime of reduced NiSMM is related to the amount of metallic nickel present. This fact is supported by the results obtained for reduced NiIXSMM.

The product selectivity of the reduced NiSMM and NiIXSMM was not significantly different to that obtained for unreduced NiSMM and NiIXSMM except for the initial shift to heavier oligomers in the case of reduced NiSMM. A similar shift to long chain products was observed for the CO treated samples. NMR data for the liquid product of the reduced samples generally showed a higher degree of branching (Ø.62) compared to the unreduced samples (Ø.5). As discussed earlier the degree of branching increases with increasing oligomerizing activity. The graphitic coke content decreased in the order : reduced NiSMM (763 K) > reduced NiSMM (723 K) > reduced NiIXSMM > CO treated NiSMM. Propene oligomerization over reduced NiSMM results in a rapid coke deposition (2.8% after 3Ø h on stream), whereas the CO treated catalyst samples have a much lower graphitic coke content (1.7% after 48 h). It is therefore probable that the generation of Bronsted sites upon reduction of the catalyst improves the overall oligomerizing activity but that the metallic nickel may be acting as a dehydrogenating catalyst causing increased coke formation. This proposal is supported by the fact that upon the removal of the nickel, the coke deposition rate decreased.

An oligomerization experiment using 7% NiSMM extrudates at a lower WHSV (1.6 h^{-1}) showed that the catalyst maintained a 9Ø% conversion by mass for 72 h (Figure 4.24). It is interesting to note that the liquid product spectrum is very similar to that obtained using a 1Ø6 - 212 micron fraction at WHSV of 8 h^{-1}. However, there is the possibility that the product spectra may be significantly different for an oligomerization reaction over this fraction at WHSV of 1.6 h^{-1}. At this lower space velocity propene molecules have a longer residence time in the catalyst bed and therefore increased exposure to the active sites

may result in the formation of heavier weight oligomers. A direct comparison between extrudate and powder catalysts cannot be made since the powder would show a higher active surface area / unit mass than the extrudates. Using the powder form in the catalyst bed increases the pressure drop which may influence selectivity. A similar experiment using 1/16" SMM extrudates at WHSV of approximately 1 h^{-1} was performed (Fletcher et al, 1984) and it was observed that SMM deactivated after 30 h on stream.

The liquid fuel was separated into a petrol (< 450 K) and a diesel (> 450 K) fraction. The petrol fraction exhibited a reasonably high RON of 94.5. The high bromine number (126.6) indicates that the product has a high olefin content. Although the fuel has a high RON, the ASTM distillation curve does not meet SABS specifications. This is, however, not critical since upon spiking the product with, for example, monomer the 10% evaporation point will drop somewhat. The diesel fraction was hydrogenated at 594 K and 150 atm for 9 h, and the bonds were saturated as indicated by the low Bromine number. The product showed a low cloud point, thus the heavier fractions (hexamer^{+}) could be used as a source of lubricating or transformer oils. The hydrogenated diesel product has a cetane number less than 35 and showed good viscosity and density characteristics. The hydrogenated C_{12} - C_{18} product could also be used as a high performance jet fuel.

The carbonaceous deposits on the catalysts after reaction consisted of a fraction removable by nitrogen in the temperature range 473 to 873 K and a fraction only removed by air at 773 - 873 K. The two fractions were assumed to be long chain hydrocarbons which "evaporated" from the catalyst surface upon heating in nitrogen and a "graphitic" fraction.

Although SMM, NiIXSMM and NiSMM have layered structures as opposed to the cagelike structure of the zeolites, there was still a large hydrocarbon build up (13 - 15%). This observation may imply that there is a strong adsorption of these hydrocarbons to the active sites of the catalysts. Fletcher (1984) showed that SMM, after deactivation by the deposition of coke during the reaction, can be regenerated in dry air. The regenerated catalyst gave a similar oligomerizing activity and selectivity to fresh SMM. Bercik et al (1978) found that NiSMM was capable of air regeneration. A study by Reid (1986) showed that regeneration in air restored 7% NiSMM's original activity. However, regeneration in flowing nitrogen resulted in no activity. These observations suggest that the catalyst deactivation is probably due to the deposition of "graphitic" coke, blocking the stronger and more active sites. The high boiling point hydrocarbon fraction may adsorb to the weaker acid sites. Regeneration in air thus removes both forms of deposits resulting in a catalyst with a similar acid site distribution to fresh NiSMM.

In conclusion, this study has found that :

i) the incorporation of matrix nickel enhances the catalytic activity of SMM.

ii) there is an optimum Ni loading in ion exchanging Ni with SMM.

iii) the lower the polarizing power of the cation present in SMM, the higher the initial activity.

iv) the reduction of the interlayer Ni^{2+} ions removes the induction period associated with SMM and increases catalyst lifetime.

v) the reduction of matrix nickel results in high initial activity, followed by deactivation.

vi) the metallic nickel formed upon reduction may be acting as a dehydrogenating catalyst causing increased coke formation during oligomerization over reduced NiSMM.

vii) the introduction of the wet feed resulted in poor catalyst lifetime. The rapid deactivation is attributed to the conversion of Lewis sites to Bronsted sites in the presence of water.

viii) product selectivity for the above catalysts are similar. However, the reduced NiSMM and CoIXSMM samples show an initial shift to long chain oligomers.

ix) the diesel product had a cetane number less than 35. This fraction exhibited good density and viscosity characteristics.

To adequately explain the differences in the oligomerizing activity of the various forms of the catalyst discussed, it is essential that acid site distribution studies be performed. These studies would include :

i) the determination of acid sites on NiSMM.

ii) the influence of exchange ions on the acidity of SMM.

iii) the effect of the reduction of Ni^{2+} ions (matrix and exchanged) on the acidity of SMM.

6. REFERENCES

Addy, K.D. and Innes, W.B. (1952), Ind. Eng. Chem., 42, 866.

Anderson, J.R., Mole, T. and Christov, V. (1980), J. Catal., 61, 477 - 484.

Ashley, L.E. and Hill, T. (1966), U.S. Pat. 1, 102, 298.

Banks, R.L. (August 1979), Chemtech, 494.

Becker, K.A., Fabianska, K and Kowalak, S. (1985), Acta. Phys. Chem., 31, 63.

Benesi, H.A. (1957), J. Phys. Chem., 61, 970 - 973.

Bercik, P.G., Metzger, K.J. and Swift, H.E. (1978), Ind. Eng. Chem. Prod. Res. Dev., 17 (3), 214.

Black, E.R., Montagna, A. and Swift, H.E. (1976) U.S. Patent 3, 966, 642.

Blackmond, D.G., Goodwin, J.G. and Lester, J.E. (1982), 78, 34 - 43.

Boudart, M. (1972), AJChE Journal, 18 (3), 465.

Bovey, J.A. (1969), "Nuclear Magnetic Resonance Spectroscopy", Academic Press, New York.

Brindley, G.W. (1964), Clays and Clay Minerals, Fourteenth Natl. Conf., 31.

Brown, G. (Ed) (1972), "The X-Ray Identification and Crystal Structures of Clay Minerals," Jarrold and Sons Ltd. Norwich.

Capell, R.G. and Granquist, W.J. (1966), U.S. Pat. 3, 252, 889.

Cariatti, J. (1983), Clays and Clay Minerals, 31 (2), 155 - 157.

Carter, J.L., Cusumano, J.A. and Sinfelt, J.H. (1966), J. Phys. Chem., 70 (7), 2257 - 2263.

Coenen, J.W.E. (1978), Int. Congr. Catalysis, 89 - 107.

Coleman, N.J. and Mc Auliffe, C. (1954), Clays and Clay Minerals, 3rd Natl. Conf., 282 - 289.

Cook, E.B.J. and Steele, J.W. "The determination of minor amounts of chloride and flouride in tourmaline and other silicate materials," National Institute for Metallurgy.

Cross, W.E., Kemball, C. and Leach, H.F. (1971), Inorg. Phys. Theor., J. Chem. Soc. (A), 3315.

Csiesery, S.M. and Kittrell, J.R. (1972), U.S. Pat. 3, 632, 500.

Datka, J. (1980), J.C.S. Faraday 1, 76, 2437.

Davidtz, J.C. (1976), J. Catal., 43, 260.

Dietz, W.A. (1967), Journal of Gas Chromotography, Feb., 68 - 71.

Doi, Y., Murata, M. Yano, K and Keii, T. (1982), Ind. Eng. Chem. Prod. Res. Dev., 21, 580.

Dorling, J.A. and Moss, R.L. (1966), J. Catal., 5, 11.

Dry, M.E. (1982), Chemtech, December, 744 - 750.

Eberhart, J.P., (1963) Bull. Soc. Fr. Mineral. Cryst, 86, 213.

Elliot D.J. and Lunsford J.H., (1979), J. Catal., 57, p11.

Emmet, P.H. Ed, (1954), Catalysis Vol. 1, McGraw Hill, New York.

Endo, T. Mortland, M.M. and Pinnavaia, T.J. (1981), Clays and Clay Minerals, 29, 153.

Farmer, V.C. and Mortland, M.M. (1966), J.Chem.Soc. (A), 344.

Farmer, V.C. and Russell, J.D. (1964), Spectrochimica Acta, 20, 1149

Fasol, R.E. (1983), M.Sc. Thesis, University of Cape Town.

Fletcher, J.C.Q. (1984), Ph.D. Thesis, University of Cape Town.

Flory, Paul J. (1964),"Principles of Polymer Chemistry", Cornell Univeristy Press, 222.

Frenkel, M. (1974), Clays and Clay Minerals, 22, 435.

Gaaf, J., van Santen, R., Knoester, A. and van Ningerden, B. (1983), J.Chem.Soc.

Gallezot and Imelik (1973), J. Phys. Chem., 77, 652.

Galya, T.G., Ocelli, M.L., Hsu, J.T. and Young, D.C. (1985), Journal of Molecular Catalysis, 32, 395.

Germain, J.E. (1969), "Catalytic Conversion of Hydrocarbons", Chapter 4, Academic Press, London.

Ghosh, A.K. and Kydd, R.A. (1986), J. Catal., 100, 186.

Glockner, P.W. and Barnett, K.W. (1970), U.S. Pat. 3, 527, 839.

Grim, R.E. (1968), "Clay Mineralogy", 2nd edn. McGraw Hill, 194.

Granquist, W.J. and Kennedy, J.V. (1967), Clays and Clay Minerals, Proceedings of 15th Conf., Pergamon Press, New York, 103.

Granquist, W.J. and Pollack, S.S. (1967) Amer. Miner., 52, 212.

Granquist, W.J., Hoffman, G.W. and Boteler, R.C. (1972), Clays and Clay Minerals, 20, 323.

Granquist, W.J. (1976), U.S. Patent 3, 976, 744.

Haag, W.O. (1967), Chemical Engineering Progress - Symposium series, 63 (73), 140 - 147.

Hassan, S.W., Panchenkov, G.M. and Kuznetsov, O.I. (1977), Bull. Chem. Soc. Japan., 50 (10), 2597.

Hattori, S.W., Milliron, D.L. and Hightower, J.W. (1973), Preprints Div. Pet. Chem., 18, No. 1.

Heinerman, J.J.L., Freriks, J.L., Gaaf, J., Pott, G.T. and Coolegem, J.G. (1983), J. Catal., 80, 145 - 153.

Helfferich, F. (1962), "Ion Exchange", McGraw Hill, New York, p.72.

Herskowitz, M. and Smith, J.M. (1978), Journal of the Amer. Inst. of Chemical Engineers, 24, 439 - 449.

Hill, T. (1967), U.S. Patent 1, 151, 166.

Hoffman, G.W. and Granquist, W.J. (1974), U.S. Pat. 3, 816, 343.

Hogan, J.P., Banks, R.L., Tanning, W.C. and Clark, A. (1955), Ind. Eng. Chem., 47 (4), 752.

Holm, V.C.F., Bailey, G.C. and Clark, A. (1957), Ind. Eng. Chem., 49 (2), 250.

Hoogendoorn, J.C. (1974), The Sasol Story, Sasol.

Hughes, J.R. and White, H.M. (1967), J. Phys. Chem., 71, 2192.

Iiyama, J.T. and Roy, R. (1963), Clays and Clay Minerals, Proc. Nat. Conf., 10, 4 - 21.

Imai, H., Hasegawa, T. and Uchida, H. (1968), Bull. Chem. Soc. Jpn., 41, 45.

Ipatieff, V.R. and Corson, B.B. (1935), Ind. Eng. Chem., 27, (9), 1069.

Ipatieff, V.R. and Schaad, R.E. (1938), Ind. Eng. Chem., (5) 596.

Jaffe, J. and Kittrell, J.R. (1972) U.S. Pat. 3, 671, 425.

Jager, B., (1978), Fischer - Tropsch Synthesis, Spring School in Coal Conversion, Rand Afrikaans University.

Jager, B., Holtkamp, W. and Gaensslen, H. (1982), International Coal Conversion Conference, CSIR, South Africa.

Jasra, R.V. and Bhat, S.G.T. (1985), Advances in Catalysis, Science and Technology, Proc. 7th Natl. Symp. on Catalysis, 423.

Johns, W.D. and Shimoyama, A. (1972), Amer. Ass. Petrol. Geol. Bull., 56, 2160.

Johnson, O. (1955), J. Phys. Chem., 59, 827.

Kerns, R.L. and Mankin, C.J. (1968), Clays and Clay Minerals, 16, 73

Kittrell, J.R., Langlois, G.E. and Scott, R. (1971), U.S. Pat. 3, 625, 865.

Kojima, M., Fletcher, J.C.Q. and O'Connor, C.T. (1986), Appl. Cat., 28, 169.

Kunin, R. (1970), "Ion Exchange resins", McGraw Hill, New York, p338.

Langlois, G.E. (1953), Ind. Eng. Chem., 45 (7), 1470.

Langner, B.E. (1981), Ind. Eng. Chem. Process. Des. Dev., 20, 326.

Lapidus, A.L., Isakov, YA.I., Rudakova, L.N., Minachev, KH.M., and Eidus, YA.T. (1973), Symp. Mech. Hydro. Reactions, Hungary, 403.

Lawson, J.D. and Rase, H.T. (1970), Ind. Eng. Chem. Prod. Res. Develop., 9(3), 317 - 324.

Lewis, D.R. (1955), Clays and Clay Technology, First Natl. Conf., 54

Malaskey, B.F. (1972), U.S. Pat. 3, 682, 811.

Marsh, S.K., Owen, H. and Wright, B.S. (1984), U.S. Patent 4, 456, 781.

Mathers, A.C., Weed, S.B. and Coleman, R.T. (1954), Clay and Clay Minerals, 3rd Natl. Conf. 403 - 412.

Mathleson, D.W. Ed (1967), "Nuclear Magnetic Resonance for Organic Chemists", Academic Press, New York.

McMahon, J.F., Bednars, C. and Solomon, E. (1963), Adv. Petr. Chem. Refin., 7, 285 - 315.

Mortland, M.M. and Raman, K.V. (1968), Clays and Clay Minerals, 16, 393.

Noll, W. (1930), Chem. Erde., 10, 129 - 154.

Oblad, A.G., Mills, G.A. and Heinemann, H., (1958) in PH Emmet, Catalysis, 6, Chapter 4, Reinholdt Publishing Corp., Baltimore.

Occelli, M.L., Hsu, J.T. and Galya, L.G. (1985), J. Mol. Cat., 32, 377.

Panametrics Instrument Guide.

Pine, L.A., Roberts, D.T. and Tolley, G.B. (1970), U.S. Pat. 3, 518, 323.

Rautenbach, M.W. (1986), Ph.D. Thesis, University of Cape Town.

Reid, G.T. (1986), Honours Project, Dept. Chem. Eng., University of Cape Town.

Richardson, J.T. (1967), J. Catal., 9, 182 - 194.

Richardson, J.T. (1971), J. Catal., 21, 122 - 129.

Robschlager, K.H.W., Emeis, C.A. and van Santen, R.A., (1984), J.Catal., 86, 1 - 8.

Russell, J.D. and White, J.L. (1966), Clays and Clay Minerals, Proceedings of 14th Natl. Conf., 181.

Schainberg, I. and Kemper, W.D. (1966), Soil. Sci. Soc. Am. Proc. 30, 707.

Schmerling, L. and Ipatieff, V., (1950), Advances in Catalysis, 2, 21.

Schultz, R., Engelbrecht, R.M., Moore, R.N. and Wolford, L.T. (1966) J. Catal., 6, 419.

Schumann, W. (1983), M.Sc. Thesis, University of Cape Town.

Shephard, F.E., Rooney, I.J. and Kemball, C. (1962) J. Catal., 1, 379.

Sinfelt, J.H. and Yates, D.C. (1967), J. Catal., 8, 82.

Snel, R. (1982), Chemica Scripta, 20, 99 - 101.

Snel, R. (1986), CSIR Report, CENG 598, 1.

Solomon, D.H. and Rosser, M.J. (1965), J. Appl. Polymer Sci., 9, 1261.

Solomon, D.H. (1968), Clay and Clay Minerals, 16, 31-39.

Swartzen-Allen, S.L. and Matijevic,E.(1974), Chemical Reviews, 74, 385.

Swift, H.E. and Black, E.R. (1974), Ind.Eng. Chem. Prod. Res. Develop., 13 (2), 106.

Swift, H.E (1977), Advanced Materials in Catalysis, Academic Press, p209.

Swift H.E. and Vogel, R.F. (1979), U.S.Pat. 4, 138, 326.

Tabak, S.A. (1981), U.S. Patent 4, 254, 295.

Tabak, S.A. Krambeck, F.J. and Garwood, W.E. (1986), AIChE Journal, 32 (9), 1526 - 1531.

Taylor, W.F, Yates D.C. and Sinfelt, J.H. (1964), J.Phys. Chem, 68 (10), 2962.

Thomas, C.L. (1945), Ind.Eng. Chem., 37, 543.

Thomas, C.L. and Barmby, D.S. (1968), J.Catal., 12, 341.

Uytterhoeven, J.B., Christner, L.G and Hall, W.K. (1965), J.Phys. Chem., 69, 2117.

Van Olphen, H. (1963), "An Introduction to Clay Colloid Chemistry", Interscience publishers, New York, 66.

Varian Techron Pty Ltd (July, 1979), "Analytical methods for flame spectroscopy".

Vedder, W. and Wilkens, R.W.T. (1963), Amer. Mineral., 54, 482.

Voge, H.H., In P.H. Emmet (Ed) (1958), Catalysis 6, Chapter 5, Reinhold Publishing Corp., Waverly Press, Baltimore.

Walker, G.F.(1967), Clay Minerals, 7, 111.

Ward, J.W. (1967), J. Catal., 9, 225 - 236.

Webb, T.L. (1981), Chemsa, August, 192-195.

Welz, B.(1976), "Atomic Absorption Spectroscopy", New York, p. 121.

Wendlandt, W.M. (1964), "Thermal Methods of Analysis", Interscience publishers, New York.

Wiese, H.K. (1977), U.S. Pat. 4, 029, 601.

Wright, A.C., Granquist, W.T. and Kennedy, J.V. (1972), J. Catal., 25, 65.

Yates, D.C. and Sinfelt, J.H. (1967), J.Catal., 8, 348.

APPENDIX 1

i) Atomic Absorption Spectroscopy

The table below gives a list of the elements determined, the wave lengths, flames employed, optimum working range and interferences.

ELEMENT	WAVE-LENGTH (nm)	OXIDIZER	OPT WORKING RANGE (ppm)	INTERFERENCES
Ni	232	AIR	3 - 12	NON-ATOMIC ABSORPTION
	341.5	AIR	15 - 60	-
Co	240.7	AIR	3 - 12	HIGH Ni CONC LEVELS
	304.4	AIR	50 - 200	"
Zn	213.9	AIR	0.4 - 1.6	NON-ATOMIC ABSORPTION
Na	330.2	AIR	100 - 400	NA PARTIALLY IONIZES IN AIR-ACETYLENE FLAME

ii) Method of standard additions

The method of standard additions involves using three aliquots of the same sample. The first aliquot was diluted to 250 ml; the second solution was spiked with a standard so that the concentration of this solution is approximately twice that of the unknown, and the third three times the unknown.

The absorbances, A_1, A_2 and A_3 were measured and a calibration curve constructed as shown in the Figure 7.1. The concentration (x) of the original sample is determined by extrapolating to the concentration axis.

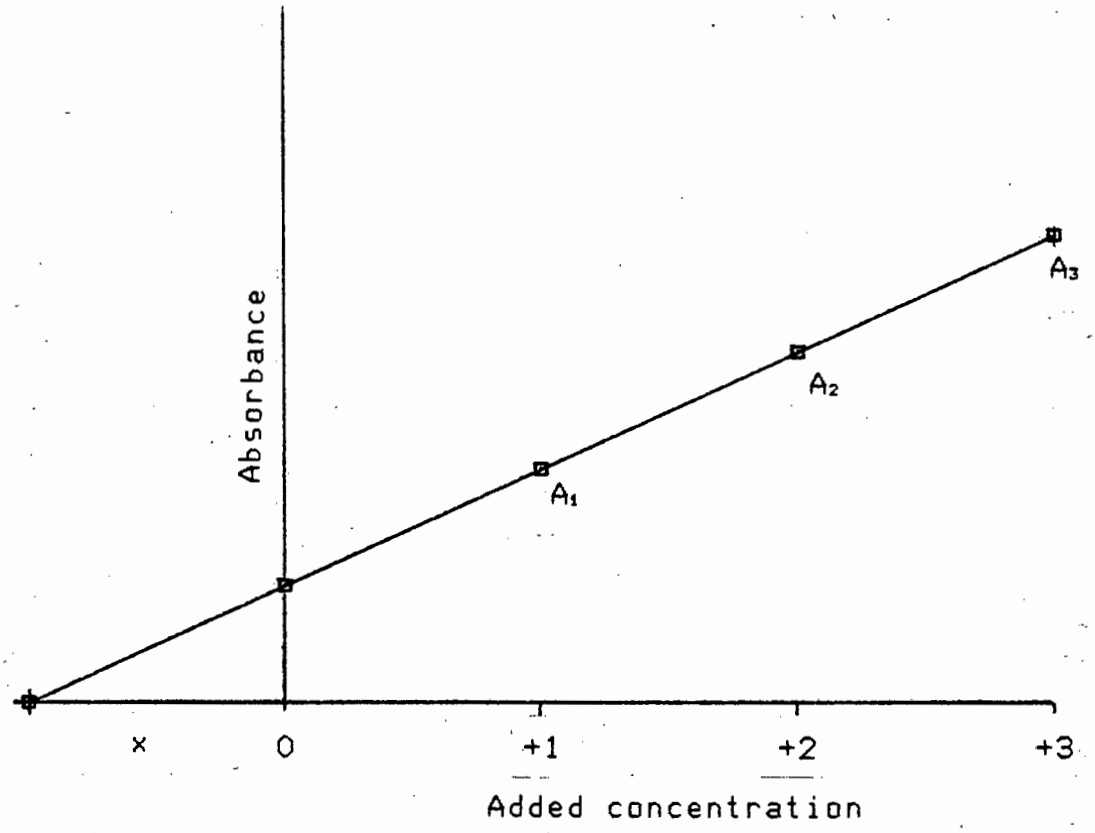

Figure 7.1 Method of standard additons

APPENDIX 2 : OPERATION OF INTEGRAL REACTOR

1. Start-up

After cooling the reactor to room temperature, the feed was diverted past the reactor by means of the bypass line at a similar flow rate to that used during operation (24 g/h). This was continued for at least 30 minutes to remove the initial wet batch of feed. The gaseous feed was then introduced into the reactor at atmospheric conditions, and the reactor system was flushed until approximately 0.1 of feed passed over the catalyst bed. The backpressure regulator was then set at 5 MPa, and the reactor was allowed to fill with feed at the same rate as during flushing.

This procedure ensured that the feed was adequately dried (residence time of the liquid feed in the molecular sieve bed was approximately 4 h). Once the reactor was filled (about 1.5 h), the pump setting was increased slowly until the pressure was raised to the set point and feed issued from the exit gas meter. The reactor was allowed to purge itself of non-condensable gases and the pump settings were adjusted to give the required flow rate.

The reactor temperature was raised slowly to the desired temperature by stepping up the voltage regulator gradually. Typically, a bed temperature of 413 K was reached after 1 to 2 h. Because of the heat of reaction, the Eurotherm controller was set at about 388 K (140V). It should be noted that a phase change of the feed, resulting in volume expansion, occurred in the vicinity of 373 K ($T_{c\ PROPENE}$ = 365.1 K, $T_{c\ PROPANE}$ = 370 K).

Once the bed reached the reaction temperature, the reaction was allowed to proceed for the time taken to empty the dead volume between the catalyst bed and the backpressure regulator after which the catch-pot was emptied. This time was defined as time zero for the reaction. At this stage, the feed cylinder was weighed for mass balance purposes.

2. STEADY STATE OPERATION

The following data was recorded at various time intervals :

- gas meter reading and effluent gas temperature
- mass of liquid product collected
- temperature profile down catalyst bed
- GC analysis of the gas and liquid samples collected

3. SHUTDOWN

The reaction was terminated by isolating the pump from the reactor and releasing the backpressure. The reactor was then cooled under flowing nitrogen. The catalyst was removed and stored in a sealed bottle for coke analysis.

APPENDIX 3 : ANALYTICAL METHODS

3.1. Typical gas chromatogram and gas component peak table.

Figure 7.2 shows a typical gas chromatogram and the assignment of peaks. Table 7.1 summarises these peaks and gives their approximate reponse time and response factors :

GAS COMPONENT	RENTENTION TIME (min)	RESPONSE FACTOR
Methane	3.5Ø	1.Ø7
Ethane	4.25	1.Ø
Propane	6.25	1.Ø6
Propene	7.55	Ø.82
Iso-Butane	1Ø.Ø5	1.Ø
N-Butane	11.5Ø	Ø.8Ø
N-Butene	14.35	1.Ø
Iso-Butene	15.1Ø	1.Ø
T2-Butene	15.6Ø	1.Ø
C2-Butene	16.3Ø	1.Ø
C5's	19.15 : 2Ø.3Ø	1.Ø

TABLE 7.1 COMPONENTS AND THEIR RESPECTIVE RETENTION TIMES

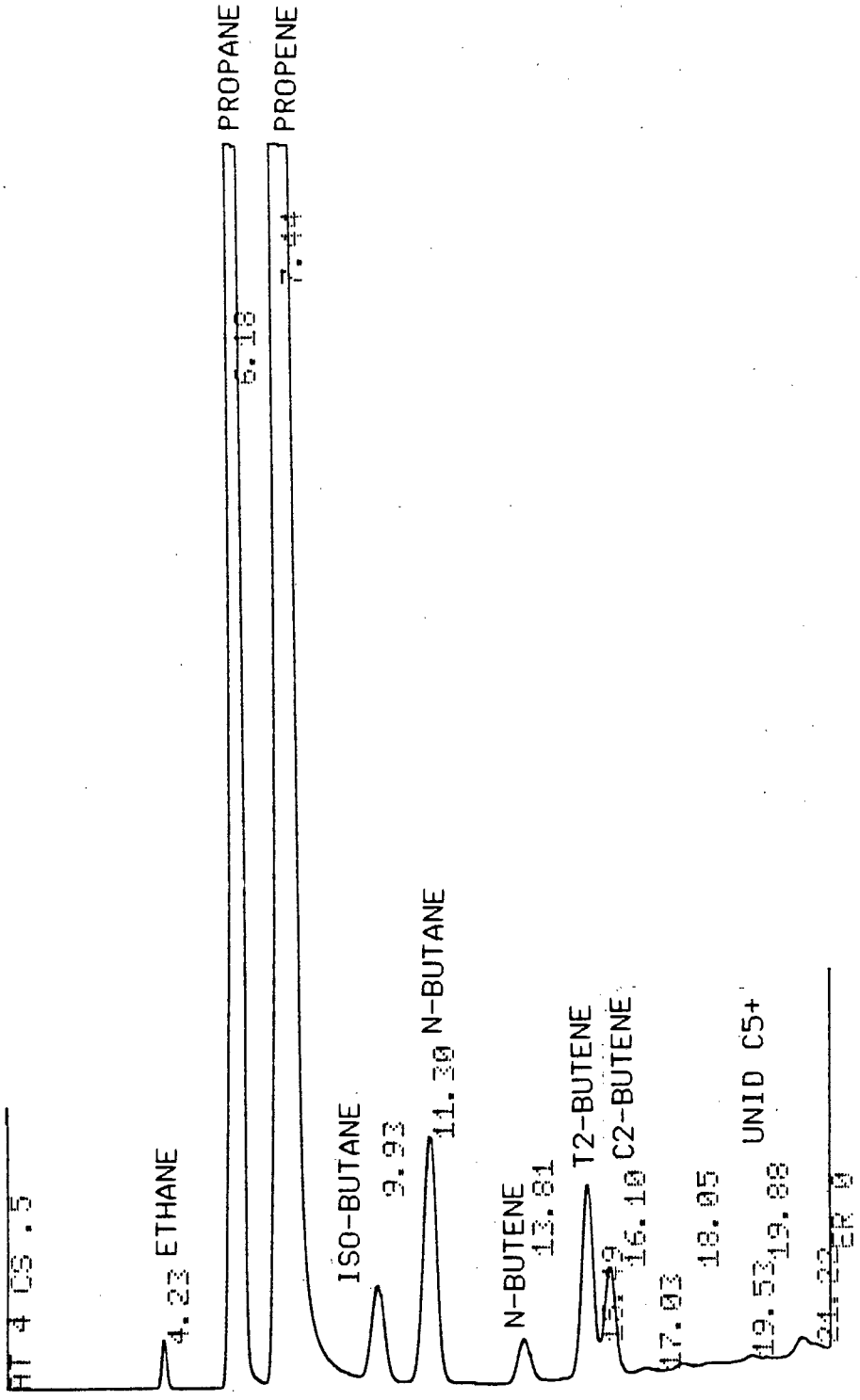

Figure 7.2 Typical gas chromatogram

3.2 PROTON NMR SPECTRUM OF LIQUID PRODUCT SAMPLE

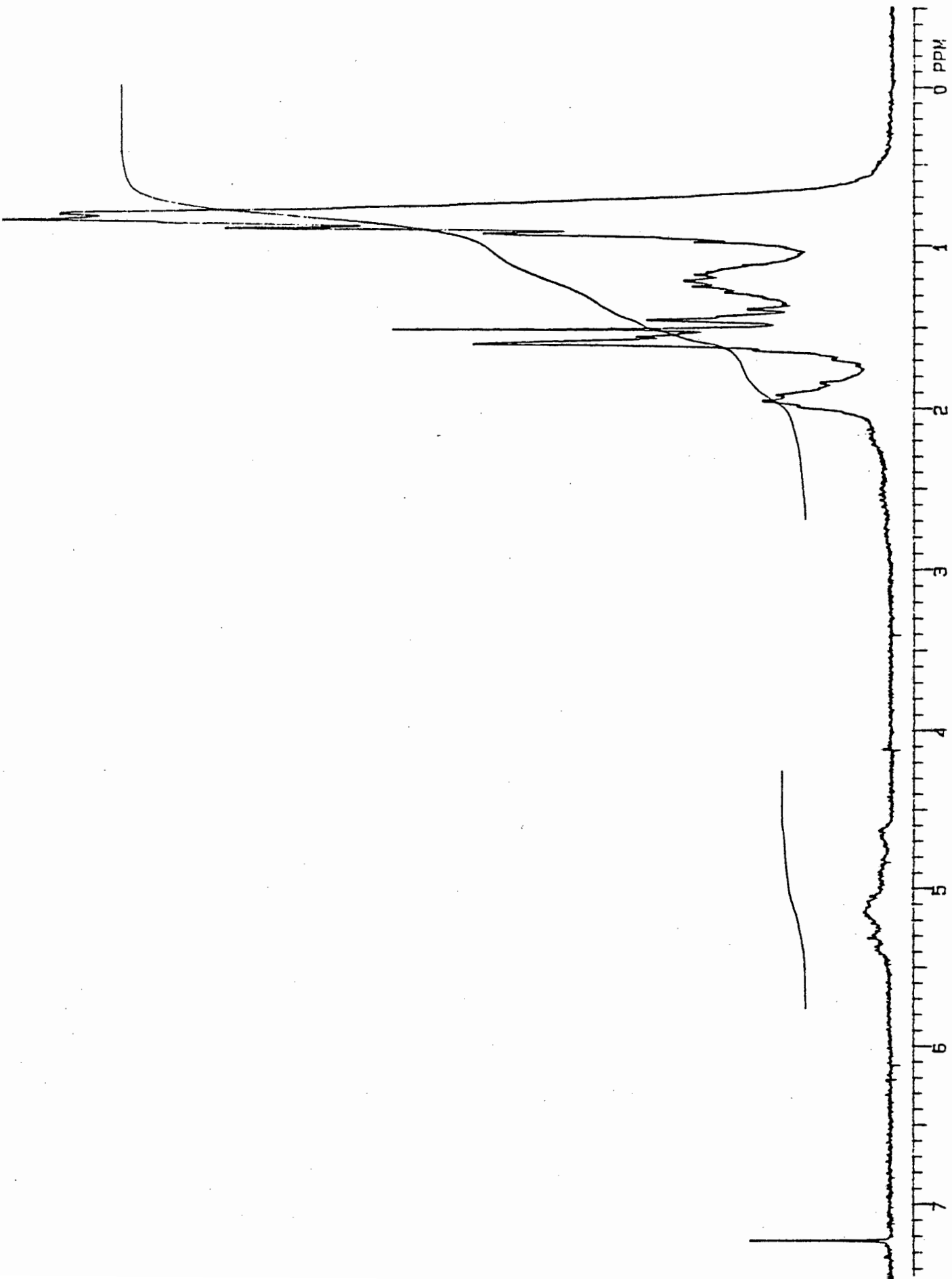

3.3 TG-DTA CURVE OF DEACTIVATED NH_4^+-SMM

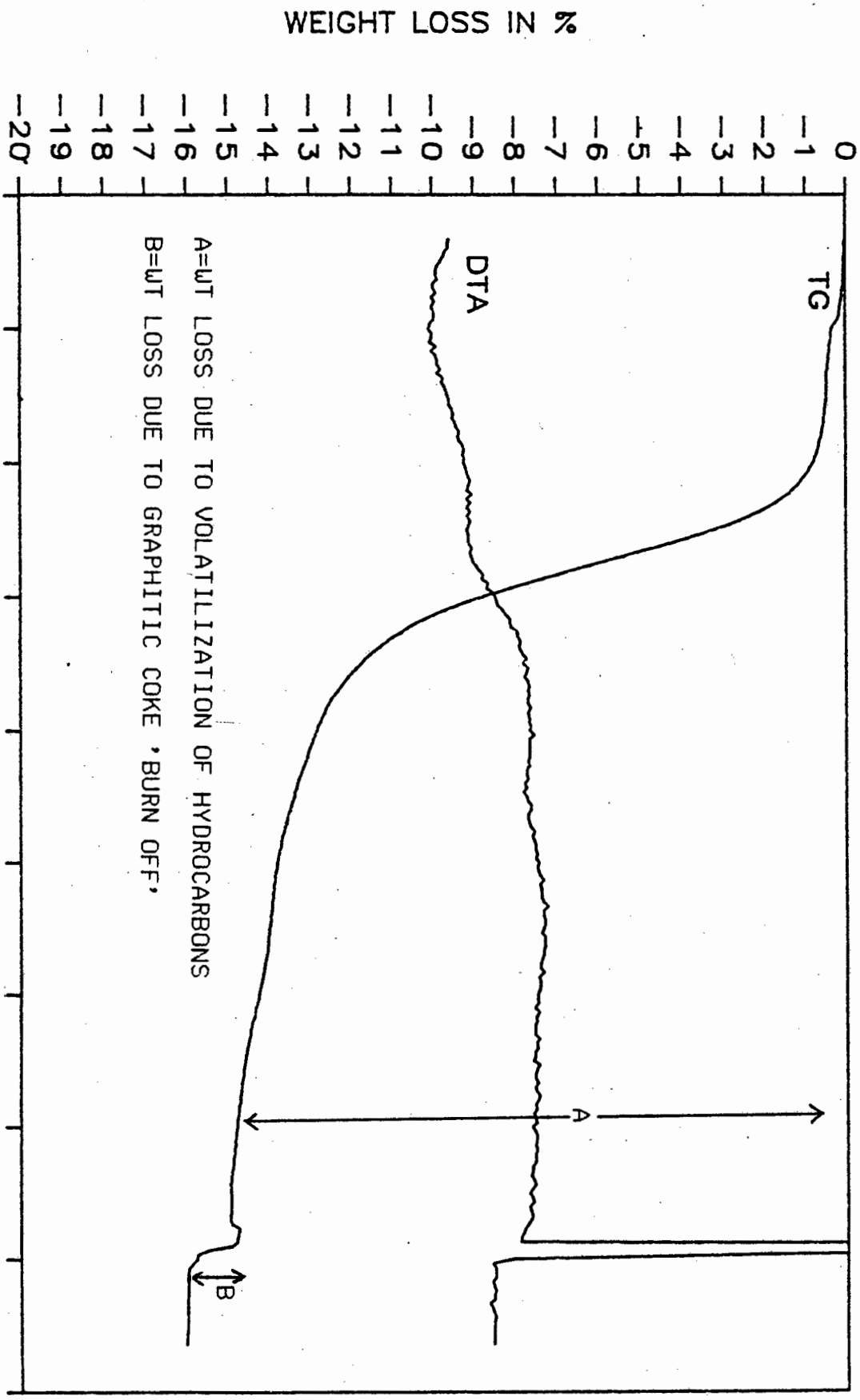

3.4 STANDARD FUEL TESTS

TEST METHOD	ASTM / IP CODE	
	MOTOR GASOLINE	DIESEL FUEL OIL
Distillation	ASTM D86/IP123	ASTM D86/IP123
Vapour pressure (Reid)	ASTM D323/IP69	
R.O.N.	ASTM 2699	
M.O.N.	ASTM 2700	
Induction period	ASTM D525/IP40	
Existing gum	ASTM D381/IP131	
Potential gum	ASTM D873/IP138	
Sulphur content	ASTM D1266/IP107	ASTM D129/IP61
Copper corrosion	ASTM D130/IP154	ASTM D130/IP154
Vapour liquid ratio	ASTM D2533	
Total acidity	ASTM D3242	
Flash point		ASTM D93/IP34
Cetane No.		ASTM D613/IP41
Cold Filter plugging point		IP309
Carbon Residue		ASTM D524/IP14
Ash content		ASTM D482/IP4
Water content		IP74
Sediment content		ASTM D473/IP53
Viscosity		ASTM D445/IP71
Anilene point		ASTM D611/IP 2